

# DISSERTATION

## QUASI-EQUILIBRIUM CONDITIONS OF URBAN GRAVEL-BED STREAM CHANNELS IN SOUTHERN ONTARIO, CANADA, AND THEIR IMPLICATIONS FOR URBAN-STREAM RESTORATION

Submitted by

William Kenneth Annable

Department of Civil and Environmental Engineering

In partial fulfillment of the requirements

For the Degree of Doctor of Philosophy

Colorado State University

Fort Collins, Colorado

Fall 2010

Doctoral Committee:

Department Head: Luis A. Garcia

Advisor: Chester C. Watson

Brian P. Bledsoe  
J. Craig Fischenich  
Pierre Y. Julien

Copyright by William Kenneth Annable 2010

All Rights Reserved

## ABSTRACT

### QUASI-EQUILIBRIUM CONDITIONS OF URBAN GRAVEL-BED STREAM CHANNELS IN SOUTHERN ONTARIO, CANADA, AND THEIR IMPLICATIONS FOR URBAN-STREAM RESTORATION

Urban gravel-bed stream channels in southern Ontario, Canada, identified to be in a state of quasi-equilibrium have been studied over the past 15 years and compared against rural gravel-bed stream channels of the same hydrophysiographic region. Bankfull width and depth versus bankfull discharge were not found to increase as a function of increasing urbanization as has been found in many other studies. The observed annual frequency of bankfull discharge was typically less than a 1-year return period with many sites ranging between two to eighteen bankfull events per year with higher intensity and shorter duration urban flood responses.

The cumulative volume of bankfull and larger flood events from the urban-stream channels were very similar to the same annual event volumes in the rural comparison study reaches. Bed-material supply was found to decrease with increasing urbanization and the reduction in bed-material supply appears to be offset by the smaller bankfull channel width, depth, and access to floodplains during large flood events. Field evidence may also suggest an even greater reduction in channel width trajectory, relative to the

rural setting, with floodplains to maintain quasi-equilibrium conditions as bed-material supply continues to decrease with increased anthropogenic activity.

Compared to surrounding rural watersheds, urban belt widths were found to decrease, while meander wave lengths and radii of curvature were found to increase as a function of bankfull width. The stream-wise elongation of meander wave lengths (and thus increase in radii of curvature) are a result of increased flood flow frequency and volume in the urban environments combined with reductions in bed-material supply.

An increased frequency in riffles and pools was also observed along each reach. Additional pools appeared along straight sections between bends, although they were shallower than pools on bends. The changes in bedforms result from brief but frequent discharge events that exceed critical shear values, resulting in sediment pulsing and the frequent placement of keystone clasts that create frequent riffle (and pool) development. Field observations of standing wave patterns in flood flows also support the role of ‘dune-like’ formations as a means of maximizing flow resistance.

Several methods of estimating channel-forming discharge were also evaluated to test their applicability in the urban condition. Bankfull stage was identified at a series of locations along each study reach and it was found that the most consistent observations of bankfull discharge occurred during flood conditions where bankfull stage was identified at the top of point bars along the convex arc of bends. The largest errors in estimation occurred at gauge stations where cross-sectional geometry had been altered to conform to bridges or culverts rather than the channel morphology. Independent evaluations of channel-forming discharge were conducted by eleven practitioners ranging from 10 to 43 years of experience with similar findings and errors.

Various methods of relating frequency return periods were evaluated using annual peak series discharge observations and continuous 15-minute systematic discharge records using partial duration series analysis. No specific correlations were identified between frequency return periods and land-use change. However, based upon the findings of this study, the applicability of employing annual series peak discharge data to evaluate bankfull frequency return in urban-stream channels is highly discouraged.

William Kenneth Annable  
Department of Civil and Environmental Engineering  
Colorado State University  
Fort Collins, Colorado 80523  
Fall 2010

## ACKNOWLEDGMENTS

This research would not have been possible without the financial assistance from the: Ontario Ministry of Natural Resources, Federal Department of Fisheries and Oceans, Ontario Ministry of Transportation, Ontario Ministry of the Environment, Credit Valley Conservation Authority, Grand River Conservation Authority, Toronto and Region Conservation Authority, Central Lake Ontario Conservation Authority, Halton Region Conservation Authority, Niagara Region Conservation Authority, and Southern Ontario Chapter of the American Fisheries Society. In addition, the hydraulic data, supplied by the Water Survey Division of the Monitoring and Systems Branch of the Inland Water Directorate, Environment Canada, were invaluable in conducting this research.

I am eternally indebted to Dr. Chester Watson, my advisor, who was willing to play along with this trek. Thanks for sharing your tool box of knowledge and experience – among the less obvious and of equal importance, has been your dry sense of humor and a quiet, yet strikingly influential, disposition. Dr. Pierre Julien at the drop of a hat was always willing to embark upon countless numerical and theoretical conversations on sediment transport and river mechanics. It was also wonderful to have another Canadian around with a similar accent. Thanks also to Dr. Brian Bledsoe and Dr. Craig Fischenich for providing thoughtful reviews and comments on the dissertation and serving on my committee.

There are so many students and friends that helped with the field research, data collection, and analysis over the years. Of particular note were the efforts of Derek Brunner, Mark Hartely, Alex Samules, Terry Ridgway, Victoria Lounder, Mike Fabro, and the countless CO-OP students that assisted with sampling and sediment analysis over the years. A special acknowledgement has to be made to Peter J. Thompson who tirelessly picked through all of the Environment Canada data and ensured quality assurance/quality control with all of the 15-minute data – a very tedious but invaluable contribution.

I met so many wonderful faculty, staff, and students in my short time at CSU that I would like to take the time to thank each and every one of you. However, for the sake of brevity – THANKS! There are, however, three particular individuals at CSU that have earned a special spot in my memories. Gloria Garza – I have seldom met people in life with the exuberance and the willingness to help that you possess; and always with a smile, a laugh, and often a joke. Mark Velleux – I never expected to have a roommate while at CSU, but I got one. Projects were a lot more fun with someone around to bounce ideas off of and to collaborate on different numerical techniques. Brett Jordan – a straight-shooting stand-up friend. More importantly, another compatriot who has the love of the river instilled in his blood.

My wife Sheri has been a patient partner for many years with all of my academic pursuits. I am and will always be indebted to your understanding and support throughout the years of continual theses writing, field work, and conferences. I had a lifetime of experiences to make up for and explore with you which were put on hold for so many years. The strain was obviously too great.

Bill Blackport, Pat Crabbe, Shaun Frape, Monique Hobbs, Dave Rosgen, and Tina Wallace have been very special friends throughout the years. You have all lifted my spirits, nurtured my soul, and have been sounding boards throughout life's trials and tribulations. You can't choose your family but we all choose our friends. I have chosen very well over the years and I am very grateful to each of you for sharing your lives and experiences with me.

My son Cory has been a joy and one of the best teachers of my life. Children have a wonderful way of making a parent explore and understand things far greater than themselves. I look forward to having many ski trips with you and finding new things to explore together.

My parents Mae and Ken Annable never had delusions of grandeur with respect to the lifelong aspirations of their kids. Simply, we were just encouraged to "*do our best.*" Well, I am not sure if I have gotten to my best yet, but I think I'm a little closer now than when I started university some 26 years ago! Thanks for all of your love and support throughout the years.

Finally, there was no rational reason for undertaking a second PhD. Simply, I did it to close a loophole, because I bloody well felt like it, and I thought it was the right thing to do for the environment! Thanks to the doctors, nurses, and research in oncology which provided me with the opportunity to see this through to fruition.



# AUTOBIOGRAPHY

## ***WILLIAM KENNETH ANNABLE***

- Bachelors of Science, University of Waterloo, 1987
- Bachelors of Environmental Studies, University of Waterloo, 1990
- Masters of Science, Earth Sciences, University of Waterloo, 1993
- Masters of Science, School of Engineering, University of Guelph, 1995
- Doctorate of Philosophy, Department of Earth Sciences, University of Waterloo, 2003
- Professional Geoscientist, Province of Ontario, 2003
- Professional Engineer, Province of Ontario, 2005
- Doctorate of Philosophy, Department of Civil and Environmental Engineering, Colorado State University, 2010

## DEDICATION

I have been very fortunate over the past number of years to collaborate and wade rivers with so many of the notable leaders in this field, colleagues, and students. However, in the winter of 2006, I (and many other people) lost a good friend and mentor – Dr. Luna B. Leopold. I met Luna late in his life when I began working on my second masters at the University of Guelph researching rural rivers in Ontario, Canada. Luna examined my data set in the early 1990s and had strongly supported and encouraged my efforts. A friendship ensued to his passing. His teachings, rigor, tenacity, and respect for the river and environmental systems founded much of my ethics that I hold dear to this day. “*The knowledge is in the river. Let the river be your guide*” he would repeatedly command. May we all be guided by your legacy. See you down the river!

## TABLE OF CONTENTS

<b>ABSTRACT.....</b>	<b>ii</b>
<b>ACKNOWLEDGMENTS .....</b>	<b>v</b>
<b>AUTOBIOGRAPHY .....</b>	<b>viii</b>
<b>DEDICATION.....</b>	<b>ix</b>
<b>LIST OF FIGURES .....</b>	<b>xiii</b>
<b>LIST OF TABLES .....</b>	<b>xviii</b>
<b>LIST OF SYMBOLS, UNITS, AND ABBREVIATIONS.....</b>	<b>xix</b>
<b>CHAPTER 1 INTRODUCTION.....</b>	<b>1</b>
1.1 OBJECTIVES .....	4
1.2 DISSERTATION ORGANIZATION.....	5
<b>CHAPTER 2 QUASI-EQUILIBRIUM CONDITIONS OF GRAVEL-BED URBAN-STREAM CHANNELS.....</b>	<b>7</b>
2.1 INTRODUCTION.....	7
2.2 METHODS.....	9
2.2.1 Study Area and Site Selection.....	10
2.2.2 Site Conditions .....	11
2.2.3 Channel and Hydraulic Geometry.....	16
2.2.4 Hydrology.....	19
2.2.5 Bed- and Bank-material Characteristics.....	22
2.2.6 Bed-material Transport Capacity .....	28

2.2.7	Statistical Analysis .....	30
2.3	RESULTS.....	32
2.3.1	Channel and Hydraulic Geometry .....	32
2.3.2	Hydrology.....	39
2.3.3	Bed-material Characteristics .....	48
2.3.4	Channel Bed-material Transport Capacity .....	50
2.4	DISCUSSION .....	55
2.5	SUMMARY .....	58
<b>CHAPTER 3 PLANFORM AND BED MORPHOLOGY CHARACTERISTICS.....</b>		<b>61</b>
3.1	INTRODUCTION.....	61
3.2	BACKGROUND.....	63
3.2.1	Bed Morphology .....	64
3.3	METHODS.....	66
3.3.1	Bed Material.....	68
3.4	RESULTS.....	71
3.4.1	Bed Morphology .....	74
3.4.2	Discharge Pulsing.....	80
3.5	SUMMARY .....	84
<b>CHAPTER 4 ESTIMATING CHANNEL-FORMING DISCHARGE IN URBAN WATERCOURSES .....</b>		<b>86</b>
4.1	INTRODUCTION.....	86
4.2	FIELD METHODS .....	91
4.3	INDEPENDENT CALIBRATION .....	94
4.4	EFFECTIVE DISCHARGE .....	99

4.5	HYDRO-GEOMORPHIC METHODS.....	104
4.6	FLOW-FREQUENCY METHODS.....	109
4.7	CATCHMENT RELATIONSHIPS .....	115
4.8	SUMMARY .....	117
<b>CHAPTER 5 CONCLUSIONS AND RECOMMENDATIONS .....</b>		<b>120</b>
5.1	RECOMMENDATIONS .....	125
<b>REFERENCES.....</b>		<b>128</b>

## LIST OF FIGURES

Figure 2.1. Site location map: a) screening area, and b) site location references. ....	11
Figure 2.2. Urban land-use assemblages within effective catchment areas.....	14
Figure 2.3. Event definition and threshold criteria. ....	21
Figure 2.4. Average bankfull width ( $\overline{W}_{bf}$ ) and average bankfull depth ( $\overline{D}_{bf}$ ) versus bankfull discharge ( $Q_{bf}$ ). ....	33
Figure 2.5. Dimensionless average bankfull width ( $\hat{W}$ ), dimensionless average bankfull depth ( $\hat{D}$ ), and channel bed slope ( $S_o$ ) versus dimensionless bankfull discharge ( $\hat{Q}$ ). ....	35
Figure 2.6. Annual duration flow exceeding critical bank shear stress ( $F_{Bk}$ ) versus the annual percent shear stress exceeding critical shear of the a) median bed material ( $F_{Bed50}$ ), and b) the 84 <sup>th</sup> -percentile bed material ( $F_{Bed84}$ ). ....	38
Figure 2.7. Bankfull discharge ( $Q_{bf}$ ) versus effective catchment area ( $A_{eff}$ ). ....	40
Figure 2.8. Annual frequency of bankfull discharge events ( $N_e$ ) versus percent urban land use. ....	42
Figure 2.9. Annual return period of bankfull discharge using: a) annual frequency of bankfull discharge events ( $1/N_e$ ), and b) maximum annual instantaneous discharge data. ....	43

Figure 2.10. a) flood intensity and b) flashiness index versus effective catchment area ( $A_{\text{eff}}$ ).	44
Figure 2.11. Annual flow volume ( $V_{\text{tot}}$ ) versus effective catchment area ( $A_{\text{eff}}$ ).	46
Figure 2.12. Annual cumulative a) volume ( $V_{\text{ae}}$ ) and b) duration ( $T_{\text{ae}}$ ) of events where bankfull discharge has been equaled or exceeded; and, annual cumulative c) volume ( $V_{\text{abf}}$ ) and d) duration ( $T_{\text{abf}}$ ) of discharge exclusively exceeding bankfull discharge versus effective catchment area ( $A_{\text{eff}}$ ).	47
Figure 2.13. Annual bed-load transport yield capacity versus effective catchment area ( $A_{\text{eff}}$ ) using Einstein-Brown equation (Brown, 1950). <i>Note:</i>	49
Figure 2.14. Bed-load rating curves.	51
Figure 2.15. Urban reach a) bed-load rating curve exponents ( $\beta_s$ ) versus percent urban land use, and b) annual bed-load yields versus effective catchment area ( $A_{\text{eff}}$ ).	53
Figure 2.16. Effective discharge ( $Q_{\text{eff}}$ ) versus bankfull discharge ( $Q_{\text{bf}}$ ).	55
Figure 3.1. Standing wave pattern in Little Etobicoke Creek at York Mills (Site 7) at $32.4 \text{ m}^3/\text{s}$ . Bankfull discharge is $23.8 \text{ m}^3/\text{s}$ .	62
Figure 3.2. Study reach images.	67
Figure 3.3. Typical measurements of longitudinal profile.	68
Figure 3.4. Belt width, meander wave length, and radius of curvature ( $R_C$ ) versus average bankfull width for urban and rural streams in the same hydrophysiographic province.	72

Figure 3.5. Belt width, meander wave length, and radius of curvature ( $R_C$ ) versus average bankfull width for urban and rural Ontario streams (Leopold and Wolman, 1960; Williams, 1986).....	73
Figure 3.6. a) inter-pool length ( $\bar{L}_{IP}$ ) by bankfull width ( $\bar{W}_{bf}$ ) versus meander wave length ( $\bar{\lambda}$ ) by $\bar{W}_{bf}$ and b) riffle slope ( $\bar{S}_R$ ) by bed slope ( $S_O$ ) versus riffle length ( $\bar{L}_R$ ) by bankfull width ( $\bar{W}_{bf}$ ).....	75
Figure 3.7. Pool depths ( $D_P$ ) at bankfull stage by average reach bankfull depth ( $\bar{D}_{bf}$ ) versus radius of curvature ( $R_C$ ) by average reach bankfull width ( $\bar{W}_{bf}$ ) for a) bend pools and b) box-and-whisker plot for in-line pools. ....	77
Figure 3.8. Riffle crest to pool invert height ( $H_{LP}$ ) by length of crest of riffle to pool invert ( $L_{LP}$ ).....	79
Figure 3.9. Average annual number of observed discharge events where critical shear of $D_{50}$ particle grain sizes ( $Q_{C50}$ ) versus $D_{84}$ particle grain sizes ( $Q_{C84}$ ) are exceeded.....	80
Figure 3.10. Average annual duration of time exceeding thresholds of $\tau_{X84}$ versus $\tau_{C50}$ . ....	82
Figure 3.11. Number of observed clast particles versus clast-travel distance ( $L_{\square}$ ) by average bankfull width. ....	84
Figure 4.1. Longitudinal thalweg profile bankfull stage regression. ....	92
Figure 4.2. Discharge from bankfull stage estimate at gauge station versus observed bankfull discharge at top of point bars during flood event. ....	94



Figure 4.3. Independent evaluation of bankfull stage versus field observed bankfull discharge during flood events at a) upper-limits of point bars on the convex arc of bends, b) riffles, and c) gauge station. ....	97
Figure 4.4. Field-identified bankfull stage using snow-melt limit where $Q_{bf}$ is the stage associated with bankfull discharge (Redhill Creek at Hamilton). ....	99
Figure 4.5. Flow conditions used in effective-discharge estimate from the Little Don River and Don Mills sites for a) hydraulic geometry observed at gauge station and representative cross section versus discharge and b) discharge versus time for different systematic time observation intervals.....	100
Figure 4.6. Effective-discharge analysis using Wilcock and Kenworthy (2002). Bed-load discharge versus discharge for 15-minute flow observation data at gauge station cross section (15), representative cross section (15), and hourly data (60) at representative cross sections for a) Little Don River at Don Mills (Site 7), b) Mimico Creek at Islington (Site 8), and c) Spencer Creek at Dundas (Site 10).....	104
Figure 4.7. Total channel shear, specific stream power, width/depth ratio, and discharge velocity versus discharge for a representative cross section. One-hundred discrete evenly-distributed discharge simulation events between $Q_{min} \leq Q \leq Q_{100}$ .....	105
Figure 4.8. a) discharge velocity, and b) width/depth ratio versus longitudinal distance. ....	107

Figure 4.9. Field-observed bankfull discharge versus predicted channel-forming flow from one-dimensional model analysis using local maxima values of a) discharge velocity, b) total channel shear, c) specific stream power, and d) width/depth ratio.....	108
Figure 4.10. Recurrence interval versus discharge (Red Hill Creek at Hamilton (Site 9)). .....	110
Figure 4.11. Predicted bankfull discharge for the 1.5-year return interval versus field-observed bankfull discharge for a) for Weibull analysis, and b) Log Pearson III analysis. ....	112
Figure 4.12. Discharge return period a) $Q_2$ , b) $Q_5$ , and c) $Q_{10}$ by bankfull discharge ( $Q_{bf}$ ) versus effective catchment area ( $A_{eff}$ ) for urban streams and rural streams in the same hydrophysiographic region. ....	113
Figure 4.13. Bankfull discharge ( $Q_{bf}$ ) by effective discharge ( $Q_{eff}$ ) versus discharge return period a) $Q_2$ , b) $Q_5$ , and c) $Q_{10}$ ( $Q_X$ ) by the annual average median discharge ( $Q_{ma}$ ) for urban streams and rural streams in the same hydrophysiographic region. ....	114
Figure 4.14. Bankfull discharge return period ( $T_{bf}$ ) versus watershed urban land use for urban streams and rural streams in the same hydrophysiographic region .....	115
Figure 4.15. Bankfull discharge ( $Q_{bf}$ ) versus a) effective discharge, and b) stream-network length for urban streams and rural streams in the same hydrophysiographic region. ....	116

## LIST OF TABLES

Table 2.1. General urban reach characteristics .....	12
Table 2.2. Reach geometry and pebble count characteristics. ....	33
Table 2.3. Bed-material and transport characteristics.....	36
Table 2.4. Channel bank characteristics. ....	37
Table 3.1. Reach geometry and bed-material characteristics. ....	81
Table 4.1. General urban site characteristics and channel-forming flow metrics.....	90

## LIST OF SYMBOLS, UNITS, AND ABBREVIATIONS

### Symbols

$A$	=	discharge cross-sectional area [ $L^2$ ]
$A'$	=	dimensionless transport function parameter [-]
$A_d$	=	topographic catchment area [ $L^2$ ]
$A_{\text{eff}}$	=	effective catchment area [ $L^2$ ]
$A_p$	=	meander amplitude [ $L$ ]
$A_U$	=	urban effective catchment area [ $L^2$ ]
$c_1 - c_6$	=	hydraulic geometry coefficients [-]
$D$	=	discharge depth, channel depth [ $L$ ]
$\hat{D}$	=	dimensionless bankfull depth [-]
$D_{16}$	=	grain-size fraction diameter [ $L$ ]
$D_{25}$	=	grain-size fraction diameter [ $L$ ]
$D_{50}$	=	median grain-size fraction diameter [ $L$ ]
$D_{50p}$	=	median pebble count grain diameter [ $L$ ]
$D_{75}$	=	grain-size fraction diameter [ $L$ ]
$D_{84}$	=	grain-size fraction diameter [ $L$ ]
$D_{\text{bf}}$	=	bankfull depth [ $L$ ]
$\overline{D}_{\text{bf}}$	=	average bankfull depth [ $L$ ]

$D_{gr}$	=	representative grain-size diameter of gravel fraction [L]
$D_i$	=	bed (pavement) sample diameter of the $i^{th}$ percentile [L]; grain diameter of percentile $i$ [L]
$D_p$	=	pool depth [L]
$D_{sa}$	=	representative grain-size diameter of sand fraction [L]
$e_1 - e_6$	=	hydraulic geometry exponents [-]
$F_{Bed}$	=	annual percent fraction of year where critical shear of bed material is exceeded [-]
$F_{Bed50}$	=	annual percent fraction of year where critical shear of the $D_{50}$ bed-material size is exceeded [-]
$F_{Bed84}$	=	annual percent fraction of year where critical shear of the $D_{84}$ bed-material size is exceeded [-]
$F_{Bk}$	=	annual percent fraction of year where critical shear of band material is exceeded [-]
$F_i$	=	grain-size fraction $i$ of either sand or gravel [-]
$F_r$	=	Froude number [-]
$F_s$	=	surface sand content [-]
$g$	=	gravitational acceleration [L/T <sup>2</sup> ]
$gr$	=	transport function gravel fraction [-]
$G$	=	specific gravity [-]
$H_{LP}$	=	riffle crest to pool invert vertical height [L]
$H_{LR}$	=	change in vertical elevation from upstream to downstream limit of a riffle [L]

$H_R$	=	change in elevation of a riffle [L]
$H_{RP}$	=	vertical height from riffle (or step) crest to downstream pool invert [L]
$L_{IP}$	=	horizontal distance between adjacent pool inverts [L]
$\bar{L}_{IP}$	=	average horizontal distance between adjacent pool inverts [L]
$L_{LP}$	=	horizontal length of crest of riffle to pool invert (measured along centre line) [L]
$L_R$	=	riffle length [L]
$\bar{L}_R$	=	reach average riffle length [L]
$L_{RP}$	=	length from riffle (or step) crest to downstream pool invert [L]
$L_{\square}$	=	particle travel distance [L]
$n$	=	Manning's roughness coefficient [ $T/L^{1/3}$ ]
$N_C$	=	observed number of annual discharge events exceeding critical discharge [-]
$N_e$	=	number of observed events [-]
$P$	=	discharge wetted perimeter [L]
$\hat{P}$	=	specific stream power [ $M/L^2T^2$ ]
$q_{bi}$	=	volumetric bed-load transport per unit width [ $L^3/T$ ]
$q_{bj,i}$	=	volumetric transport rate per unit width of grain size $i$ [ $L^3/T$ ]
$Q$	=	discharge [ $L^3/T$ ]
$\bar{Q}$	=	mean annual discharge [ $L^3/T$ ]
$\hat{Q}$	=	dimensionless bankfull discharge [-]
$Q^+$	=	increased discharge [ $L^3/T$ ]
$Q_s^+$	=	increased bed-material load fraction [ $M/T$ ]

$Q_s^-$	=	decreased bed-material load fraction [M/T]
$Q_2$	=	2-year return discharge [ $L^3/T$ ]
$Q_5$	=	5-year return discharge [ $L^3/T$ ]
$Q_{10}$	=	10-year return discharge [ $L^3/T$ ]
$Q_{100}$	=	100-year return period discharge [ $L^3/T$ ]
$Q_{Bed}$	=	instantaneous bed-material transport rate [M/T]
$Q_{bf}$	=	bankfull discharge [ $L^3/T$ ]
$Q_C$	=	critical discharge [ $L^3/T$ ]
$Q_{C50}$	=	discharge exceeding critical shear stress of the $D_{50}$ grain size [ $L^3/T$ ]
$Q_{C84}$	=	discharge exceeding critical shear stress of the $D_{84}$ grain size [ $L^3/T$ ]
$Q_{eff}$	=	effective discharge [ $L^3/T$ ]
$Q_i$	=	observed instantaneous time-series discharge [ $L^3/T$ ]
$Q_{ma}$	=	mean annual flood peak discharge [ $L^3/T$ ]
$Q_{min}$	=	minimum annual discharge [ $L^3/T$ ]
$Q_T$	=	percent bed-material load [-]
$Q_X$	=	discharge of return frequency X [ $L^3/T$ ]
$R_C$	=	meander radius of curvature [L]
$\bar{R}_C$	=	reach average radius of curvature [L]
$R_h$	=	hydraulic radius [L]
$Re_{pi}$	=	particle Reynolds number [-]
$sa$	=	transport function sand fraction [-]
$S_f$	=	channel friction slope [-]
$S_o$	=	channel bed slope [-]

$\bar{S}_R$	= reach average riffle slope [-]
$T$	= temperature [-]
$T_{abf}$	= annual duration of flow exclusively exceeding bankfull discharge [T]
$T_{ae}$	= sum of annual duration of all events where bankfull discharge has been exceeded [T]
$T_{bf}$	= event duration exclusively exceeding bankfull discharge [T]
$T_C$	= cumulative annual duration of flows exceeding critical discharge [T]
$T_e$	= event duration [T]
$u^*$	= shear velocity [L/T]
$\bar{V}$	= average discharge velocity [L/T]
$V_{abf}$	= sum of annual volume of flow exclusively exceeding bankfull discharge [L <sup>3</sup> ]
$V_{ae}$	= sum of annual volume of all events where bankfull discharge has been exceeded [L <sup>3</sup> ]
$V_{bf}$	= event volume exclusively exceeding bankfull discharge [L <sup>3</sup> ]
$V_e$	= event volume [L <sup>3</sup> ]
$V_{mc}$	= main channel discharge velocity [L/T]
$V_{tot}$	= total annual discharge volume [L <sup>3</sup> ]
$W$	= discharge top width [L]
$\hat{W}$	= dimensionless bankfull width [-]
$W_{bf}$	= bankfull width [L]
$\bar{W}_{bf}$	= average bankfull width [L]
$W_{fp}$	= flood-prone width [L]



$W_i^*$  = dimensionless transport function [-]

$\hat{y}$  = dimensionless depth [-]

$Y_{\text{Bed}}$  = annual bed-load sediment yield [M]

$Z$  = tractive force ratio [-]

### **Greek Symbols**

$\alpha_s$  = bed-material rating curve coefficient [-]

$\beta$  = specific stream power [M/T<sup>3</sup>]

$\beta_H$  = hydraulic shear coefficient [-]

$\beta_s$  = bed-material rating curve exponent [-]

$\gamma$  = specific weight of water [M/L<sup>2</sup>S<sup>2</sup>]

$\gamma_s$  = specific weight of a solid [M/L<sup>2</sup>S<sup>2</sup>]

$\Gamma$  = meander belt width [-]

$\zeta$  = user specified lower bed-material transport threshold [L<sup>3</sup>/T]

$\lambda$  = meander wave length [L]

$\bar{\lambda}$  = average meander wave length [L]

$\nu$  = kinematic viscosity [L<sup>2</sup>/T]

$\rho$  = fluid density [M/L<sup>3</sup>]

$\sigma_T$  = total shear [M/LT<sup>2</sup>]

$\tau_b$  = channel bed shear stress [M/LT<sup>2</sup>]

$\tau_c$  = critical shear stress [M/LT<sup>2</sup>]

$\tau_{C50}$  = critical shear stress of the D<sub>50</sub> grain size [M/LT<sup>2</sup>]

$\tau_{C84}$  = critical shear stress of the D<sub>84</sub> grain size [M/LT<sup>2</sup>]

$\tau_{CB}$	= critical bank shear stress [M/LT <sup>2</sup> ]
$\tau_{Cgr}^*$	= critical shear stress of gravel fraction [M/LT <sup>2</sup> ]
$\tau_{Ci}^*$	= critical dimensionless Shields number [-]
$\tau_{CS}^*$	= critical shear stress of sand fraction [M/LT <sup>2</sup> ]
$\tau_i^*$	= dimensionless Shields shear stress associated with particle diameter i [-]
$\tau_o$	= shear stress [M/LT <sup>2</sup> ]
$\tau_{SCi}^*$	= critical dimensionless Shields number [-]
$\tau_{Si}^*$	= dimensionless Shields number [-]
$\phi$	= bank-slope angle [-]
$\phi'$	= dimensionless transport-function parameter [-]
$\psi$	= dimensionless transport function parameter [-]
$\omega_o$	= clear-water settling velocity [L/T]
$\bar{\omega}$	= width : depth ratio [-]
$\Omega$	= channel sinuosity [-]

### Units of Measure

(-)	no units
°C	degree(s) Celsius
kg/s	kilogram(s) per second
km	kilometer(s)
km <sup>2</sup>	square kilometer(s)
m	meter(s)
m/m	meter(s) per meter

m/s	meter(s) per second
m/year	meter(s) per year
m <sup>2</sup> /s	square meter(s) per second
m <sup>3</sup>	cubic meter(s)
m <sup>3</sup> /hour	cubic meter(s) per hour
m <sup>3</sup> /s	cubic meter(s) per second
mg/L	milligram(s) per liter
mm	millimeter(s)
N/m <sup>2</sup>	Newton per square meter
Pa	Pascal
%	percent
W/m <sup>2</sup>	Watt per square meter
yr(s)	year(s)

### **Abbreviations**

ASCE	American Society of Civil Engineers
ANOVA	ANalysis Of VAriances
DEMs	digital elevation models
GIS	geographic information system
GPS	global positioning system
FISRWG	Federal Interagency Stream Restoration Working Group
H:V	Horizontal:Vertical
HEC-RAS	Hydrologic Engineering Centers River Analysis System
ID	identification

NCD	natural channel design
No.	number
NRC	National Research Council
OMNR	Ontario Ministry of Natural Resources
RFID	radio frequency identification
SIBs	standard iron bars
USACE	U. S. Army Corps of Engineers
USDAFS	U. S. Department of Agriculture Forest Service
USGS	U. S. Geological Survey

# **CHAPTER 1**

## **INTRODUCTION**

Sedimentary deposition has been occurring over the planet for approximately 4.2 billion years from fluvial, mechanical, and aeolian erosion of sub-aerial crustal regions (Froude *et al.*, 1983). Over this time period, fluvial processes have played a significant role in molding Earth's landscapes and river valleys. During the geologic evolutionary time scale, river networks experience erosional cycles (Davis, 1899; Leliavsky, 1955; Leopold *et al.*, 1964; Schumm 1969, 1977; Schumm *et al.*, 1984). The cycles are typified by long durations (hundreds to hundreds of thousands of years) of quiescent evolution whereby bed- and bank-erosion rates are relatively low with the surrounding geology, sediment supply, flow regime, vegetative communities, and land use for a given catchment area (Lane, 1955). Long durations of quiescent evolution are interrupted by abrupt incursions upon the landscape (i.e., changes in slope, land use, flow regime, or sediment regime), which result in relatively rapid rates (decades to hundreds of years) of channel degradation.

Recently human-kind, in the geologic time scale, has had profound effects upon Earth's landscapes. Anthropogenic manipulations of upland regions for agricultural, resource, transportation, and occupational exploits have resulted in rivers responding to the land-use stressors (Wohl, 2000). In attempts to mitigate channel change, humans

have imposed a litany of channel works to counter geologic evolution including: conversions of watercourses into storm-sewer networks and floodways, hardening of channel beds and banks to mitigate stream-channel erosion (which may include materials such as concrete, riprap, gabion baskets, etc.), introduction of grade-control structures, construction of reservoirs, storm-water management facilities, and bio-engineering. Concomitantly, these measures have often resulted in the decline of riparian corridor diversity and aquatic health (e.g., Leopold (1949), Booth and Jackson (1997), Paul and Meyer (2001), Morley and Karr (2002), Booth *et al.* (2004), and Freeman and Schorr (2004)).

In the past 25 years, there has been an evolving intellectual and resource-management shift towards restoring or rehabilitating many degraded river systems throughout the world (e.g., Federal Interagency Stream Restoration Working Group (FISRWG, 1998), Shields *et al.* (2003), and Bernhardt *et al.* (2005)); which is also commonly referred to as natural channel design (NCD). These initiatives have been motivated by attempting to increase the bio-diversity of riparian corridors, reducing infrastructure maintenance costs, reducing sediment loadings to river networks, and improving water quality, amongst other initiatives (FISRWG, 1998). Objectives of this approach are to: develop stable dimensions, patterns, and profile forms for the given watercourse, floodplain, valley form, and geology; maintain sediment continuity; maintain geo-technical slope stability; reduce risk of flooding; and provide a thriving ecological community (e.g., Imhof *et al.* (1996), FISRWG (1998), and Shields *et al.* (2003)). From a river mechanics perspective the NCD approach is to develop a river channel in a state of quasi-equilibrium. Quasi-equilibrium is here defined as a channel

that maintains both discharge and sediment continuity throughout the entire flow regime, while maintaining relations amongst discharge, velocity, width, depth, slope, and roughness (Langbein and Leopold, 1964). The relations do not imply static conditions; rather, the channel adjusts with time, while maintaining hydraulic geometry relations unique to the given geology, valley configuration, climate, vegetative communities, and land use.

One category of land usage that has garnered particular attention in NCD has been urban or urbanizing assemblages. Although it is not entirely certain whether urban watersheds experience greater net amounts of river degradation relative to rural or wildland settings over evolutionary time scales, their rates of channel change, increased maintenance costs, and changes in ecology at the human time-scale are perceived to be of higher importance. Simply, these are the areas where large percentages of the Earth's populations reside focusing attention towards these regions.

Considerable research over the past half century has focused on the degradational effects from urbanization on stream channels (e.g., Carter (1961), Wolman (1967), Leopold (1968), Hollis (1975), Packman (1979), Whipple *et al.* (1981), Dyhouse (1982), Booth (1990, 1991), MacRae and Rowney (1992), Henshaw and Booth (2000), MacRae (1997), Doll *et al.* (2002), Bledsoe and Watson (2001), Konrad *et al.* (2005), and Jordan *et al.* (2009)). However, there is a dearth of studies on the quasi-equilibrium characteristics of urban-stream channels (if they exist) which could strengthen our understanding of urban-stream systems and possibly lead to improved designs. Most NCDs in urban regions have therefore relied upon the hydraulic and morphologic relationships derived from rural or wildland watersheds (e.g., Leopold *et al.* (1964), Bray

(1972), Andrews (1984), Hicks and Mason (1991), and Annable (1996a,b)) to proffer design plans, assuming that the quasi-equilibrium conditions in rural and urban land-use areas are transferable.

If the conditions unique to urban watersheds are not fully realized and design tools employed that are inconsistent with the urban state (i.e., considerations in the changes in overland flow routing, sediment supply and transport, channel evolution, etc.), an intended positive NCD may fail and initiate a further rapid rate of channel degradation that was not anticipated (e.g., Alexander, 1999). Further, if the processes unique to urban streams are not sufficiently quantified and NCD projects continue to employ observations and theory that many not be entirely applicable to the land-use condition, the liability and cost of undertaking NCD projects and ensuing maintenance may become prohibitive.

## **1.1 OBJECTIVES**

At the conclusion of a research project by Annable (1996a,b) investigating the quasi-equilibrium morphologic, hydraulic, and sedimentological relationships of rural rivers in southern Ontario, Canada, several researchers and practitioners identified limitations in the data set when applied to urban or urbanizing stream channels. At that time and to present, most stream-restoration projects in the region have been focused towards urban or urbanizing watersheds where erosion control and the preservation of aquatic ecosystems have been of paramount consideration. Researchers and practitioners have been concerned with how transferable the practice of NCD is to urban regions (relative to rural or wildland settings), and if there are differences in the external



variables of urban watersheds (e.g., flow and sediment) that require different knowledge sets to culminate in successful urban-stream restoration designs.

The objective of this work is, therefore, fundamental in approach: it is to determine if quasi-equilibrium urban-stream channels exist. If such reaches exist, study their hydrologic, sedimentological, and geomorphic characteristics. Further, compare the urban-stream reaches to rural reaches identified to be in a state of quasi-equilibrium characteristics in the same hydrophysiographic region. The objectives of this research are as follows:

- canvas gauged urban or urbanizing watersheds within southern Ontario and determine if river reaches close to gauge stations (where continuity of flow can be assumed) exhibit a state of quasi-equilibrium either by maintaining previous channel form or adapting to the change in land-use conditions,
- where reaches are identified to be in a state of quasi-equilibrium, collect river data over a multi-year period to characterize the hydraulic, geomorphologic, and sedimentological conditions of each reach, and
- compare the characteristics of urban and rural streams identified to be in a state of quasi-equilibrium of the same hydrophysiographic region and identify their principal similarities and differences. Finally, identify conditions distinct to urban-stream stability.

## **1.2 DISSERTATION ORGANIZATION**

This dissertation follows the multi-part dissertation format whereby Chapters 2, 3, and 4 are organized into three distinct topics with respective introductions, methods,

observations, analyses, discussions, and summaries (manuscript format). Chapter 5 presents the general conclusions that were made during the multi-year research study. Recommendations are also offered which suggest future research avenues to pursue in complementary or contrasting avenues.

## **CHAPTER 2**

# **QUASI-EQUILIBRIUM CONDITIONS OF GRAVEL-BED URBAN-STREAM CHANNELS**

### **2.1 INTRODUCTION**

Fluvial responses to changes in watershed topography, hydrology, and sediment supply have been well studied over the past century (Davis, 1899; Leliavsky, 1955; Leopold *et al.*, 1964; Graf, 1984; Schumm *et al.*, 1984; Chang, 1988; Julien, 2002). Investigations of stream responses to urban land-use change have been more prominent since the 1960s, beginning with comparatively small watersheds where changes in hydrology and sediment delivery were identified as the principal agents of channel change (Carter, 1961; Wolman, 1967; Leopold, 1968; Hollis, 1975; Packman, 1979; Whipple *et al.*, 1981; Dyhouse, 1982). More recent studies have investigated channel responses to urbanization in larger watersheds and have also proffered strategies for mitigating the upland flow regime to minimize or reverse the impacts of channel degradation (MacRae, 1997; Booth, 1990, 1991; MacRae and Rowney, 1992; Henshaw and Booth, 2000; Doll *et al.*, 2002; Bledsoe and Watson, 2001; Konrad *et al.*, 2005; Jordan *et al.*, 2009).

A common aim in urban-stream restoration has been to maintain or return a channel to its historical (post-colonization) fluvial alignment and function rather than allowing it to evolve to a new state of quasi-equilibrium (Langbein and Leopold, 1964) that is based upon the new urban flow and sedimentological regimes. This approach is reinforced where there is existing infrastructure that may be compromised by new patterns of channel evolution, floodplain encroachment and occupation, and alterations to riparian corridor habitat and management (Brookes, 1988; Hey, 1997). However, restoration to the pre-disturbance conditions may not be achievable or may require long-term maintenance because contemporary land use has imposed a different set of irreversible controlling conditions (Kondolf and Downs, 1996).

Henshaw and Booth (2000) argue that the management of urban watercourses should not consider only maintaining or restoring a channel to its historical condition but should also explore rehabilitation alternatives that are in balance with a watershed's likely future steady-state conditions of hydrology and sediment transport. Consequently, a watercourse rehabilitated to quasi-equilibrium conditions in an urbanized watershed may have a different channel morphology and/or alignment than in its historical (post-colonization) state. However, how to determine what the quasi-equilibrium characteristics of urban watercourses are or will be has remained elusive because most previous studies have investigated the riverine degradational effects from urbanization rather than those of any new conditions of stability. Concordantly, urbanizing watersheds are in a relatively rapid rate of land-use change, while there is a dearth of studies identifying reaches that have maintained channel stability (if such exist) that could add to our understanding of urban channel stability.

In the absence of specific information on the quasi-equilibrium characteristics in urban watercourses, many researchers and practitioners rely upon the established quasi-equilibrium characteristics of rural watercourses being transferable to urban-stream settings. Data sets and relationships developed by Leopold and Wolman (1960), Kellerhals *et al.* (1972), Andrews (1980, 1984), Bray (1972), Williams (1986), Hicks and Mason (1991), Annable (1996a), Parker *et al.* (2007), and others are often employed to assist in assessing riverine urban impacts and used to develop urban-stream rehabilitation designs. However, these studies were conducted in rural or wilderness settings. It is by no means apparent how transferable such observations are to the altered flow and sedimentological regimes of urbanizing watersheds.

Some outstanding questions in regards to urban-stream channels are: 1) Do quasi-equilibrium river reaches exist within watersheds subjected to significant urbanization? 2) If so, what are their specific characteristics, and how do they compare to rural or wilderness settings in the same hydrophysiographic region? 3) Are there central tendencies common to both urban and rural fluvial processes that can be prescribed to mitigate the adverse effects of urbanization? These questions are the basis of the current study.

## **2.2 METHODS**

Twelve gravel-bed stream reaches in urban and urbanizing watersheds were measured and monitored over a 15-year period in areas of southern Ontario, Canada, underlain by unconsolidated Pleistocene deposits (i.e., not within the Canadian Shield or

areas of other resistant bedrock control, in order to avoid the complexities of bedrock channels).

### **2.2.1 Study Area and Site Selection**

The urban watercourse selection was limited to reaches where there were hydrometric gauging stations providing reliable long-term systematic hydrology records. One-hundred-sixty-eight river reaches were screened (Figure 2.1a). Reach lengths were initially limited to segments where there were no major storm-sewer outfalls or tributary confluences so that continuity of flow, relative to the gauge station location, could be assumed. Sites were eliminated that were dominantly rural, wilderness, or had flood-control structures close to the gauge stations. More sites were eliminated where aerial reconnaissance and morphometric analysis (Brice, 1973; Richard, 2001) showed that the planform geometry had significantly varied (compared to rural counterparts in similar geology) over the period of photographic record (typically a 50- to 70-year record). The remaining watercourses were inspected in the field reconnaissance and eliminated if observable down cutting had occurred or where major in-stream channel works existed.

The cull resulted in twelve urban-stream reaches (Figure 2.1b) that were subjected to detailed field studies. Within each of their watersheds, some channel degradation had occurred upstream or downstream of the study reaches. The presence of degraded channel reaches nearby helps to identify those portions in each watershed that are adjusting to changes resulting from urbanization. We, therefore, assume that the quasi-equilibrium conditions which exist within each of the detailed study reaches, either by

maintaining historical channel form or by means of short- to intermediate-term time adjustments, exhibit intrinsic reach characteristics of channel stability.

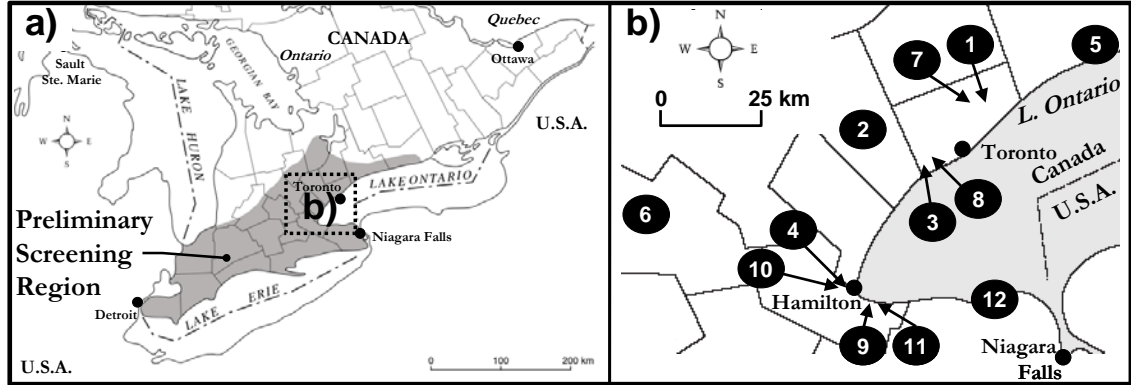


**Figure 2.1.** Site location map: a) screening area, and b) site location references.

## 2.2.2 Site Conditions

All of the urban reaches are gravel-bed stream channels, based upon the median grain size ( $D_{50}$ ) of a log-normal bed-material sampling distribution exceeding 2 mm. Each reach ranged in length between  $52 \leq W_{bf} \leq 77$ , where  $W_{bf}$  is defined as the average bankfull channel width. Eleven of the study sites have riffle-pool dominated channel morphologies (O’Neil and Abrahams, 1984; Montgomery and Buffington, 1997) and there is one run-pool dominated morphology (Table 2.1). The run-pool morphology defined here is consistent with the plane-bed definition offered by Montgomery and Buffington (1997) but it has been labeled differently to avoid confusion with the kind of plane-bed form associated with a particular flow regime in sand-bed channels (Simons and Richardson, 1963).

**Table 2.1.** General urban reach characteristics

Site Reference No.	Gauge†	Station Name	Effective Catchment Area (km <sup>2</sup> )	Urban Land Use (%)	Channel Morphology	Cross-section Relief	Adjacent Land Use
1	02HC005	Don River at York Mills	95.5	72	Riffle-pool	Semi-confined	Golf course
2	02HC017	Etobicoke Creek at Brampton	67.7	24	Riffle-pool	Floodplain dominated	Park
3	02HC030	Etobicoke Creek below QEW	215.4	62	Riffle-pool	Floodplain dominated	Park
4	02HB012	Grindstone Creek near Aldershot	83.9	13	Riffle-pool	Floodplain dominated	Park
5	02HD013	Harmony Creek at Oshawa	43.0	44	Riffle-pool	Floodplain dominated	Golf course
6	02GA024	Laurel Creek at Waterloo	57.5	34	Riffle-pool	Floodplain dominated	Park
7	02HC029	Little Don River at Don Mills	135.1	70	Riffle-pool	Floodplain dominated	Park
8	02HC033	Mimico Creek at Islington	73.8	87	Riffle-pool	Floodplain dominated	Park
9	02HA014	Redhill Creek at Hamilton	56.3	66	Riffle-pool	Floodplain dominated	Park
10	02HB007	Spencer Creek at Dundas	156.0	9	Run-pool	Semi-confined	Urban
11	02HA022	Stoney Creek at Stoney Creek	19.2	15	Riffle-pool	Floodplain dominated	Park
12	02HA027	Walker Creek at St. Catharines	5.9	99	Riffle-pool	Floodplain dominated	Park

Note: † Environment Canada Operated Gauge Stations and associated site designations.

With the exception of Sites 1 and 10, the cross-sectional relief was floodplain dominated (i.e., an unconfined floodplain). Site 1 is semi-confined to a flow depth twice bankfull depth ( $D_{bf}$ ) before there is overflow onto the floodplain. At Site 10 there is a semi-confined cross section consistent with run-pool channel morphology. Cross-sectional confinement was defined as the ratio of the channel top width ( $W_{fp}$ ) at a discharge twice bankfull depth divided by the top width associated with bankfull discharge (Rosgen, 1996). Where  $W_{fp}/W_{bf} > 2.2$ , the channel is categorized as floodplain dominated or unconfined, and where  $1.4 < W_{fp}/W_{bf} < 2.2$  the channel is considered to be semi-confined with limited floodplain access.

Digital elevation models (DEMs) at 5.0-m contour intervals were used to determine the topographic catchment area ( $A_d$ ) upstream of each hydrometric monitoring



station. The storm-sewer network, combined sewer network, and as-built infrastructure data within the topographic catchment limits were collated in a geographical information system (GIS) to determine the effective catchment area ( $A_{\text{eff}}$ ) upstream of each hydrometric station. Effective catchment area may differ from the topographic catchment area (Leopold, 1968; Booth *et al.*, 2004; Jordan *et al.*, 2009). Values of  $A_{\text{eff}}/A_d$  less than unity define a reduction in the total catchment area because some precipitation falling within the limits of  $A_d$  is routed to different catchments via drainage alterations or sewer networks. Values of  $A_{\text{eff}}/A_d$  greater than unity identify the opposite effect in basin alterations. In this study, the topographic and effective catchment areas did not vary significantly from unity ( $0.96 \leq A_{\text{eff}}/A_d \leq 1.07$ ) but it may be noted that the  $A_{\text{eff}}/A_d$  deviations did increase with decreasing watershed area.

Digital land-use classification mapping from the Ontario Ministry of Natural Resources (OMNR, 2006) differentiating ninety-nine different land-use types was used to determine the types and areal extent of urban land-use assemblages in each watershed. Anthropogenic alterations to the hydrology, hydraulic routing, and sediment supply were included in the urban land-use delineations, including roads (plus any curbs and gutters), parking lots, roof tops, turf, recreation areas, residential lands, commercial lands, and industrial lands: these were assigned to three land-use categories 1) built-up impervious, 2) built-up pervious, and 3) transportation. Their surface areas were summed within each effective catchment area to determine the urban upland catchment area ( $A_U$ ). The percent urban land use was calculated as  $(A_U/A_{\text{eff}}) \times 100$ . Figure 2.2 illustrates the spatial distribution of urban land use within each of the effective catchment areas. Only urban land-use assemblages are illustrated.

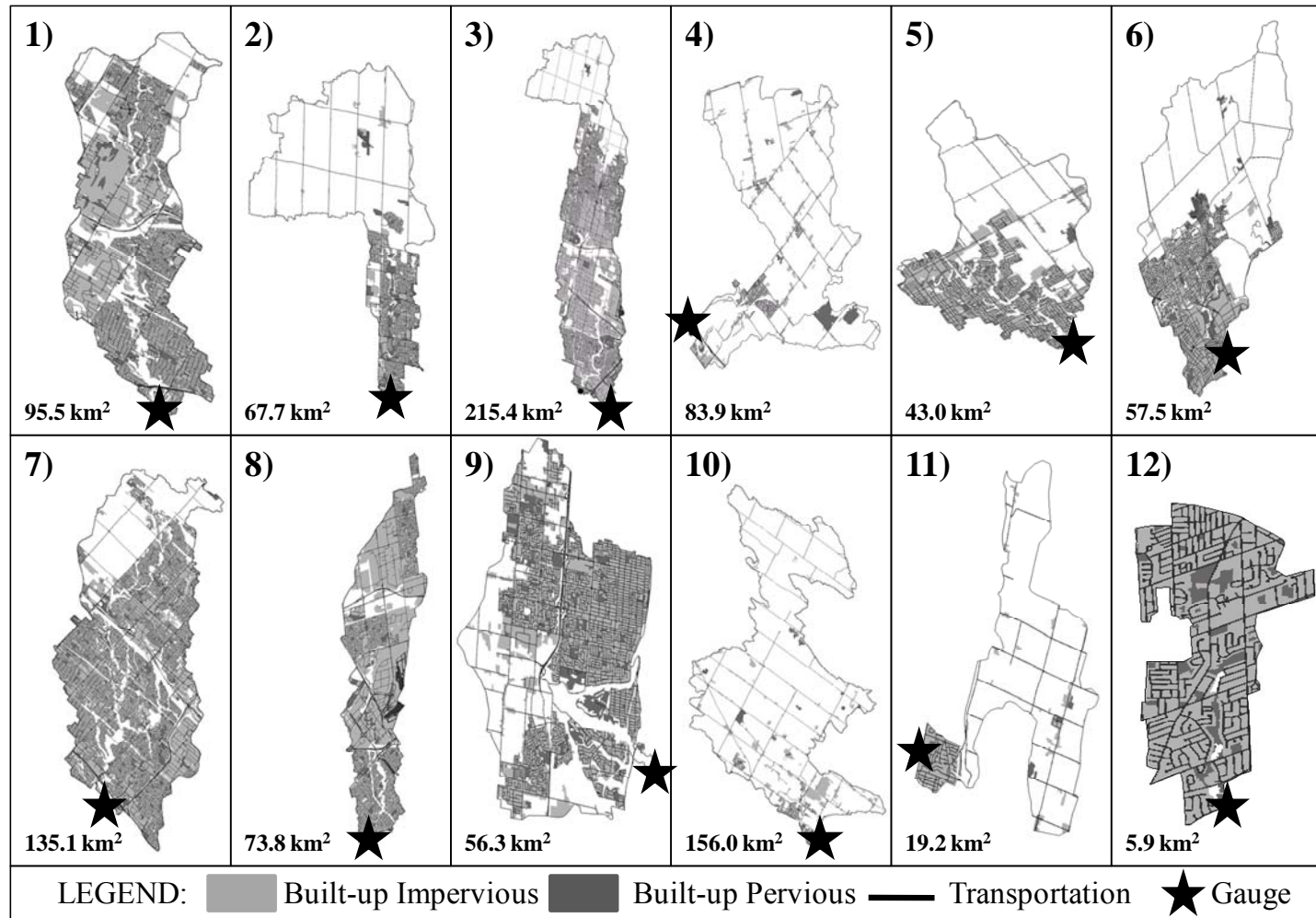


**Figure 2.2.** Urban land-use assemblages within effective catchment areas.

As shown in Table 2.1, the urban watersheds ranged between 5.9 km<sup>2</sup> and 215.4 km<sup>2</sup> in area and urban land use ranged between 9% and 99%. A set of rural gravel-bed streams studied previously by Annable (1996a) of a similar magnitude (32.3 km<sup>2</sup> to 528 km<sup>2</sup>) offer a good comparison. The urban land use varied between 1.1% and 18.3% in these watersheds. There is overlap of percent urban land use in seven of the study reaches. In the rural watersheds, however, the urban land use was dispersed throughout the watersheds such that changes in overland flow routing created by urbanization, roads, etc. were buffered by interconnecting riparian corridor reaches. Conversely, in the urban reaches, urban land use is intense proximal to the hydrometric monitoring stations where the effects of changes in urban hydrology are measured. The overlap also provides a means of investigating divergence in the frequencies of bankfull discharge in rural versus urban watersheds, as is discussed in subsequent sections.

Where there are floodplains, the land use immediately adjacent to each urban watercourse was either park land or golf courses, with the exception of Site 10 which was surrounded by urban development (residential and light industrial). The riparian corridor along each reach had a relatively dense under-story and over-story of vegetation. Vegetation densities were similar to those observed by Annable (1996a) in the rural streams in the same humid hydrophysiographic region. No significant undercut banks were observed in any of the study reaches, and the dominant plant rooting depths typically extended to the bed of the channel in most cases. It is noted that in the case of Site 12 (the smallest effective catchment area), both sides of the 3.8-m wide creek were bordered by large willow trees which significantly enhanced channel stability.

The majority of the channels are in glacial till of the Halton Clay Plain (Karrow, 1991), which underlies their banks and lower beds (below active scour depth). At Sites 3 and 9, the bankfull channels are under-fits that flow within larger glacial spillway entrenchments that have shale valley walls which outcrop intermittently along the study lengths. Site 6 is dominated by glacial fluvial deposits with fine-grained consolidated silty sandy clay levee and till deposits comprising the contemporary floodplain. All of the study sites are considered to be semi-alluvial in character, resulting from the brief 10,000-year post-Wisconsinan Glaciation period during which the stream channels are considered to be in a continuing state of evolution (Campo and Desloges, 1994; Ashmore and Church, 2001).

### **2.2.3 Channel and Hydraulic Geometry**

Longitudinal profiles were surveyed along each reach using a total station and geo-referenced using a 1<sup>st</sup>-order differential global positioning system (GPS). Fluvial features mapped included: channel thalweg, bankfull stage at the top of the convex (inside) bend on point bars and along the upper third of riffles, the crests and bottoms of riffles and runs, pool invert, terraces, and any other notable changes in channel bed slope or geomorphic features. Bed slope ( $S_o$ ) was determined from the difference in riffle crest elevations between the upper- and lower-most surveyed riffles along the measured bankfull channel centre line.

A series of cross sections were surveyed within the upper third of each riffle or run to characterize their relief, and referenced to the geodetic system. Approximately thirty to forty discrete points were surveyed at each cross section, including a discrete

point at every even meter interval within the bankfull channel limits, the top and bottom of channel banks, the thalweg, bankfull stage and terrace elevations, floodplain features, and any other observable change in slope. Parameters determined from each cross section included: bankfull width ( $W_{bf}$ ), bankfull depth ( $D_{bf}$ ), bank-slope angles ( $\alpha$ ), and flood-prone width ( $W_{fp}$ ). Permanent benchmarks were installed at cross sections on the upper third of riffles or runs to be used for long-term erosion monitoring surveys. Additional cross sections were acquired at infrastructure installations, consistent with the parameterization requirements of Hydrologic Engineering Centers River Analysis System (HEC-RAS) 4b (U.S. Army Corps of Engineers (USACE), 2004) to develop one-dimensional hydraulic models of each study reach.

To examine potential sampling bias in the current study and that of Annable (1996a), bankfull hydraulic geometry was compared to a larger data set of gravel-bed channels from North America and Europe (Parker and Anderson, 1977; Parker *et al.*, 2007). Parker *et al.* (2007) offered dimensionless bankfull cross-sectional geometry relationships of the form:

$$\hat{W} = 4.87 \hat{Q}^{0.461}, \hat{D} = 0.368 \hat{Q}^{0.405}, S_o = 0.0976 \hat{Q}^{-0.341} \quad (2.1 \text{ a – c})$$

where dimensionless bankfull discharge ( $\hat{Q}$ ), dimensionless bankfull width ( $\hat{W}$ ), and dimensionless bankfull depth ( $\hat{D}$ ) are expressed as:

$$\hat{Q} = \frac{Q_{bf}}{\sqrt{g} D_{50} D_{50}^2}, \hat{W} = \frac{W_{bf}}{D_{50}}, \hat{D} = \frac{D_{bf}}{D_{50}} \quad (2.2 \text{ a – c})$$

respectively, where  $Q_{bf}$  is the bankfull discharge and  $g$  is gravitational acceleration.

Archived Environment Canada gauge station field records of measured flow top width (W), average flow depth (D), discharge cross-sectional area (A), and average channel velocity ( $\bar{V}$ ) were collated for each urban stream to produce at-a-station hydraulic geometry relationships (Leopold and Wolman, 1960) as a function of calculated discharge (Q), in the general form:

$$W = c_1 Q^{e_1}, D = c_2 Q^{e_2}, A = c_3 Q^{e_3}, \bar{V} = c_4 Q^{e_4} \quad (2.3 \text{ a - d})$$

where  $c_1 - c_4$  and  $e_1 - e_4$  are power-function coefficients and exponents, respectively, of the best fit for each relationship. The hydraulic geometry relationships were developed in a similar fashion for rural gauge stations in the study by Annable (1996a).

The urban gauge stations were often located close to bridges for ease of sampling during high-flow events. This results in hydraulic geometry reflective of the infrastructure (confined cross sections) rather than a natural cross-sectional form. To examine at-a-station hydraulic geometry of the natural channel morphology, one-dimensional HEC-RAS models were developed from the field survey data for each reach and calibrated to the hydraulic geometry of the gauge stations (Equation (2.3)). The natural at-a-station hydraulic geometry relationships were developed for locations where cross sections were surveyed in the field at the upper third of riffles or runs, and in addition, where bed-load sampling occurred (discussed in subsequent sections). The relationships were of the general form:

$$W = \text{fn}(Q), D = \text{fn}(Q), \bar{V} = \text{fn}(Q), V_{mc} = \text{fn}(Q), R_h = \text{fn}(Q) \quad (2.4 \text{ a - e})$$

where  $V_{mc}$  is the main channel velocity,  $R_h$  is the hydraulic radius defined as  $R_h = A/P$  and  $P$  is the wetted perimeter of the channel. The relationships developed using Equation (2.4) were produced from one-hundred equally-distributed discharge simulations ranging between  $0 < Q \leq Q_{100}$ , where  $Q_{100}$  is the 100-year return period based on a Log Pearson III analysis (discussed below).

Reach-based channel roughness, used in the calibration of the one-dimensional models, was estimated employing the Wolman (1954) pebble-count method at a series of riffles, pools, and runs appropriate to each study site. Grain-size distribution results from each riffle were used to estimate the Manning's roughness coefficient ( $n$ ), employing Chow's (1959) form of the Strickler (1923) equation as defined by  $n = 0.0417 D_{50P}^{1/6}$ , where  $D_{50P}$  is defined as the log-normal median grain size of the pebble-count grain-size distribution.

## 2.2.4 Hydrology

Bankfull discharge ( $Q_{bf}$ ) was field-verified during flood events at each reach and the timing reconciled with the instantaneous discharge ( $Q_i$ ) at each urban gauge station. Bankfull discharge was defined for riffle-pool dominated morphologies as the stage on the convex arc (inside) of bends where water just begins to flow onto the floodplain (Wolman and Leopold, 1957). In the case of a run-pool dominated morphology, bankfull stage was identified as the stage where the ratio of the flowing top width ( $W$ ) to average channel depth ( $D$ ) is a minimum (Wolman, 1955).

Annual yearly maximum instantaneous discharge records for both urban and rural gauge stations were used to determine the return frequency of bankfull discharge at each

study reach. The annual flow-frequency analysis employed the Log-Pearson III method as outlined by U. S. Geological Survey (USGS) *Bulletin 17B* (1982). Given the potential event intensity and flashiness of urban-stream channels (Leopold, 1968; Hollis, 1975), all of the other hydrologic measures analyzed used systematic 15-minute interval discharge data observed at both urban and rural gauge stations. The available period of record (where 15-minute data were issued by Environment Canada) was 1969 to 2008 unless a shorter period of record was available.

The annual return frequency of bankfull discharge was also explicitly determined using the systematic time-series discharge records and enumerating the annual number of bankfull discharge (or greater) occurrences ( $N_e$ ). An event was included when  $Q_i \geq Q_{bf}$  on the rising limb of the hydrograph. The volume ( $V_e$ ) and duration ( $T_e$ ) of any event exceeding bankfull discharge was defined by the time-series limits when  $Q_i \geq \bar{Q}$  and  $Q_i < \bar{Q}$  for the rising and falling limbs of the hydrograph, respectively (Figure 2.3), where  $\bar{Q}$  is the mean annual discharge. A further condition stipulated that where two or more observations of  $Q_i$  traverse  $Q_{bf}$  on the rising or falling limbs of the hydrograph over a consecutive 3-day period, the multiple occurrences were considered a single event rather than multiple events. This constraint ensured that events associated with spring freshets and diurnal snow-melt fluctuations were not enumerated as multiple events but considered as a single discharge event. Conversely, there are frequent convective storms in the region, especially in the warmer months. Use of a minimum 3-day interval assumes that more than two independent convective storms producing independent bankfull events could occur within one week, with the proviso that the storms are separated by a 3-day interval. The constraint also stipulated that the discharge on the



falling limb of the hydrograph must cross the 25%  $Q_{bf}$  threshold in order for two events to be enumerated separately (Figure 2.3); otherwise the hydrographic response is considered a single event. The annual return frequency of bankfull discharge using observed storms was calculated as  $1/N_e$ .

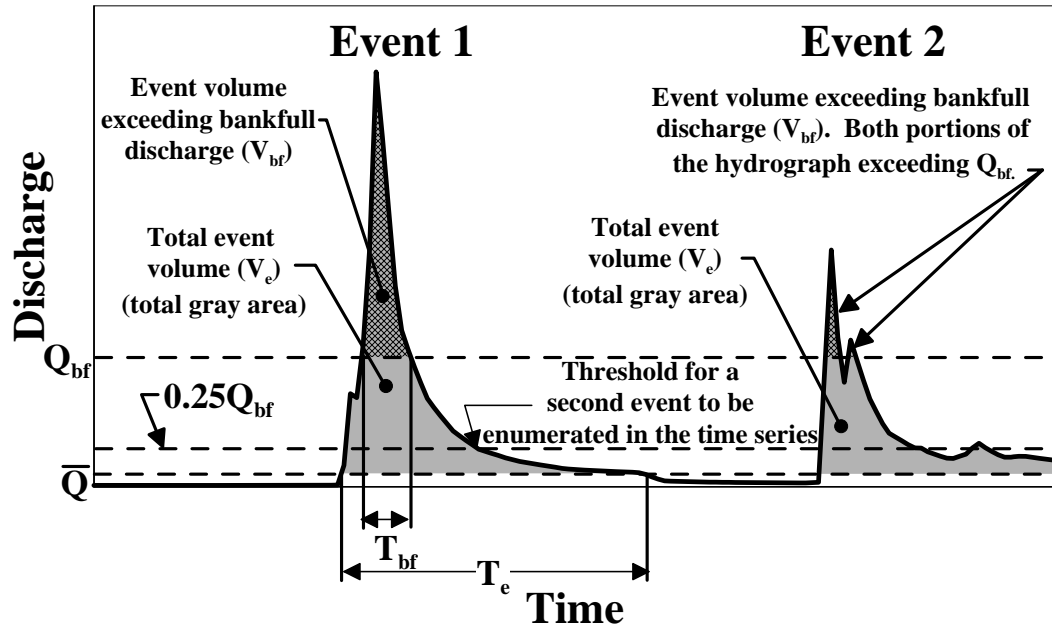


**Figure 2.3.** Event definition and threshold criteria.

The total annual discharge volume ( $V_{tot}$ ) from each effective catchment area was determined by the summation of the product of the instantaneous observed discharges and the 15-minute time interval over each entire year as  $V_{tot} = \sum_{i=1}^n Q_i \times 900$ . An event volume ( $V_e$ ) is defined as the cumulative discharge over the event duration ( $T_e$ ). Within the same event, the volume exceeding bankfull discharge ( $V_{bf}$ ) is defined as the cumulative discharge over the duration  $T_{bf}$  that exclusively equals or exceeds bankfull discharge (Figure 2.3). The annual volume ( $V_{ae}$ ) and duration ( $T_{ae}$ ) of events equaling or exceeding bankfull discharge is the annual sum of all  $V_e$  and  $T_e$  events, respectively.

Similarly, the annual volume ( $V_{abf}$ ) and duration ( $T_{abf}$ ) of flow exclusively exceeding bankfull discharge is the annual sum of all  $V_{bf}$  and  $T_{bf}$  events, respectively. Flood intensity is here defined as the largest annual event volume ( $V_e$ ) by the duration of that event ( $T_e$ ). The flashiness index is defined as the instantaneous maximum peak flow by the mean annual discharge in a given year.

### **2.2.5 Bed- and Bank-material Characteristics**

Bed-load transport measurements were not available from the rural study by Annable (1996a) and thus a direct comparison of bed-material transport capacity was not possible between the rural and urban study reaches. However, an urban versus rural comparison of bed-load transport characteristics was considered of particular relevance in evaluating the quasi-equilibrium stability characteristics unique to the urban-stream reaches. Specifically, to identify if there were any significant differences in bed-load transport characteristics derived from the change in urban hydrology.

Bed-material (pavement) and substrate (sub-pavement) samples were collected in the rural study by Annable (1996a) and were, therefore, sampled in a similar fashion here to evaluate bed-material transport characteristics in both the urban and rural study reaches. Bed-material and substrate sampling was undertaken on riffles and runs in the urban streams following the methods of Klingeman and Emmett (1982), Church *et al.* (1987), Annable (1996b), and Bunte and Abt (2001). Four to six random locations (depending on channel width) were sampled on each individual riffle or run. A serrated drum was worked into the bed of the channel with a 0.0625-mm mesh bag (Helley-Smith bed-load sampling bag) capturing flow out of an orifice on the downstream side of the

drum to ensure that all fines were captured in the excavation process. Bed samples were excavated to a depth of the largest particle size found within the drum and substrate samples were excavated to the same depth below the bed sample. Drum sizing was consistent with the recommendations of Church *et al.* (1987) and Annable (1996b) to ensure that the drum was sufficiently large to avoid bias from the mass of one or a few larger particles. Approximately eighteen to twenty-four bed samples and the same number of substrate samples were collected from each urban study site. Bed-material, substrate, and bed-load (discussed below) samples were subjected to grain-size analysis using dry sieving methods at 0.5-phi intervals (Friedman and Sanders, 1978), producing log-normal distributions. Composite reach-based grain-size distributions were determined for bed material and substrate for each reach.

As all of the urban study reaches had gravel-bed or larger average grain sizes, three sediment-transport equations were employed to evaluate transport capacity, using the at-a-station hydraulic geometry relationships of Equation (2.3) for the urban and rural study reaches. The one-dimensional model calibrated at-a-station hydraulic geometry relationships of Equation (2.4) could not be used because calibrated one-dimensional models had not been used in the earlier study of the rural watercourses (Annable, 1996a). The modified form of the Meyer-Peter Müller equation offered by Wong and Parker (2006), Einstein-Brown equation (Brown, 1950), and the Wilcock and Kenworthy (2002) were employed to evaluate the characteristics of bed-material transport. Substrate grain sizes were used in the evaluation of bed-material transport because they are found to be consistent with the grain sizes associated with bed-load transport in mostly mobile bed-material layers (Parker *et al.*, 2007).

The modified form of the Meyer-Peter Müller equation is defined for the volumetric bed-load transport ( $W_i^*$ ) per unit width ( $q_{bi}$ ) as (Wong and Parker, 2006):

$$W_i^* = \frac{q_{bi}}{\sqrt{(G-1)gD_i^3}} , W_i^* = 4.93(\tau_i^* - \tau_{SCi}^*)^{1.6} \quad (2.5a - b)$$

where  $g$  is gravitational acceleration,  $G$  is the specific gravity (which ranged between  $1.95 \leq G \leq 2.65$  for bed material between shale and granitic clasts), and  $D_i$  is the substrate grain size of interest based upon log-normal grain-size distribution. The dimensionless Shields parameter ( $\tau_i^*$ ) for a given grain size  $i$  is defined as  $\tau_i^* = \rho u_*^2 / (\gamma_s - \gamma) D_i$ , where  $\rho$  is the fluid density,  $\gamma_s$  is the specific weight of the solid, and  $\gamma$  is the weight of the fluid. Shear velocity ( $u_*$ ) is defined by  $u_* = \sqrt{\tau_b / \rho}$  where bed shear ( $\tau_b$ ) is defined as  $\tau_b = \gamma R_h S_o$  for a given discharge ( $Q_i$ ). The dimensionless critical Shields parameter  $\tau_{SCi}^*$  was determined using a modified form of Brownlie's (1981) curve as outlined by Parker *et al.* (2007) as:

$$\tau_{SCi}^* = \frac{1}{2} \left[ 0.22 \text{Re}_{pi}^{-0.6} + 0.06 \times 10^{(-7.7 \text{Re}_{pi}^{-0.6})} \right] \quad (2.6)$$

The dimensionless particle Reynolds number ( $\text{Re}_{pi}$ ) used in Equation (2.6) is defined as (Parker *et al.*, 2007):

$$\text{Re}_{pi} = \frac{\sqrt{(G-1)gD_i} D_i}{\nu} \quad (2.7)$$

where  $\nu$  is the kinematic viscosity. Values of viscosity used in Equation (2.7) were varied between  $1.51 \times 10^{-6} \text{ m}^2/\text{s} \leq \nu \leq 1.14 \times 10^{-6} \text{ m}^2/\text{s}$  following a simplified Gaussian

distribution, in order to represent the seasonal change in water temperature (T) of between  $0^{\circ}\text{C} \leq T \leq 20^{\circ}\text{C}$ ; the values were rectified in time with the flow records.

The Einstein-Brown equation is defined as (Brown, 1950):

$$W_i^* = \frac{q_{bi}}{\omega_o d_i} \quad \text{for} \quad W_i^* = \begin{cases} 2.15 \exp^{-0.391/\tau_i^*}, & \text{where } \tau_i^* < 0.18 \\ 40(\tau_i^*)^3, & \text{where } 0.52 \geq \tau_i^* \geq 0.18 \\ 15(\tau_i^*)^{1.5}, & \text{where } \tau_i^* > 0.52 \end{cases} \quad (2.8)$$

where  $\omega_o$  is the clear-water fall velocity defined by Rubey (1933). Five substrate size fractions  $i$  (i.e.,  $i = 1, 2, 3, 4$ , and  $5$  relate to  $D_{16}$ ,  $D_{25}$ ,  $D_{50}$ ,  $D_{75}$ , and  $D_{84}$  grain-size fractions, respectively) were investigated for both Equation (2.5) and Equation (2.8).

The two-fraction sediment model offered by Wilcock and Kenworthy (2002) is defined as:

$$W_i^* = \frac{(G-1)gq_{bi}}{F_i u_*^3}, \quad W_i^* = \begin{cases} 0.002\phi'^{7.5} & \text{for } \phi' < \phi' \\ A' \left(1 - \frac{\psi}{\phi'^{0.25}}\right)^{4.5} & \text{for } \phi' \geq \phi' \end{cases}, \quad \phi = \frac{\tau_b}{\tau_{ri}} \quad (2.9 \text{ a - c})$$

where field parameters were utilized for  $A' = 115$ ,  $\psi = 0.923$ , and  $\phi' = 1.27$ . The proportion  $F_i$  of size fraction  $i$  is employed differently here relative to Equation (2.5) and Equation (2.8), and is denoted as either the sand (sa) fraction or the gravel (gr) fraction of the bed-surface material. The two-fraction definition of Equation (2.9) then only has a single transport rate based on Equation (2.9) rather than the five grain fractions used in Equation (2.5) and Equation (2.8). The dimensionless critical incipient motion threshold ( $\tau_{Ci}^*$ ) used in Equation (2.9) was defined by Wilcock and Kenworthy (2002) for bed material as:

$$\tau_{Ci}^* = (\tau_{Ci}^*)_1 + [(\tau_{Ci}^*)_0 - (\tau_{Ci}^*)_1] \exp^{-14F_s} \Big], (\tau_{CS}^*)_0 = \alpha(\tau_{Cgr}^*)_0 \left( \frac{D_{gr}}{D_{sa}} \right) \quad (2.10 \text{ a} - \text{b})$$

where  $(\tau_{CS}^*)_0 = 0.035$ ,  $(\tau_{Cgr}^*)_1 = 0.011$ ,  $(\tau_{CS}^*)_1 = 0.065$ ,  $\alpha = 1.0$ ,  $F_s$  is the surface sand content, and  $D_{gr}$  and  $D_{sa}$  are the representative grains sizes of the gravel and sand fractions, respectively.

The estimated annual bed-load yield ( $Y_{Bed}$ ) from each watershed using any of Equations (2.5), (2.8), or (2.9) at-a-station was determined by:

$$Y_{Bed} = \sum_{j=1}^n \sum_{i=1}^m q_{bj,i} \cdot \min(c_{i,j} Q^{e_{i,j}}, W_{bf}) \quad (2.11)$$

where  $Y_{Bed}$  is reported in metric tonnes,  $n$  is the total number of discharge observations in any given year, and  $m$  is the total number of grain-size fractions investigated (i.e.,  $i = 1, 2, 3, 4$ , and  $5$  relating to  $D_{16}$ ,  $D_{25}$ ,  $D_{50}$ ,  $D_{75}$ , and  $D_{84}$  grain-size fractions, respectively). The minimum width limit in Equation (2.11) converts  $q_{bj,i}$  to the total flowing width of bed material that is in transport, stipulating an upper limit of bankfull width ( $W_{bf}$ ). The maximum width of  $W_{bf}$  makes the assumption that all of the bed-load transport occurs within the limits of the bankfull channel. It is noted that in the case of applying the Wilcock and Kenworthy (2002) equation only, the sand ( $D_{sa}$ ) and gravel ( $D_{gr}$ ) sizes were specified.

Stream-bed stability was evaluated in a fashion similar to those of MacRae and Rowney (1992) and Konrad *et al.* (2005). However, rather than specifying a specific return period of 0.5-year as in Konrad *et al.* (2005), (which may be subject to considerable error in urban environments (USGS, 1982; Booth, 1990; Sweet and Geratz,

2003) if not subject to the same level of scrutiny as by Konrad *et al.* (2005)), the annual fraction percent of the year ( $F_{\text{Bed}}$ ) where dimensionless shear stress exceeds dimensionless critical shear stress was used in the form:

$$F_{\text{Bed}} = \frac{1}{9n} \sum_{i=1}^n X \times 900; \quad X = \begin{cases} 1, & \text{where } \tau_i^* \geq \tau_{\text{SCi}}^* \\ 0, & \text{where } \tau_i^* < \tau_{\text{SCi}}^* \end{cases} \quad (2.12)$$

where  $n$  is the number of annual instantaneous discharge observations and the particle size  $i$  is defined here as the median ( $D_{50}$ ) or 84<sup>th</sup>-percentile ( $D_{84}$ ) bed-material (pavement) diameter.

Stream banks in all of the urban-stream channels were largely dominated by the Halton Clay Plain Till or other cohesive sediments (Chapman and Putnam, 1966; Karrow, 1991). An *in-situ* hydraulic jet tester (e.g., Hanson (1991)) to estimate critical bank hydraulic shear ( $\tau_{\text{CB}}$ ) was not available for use in this study. Instead, a series of total shear ( $\sigma_{\text{T}}$ ) measurements were obtained at each urban study site and converted to  $\tau_{\text{CB}}$  using the relationship  $\tau_{\text{CB}} = \beta_{\text{H}} \sigma_{\text{T}}$ , where  $\beta_{\text{H}}$  was specified as  $\beta_{\text{H}} = 2.6 \times 10^{-4}$  (Léonard and Richard, 2004). A series of Torvane and pocket penetrometer measurements were taken on the outside of bends at or just above the water level in the capillary fringe to obtain total shear values. Bends were selected as the locations for testing as they exhibited the steepest surfaces (often vertical), the greatest absence of roots, and are the locations associated with basal end control (Lawler *et al.*, 1997).

Stream-bank stability was evaluated in a fashion analogous to bank stability by evaluating the annual percent fraction of the year ( $F_{\text{Bk}}$ ) that the bed shear stress ( $\tau_{\text{b}}$ ) exceeds the critical shear stress of the bank material ( $\tau_{\text{CB}}$ ), in the general form:

$$F_{Bk} = \frac{1}{9n} \sum_{i=1}^n X \times 900; \quad X = \begin{cases} 1, & \text{where } Z\tau_b \geq \tau_{CB} \\ 0, & \text{where } Z\tau_b < \tau_{CB} \end{cases} \quad (2.13)$$

where  $Z$  is the tractive force ratio (Lane, 1955) defined with a maximum side slope correction factor of  $Z = 0.76$  (side slope of 1:1) to relate bank shear to bed shear. It is noted that critical bank shear stress was estimated without allowing for any mitigating effects of vegetation that can contribute to bank stability (Hickin, 1984; Thorne, 1990; Millar, 2000).

### 2.2.6 Bed-material Transport Capacity

Bed-load transport measurements were conducted in the urban study reaches employing either a 0.076-m x 0.076-m or a 0.152-m x 0.152-m Helley-Smith bed-load sampler (Helley and Smith, 1971) with hydraulic efficiency factors of 1.46 and 1.56, respectively, and using 0.0625-mm sampling bags. The specific sampler selected was based upon the pebble-count results and the average particle sizes. If the  $D_{50P}$  from the pebble count was greater than 35 mm, the 0.152-m x 0.152-m sampler was utilized, otherwise the smaller sampler was employed.

Bed-load samples were collected from pedestrian bridges, wherever possible, rather than roadway bridges. Pedestrian bridges did not constrict flood flows as significantly as roadway bridges and maintained a cross-sectional geometry more consistent with the study reach, thereby minimizing hydraulic and sediment routing. Continuity of flow between the cross section at sampling locations and gauge stations was valid in all cases. In very large flood events, roadway bridges often had to be utilized because the pedestrian bridges were inundated (wading across inundated



floodplains to pedestrian bridges was usually discontinued when flow depths exceeded 0.3 m).

Bed-load sampling followed the methods of Hubbell (1964), Emmett (1980), and Edwards and Glysson (1988). Multi-vertical samples were obtained at each cross section within the bankfull limits (typically ranging between three to nine verticals, depending upon channel width) to determine the instantaneous bed-load transport rate in a cross section. There were two or more separate samplings over the course of a hydrographic event in order to obtain bed-load transport data for both the rising and falling limbs of the hydrograph wherever possible. Although longer duration samplings are always preferable to time average the chaotic nature of bed-load transport, sample durations were typically limited to 10-minute intervals or decreased in duration to ensure that the sampling bag never exceeded approximately 75% volume occupation. Sample time was also limited in recognition of the flashiness of urban-stream hydrology because there should be a relatively constant discharge during each multi-vertical sampling pass. Post analysis, samples were corrected for the respective efficiency factors.

Instantaneous bed-material transport rates were plotted against the observed instantaneous discharges to produce bed-load rating curves of the form  $Q_{\text{Bed}} = \alpha_s Q_i^{\beta_s}$ , where  $\alpha_s$  and  $\beta_s$  are the best-fit power-fit curve-fitting coefficients and exponents for each watercourse, respectively. The annual at-a-station bed-load yield ( $Y_{\text{Bed}}$ ) for each effective catchment area was determined by:

$$Y_{\text{Bed}} = \sum_{j=1}^n \chi \alpha_s Q_i^{\beta_s} \times 900; \quad \chi = \begin{cases} 1, & \text{where } \tau_{\text{SCi}}^* \geq \tau_{\text{Si}}^* \\ 0, & \text{where } \tau_{\text{SCi}}^* < \tau_{\text{Si}}^* \end{cases} \quad (2.14)$$

where  $\zeta$  is a user-specified lower discharge threshold below which no detectable bed-material transport occurred (based upon observed discharges associated with the absence of bed material in bed-load sampling bags, and field observations). Above the observed bed-load threshold  $\zeta = 1.0$ , otherwise  $\zeta = 0.0$ . The natural at-a-station hydraulic geometry relationships of Equation (2.4) were used with Equation (2.14) to calculate the bed-material transport rates.

Bed-load sampling commenced in 1994 and continued until 2007. Within this sampling period, several of the watersheds experienced observed record discharge events. The hydrographic sampling of these events enabled the bed-load rating curves to be extended to seldom attainable limits. Effective discharge ( $Q_{\text{eff}}$ ) was determined for each stream consistent with the methods of Biedenharn *et al.* (2000) using the power-fit bed-load rating curves, minimum discharge threshold criteria outlined in Equation (2.14), and the hydraulic geometry relationships of each site defined by Equation (2.4).

### **2.2.7 Statistical Analysis**

When comparing data between the urban and rural watersheds, it is useful to determine if the data sets can be considered statistically similar. A multiple regression method making use of dummy (or indicator) variables was employed to test for coincidence between the urban and rural data set regressions. Coincidence occurs when two straight-line regressions are found to occupy the same intercept and share a common slope. The method is briefly summarized below, and is detailed in several statistical textbooks (Kleinbaum *et al.*, 1988; Paulson, 2007).

Testing for coincidence was conducted with a single linear regression model of the form:

$$\hat{y} = \beta_0 + \beta_1 x + \beta_2 z + \beta_3 xz + \varepsilon ; \quad \text{where } z = \begin{cases} 1 & \text{if watershed is rural} \\ 0 & \text{if watershed is urban} \end{cases} \quad (2.15)$$

where  $y$  and  $x$  are the variables of interest,  $z$  is the dummy variable indicating the watershed land-use type (rural or urban), and  $\varepsilon$  is the random error within the model. Two data sets are considered coincident when  $\beta_2 = \beta_3 = 0$ , which reduces the full model to a single, shared fitted line of the form  $\hat{y} = \beta_0 + \beta_1 x + \varepsilon$ . In the cases of power-fit regression comparisons (Davis, 1986), log-transforms of the variables were employed prior to undertaking tests of coincidence.

The hypothesis ( $H_0$ ) of coincidence ( $H_0: \beta_2 = \beta_3 = 0$ ), can be tested with the following F-test statistic with values derived from a full and partial regression of the model:

$$F_{\text{critical}} = F(xz, z|x) = \frac{\left( \frac{SS_{R(\text{full})} - SS_{R(\text{partial})}}{\nu} \right)}{MS_{E(\text{full})}} = \frac{\left( \frac{SS_{R(x,z,xz)} - SS_{R(x)}}{3-1} \right)}{MS_{E(x,z,xz)}} \quad (2.16)$$

where the required Mean Square (MS) and Sum of Squares (SS) values can be obtained from the overall regression ANalysis Of VAriances (ANOVA) table and the Type I (Sequential) Sum of Squares table. The hypothesis ( $H_0$ ) is not rejected when the critical value is less than the appropriate test value ( $F_{\text{critical}} < F_{\text{Test}(\alpha, \nu, n-k-1)}$ ) suggesting that there is significant evidence to conclude that the two data sets are coincident. Where the critical value of  $F$  exceeds the F-test value, this suggests that a significantly better fit will be

obtained by fitting separate regression lines to the data set then by fitting a single line. P-values are reported for each test, as the null hypothesis tests that the regression lines are significantly different, p-values greater than  $\alpha$  will result for coincident lines. For the purposes of this study,  $\alpha$  was taken as 0.05. This approach assumes that it is appropriate to pool the variances between the data sets, an innate assumption within the linear regression model.

The intercepts and slopes of the two data sets can also be examined in a similar fashion separately for similarity by testing the hypothesis ( $H_0: \beta_2 = 0$  or  $H_0: \beta_3 = 0$ , respectively). The F-statistics for these tests are shown elsewhere.

## 2.3 RESULTS

### 2.3.1 Channel and Hydraulic Geometry

A bivariate hydraulic geometry relationship was derived for average bankfull channel width ( $\overline{W}_{bf}$ ) versus bankfull discharge ( $Q_{bf}$ ) using a power-fit regression analysis (Figure 2.4). Table 2.2 lists the average bankfull hydraulic geometry characteristics of each urban study site. Average bankfull width versus bankfull discharge resulted in coefficients and exponents of fit of 4.03 and 0.41 ( $r^2 = 0.72$ ) for the urban streams and 4.25 and 0.41 ( $r^2 = 0.69$ ) for the rural streams, respectively. The urban and rural data sets were also found to be coincident ( $p = 0.90$ ), suggesting that there were no significant differences in channel width as a function of bankfull discharge between the quasi-equilibrium urban and rural reaches. Soar (2000), compiling data from Simons and Albertson (1960), Schumm (1968), Chitale (1970), Kellerhalls *et al.* (1972), and Annable (1996a) and applying a similar power-function regression analysis identified a composite

relationship with coefficients and exponents of fit of 4.13 and 0.55 ( $r^2 = 0.89$ ), which compares very well with power-function relationships of the current study.

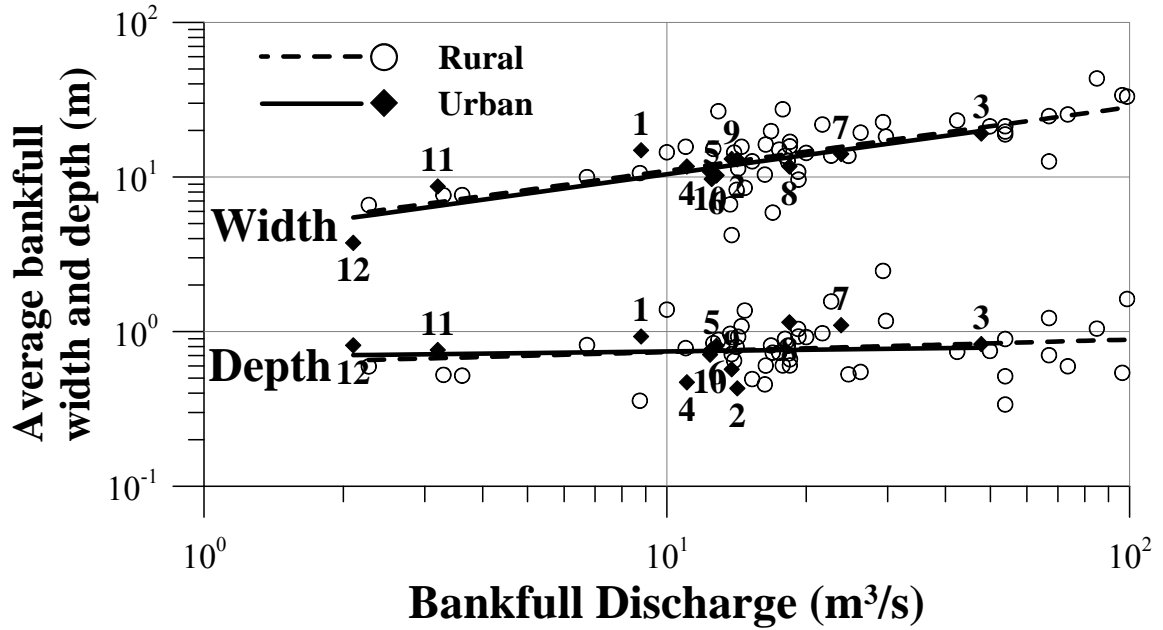


**Figure 2.4.** Average bankfull width ( $\bar{W}_{bf}$ ) and average bankfull depth ( $\bar{D}_{bf}$ ) versus bankfull discharge ( $Q_{bf}$ ).

**Table 2.2.** Reach geometry and pebble count characteristics.

Site Reference No.	Bed Slope (m/m)	Bankfull Discharge (m³/s)	Average Bankfull Width (m)	Average Bankfull Depth (m)	Pebble Count $D_{50P}$ (mm)
1	2.1E-03	8.8	14.9	0.93	30
2	4.4E-03	14.2	13.0	0.43	30
3	5.1E-03	47.8	19.1	0.83	93
4	5.0E-03	11.1	11.7	0.47	37
5	2.6E-03	12.5	9.7	0.77	19
6	1.7E-03	12.8	10.2	0.81	36
7	2.1E-03	23.8	14.1	1.10	25
8	5.5E-03	18.4	11.7	1.15	47
9	2.7E-03	13.8	13.1	0.57	35
10	1.0E-02	12.4	10.8	0.71	52
11	1.0E-02	3.2	8.7	0.76	19
12	5.1E-03	2.1	3.8	0.82	19

A bivariate power-fit regression analysis was also calculated between average bankfull depth ( $\bar{D}_{bf}$ ) versus bankfull discharge resulting in coefficients and exponents of 0.70 and 0.03 ( $r^2 = 0.23$ ) for the urban reaches and 0.61 and 0.08 ( $r^2 = 0.39$ ) for the rural study reaches (Figure 2.4). The urban and rural data sets were also found to be coincident ( $p = 0.96$ ), thus there was no statistically significant difference in channel depth as a function of bankfull discharge between the urban and rural sites. The poor coefficient of determination in average bankfull depth versus bankfull discharge is a common feature of many previous studies, which ascribe it to the variability in channel morphology, and boundary material.

Measurement bias in the current study and the rural study reaches of Annable (1996a) was evaluated against the larger database of gravel-bed rivers offered by Parker *et al.* (2007), as defined by Equations (2.1) and (2.2) using power-fit regression analysis (Figure 2.5). Results show that dimensionless width, depth, and slope versus dimensionless discharge were coincident in all cases ( $p = 0.91$ ,  $p = 0.60$ ,  $p = 0.42$ , respectively) for the combined analysis of the current rural and urban study sites and those of Parker *et al.* (2007). Based upon the combined rural and urban data sets, a coefficient and exponent of 4.163 and 0.396 ( $r^2 = 0.96$ ), respectively, compare very well with Equation (2.1a) for dimensionless width, showing no statistical differences in the data sets. Correspondingly, a coefficient and exponent of 0.336 and 0.418 ( $r^2 = 0.94$ ) were obtained for dimensionless depth, which is virtually indistinguishable from the results of Parker *et al.* (2007) given in Equation (2.1b). The regression of channel slope versus dimensionless discharge results in a coefficient and exponent of 0.031 and -0.208 ( $r^2 = 0.33$ ), respectively, which differs from that of Parker *et al.* (2007) in Equation

(2.1c). The difference is largely attributed to the scale of rivers studied; Parker's included a larger suite of rivers on shallower slopes compared to the reaches studied here, which can generate a bias in the slope regression. Thus, there appears to be no particular bias in hydraulic geometry for either the urban or rural databases of southern Ontario when compared against other gravel-bed streams from around the world.

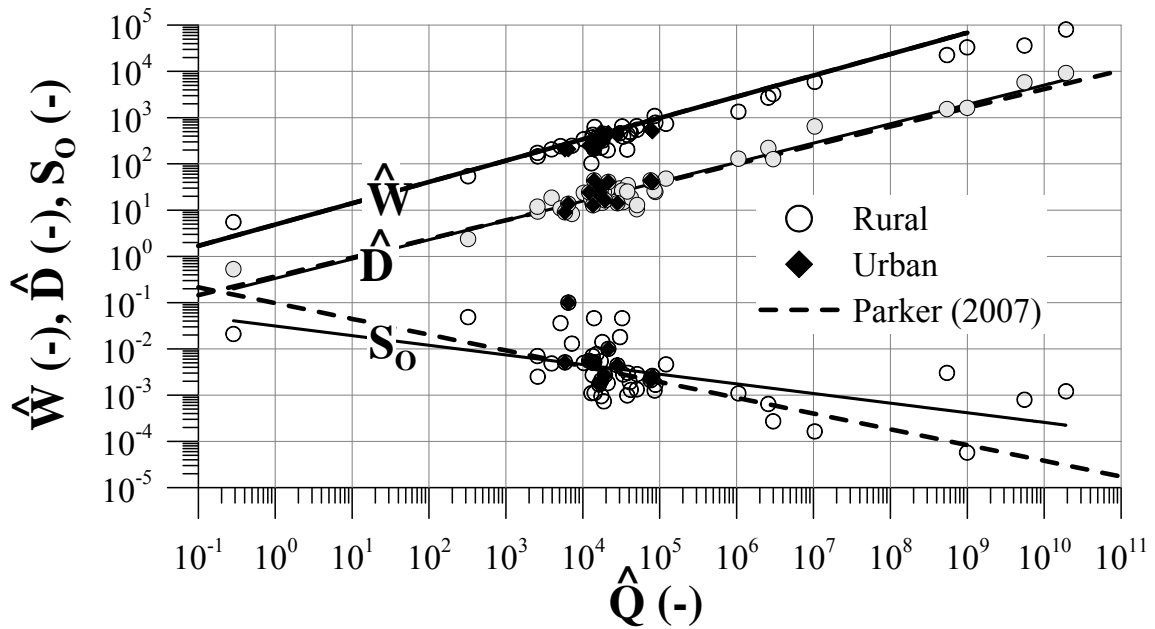


**Figure 2.5.** Dimensionless average bankfull width ( $\hat{W}$ ), dimensionless average bankfull depth ( $\hat{D}$ ), and channel bed slope ( $S_o$ ) versus dimensionless bankfull discharge ( $\hat{Q}$ ).

To further examine the hydraulic geometry characteristics of the urban study sites, the bed and bank stability were examined (Equations (2.12) and (2.13), respectively) in terms of the annual duration percent of shear stress exceeding critical shear conditions ( $F_{\text{Bed}}$  and  $F_{\text{Bk}}$ , respectively). Bed-material and bank characteristics of each urban site are outlined in Tables 2.3 and 2.4, respectively. Converted critical bank shear values obtained in this study are similar to those derived by *in-situ* jet testing by Shugar *et al.* (2007) in similar physiographic units of the same region. Although detailed bed-material

characteristics were available from the rural study by Annable (1996a), detailed bank material measurements were not. Therefore, only the urban sites were analyzed. When Equation (2.13) was applied to the hydraulic shear values converted from measured total shear using the Torvane meter, the analysis showed that in all cases the critical bank shear ( $\tau_{CB}$ ) was never exceeded in any of the urban study sites over their periods of record. Léonard and Richard (2004) found that *in-situ* jet testing of hydraulic shear was usually bound between converted total shear from pocket penetrometer measurements (commonly lower than *in-situ* testing) and converted total shear from Torvane measurements (commonly higher than *in-situ* testing). When hydraulic shear values were converted from total shear measurements using pocket penetrometer measurements, the average annual total percent duration exceeding critical shear ( $\tau_{CB}$ ) ranged between 0.14% and 6.8% of the year (1 to 24 days/year). Therefore, critical bank shear values assessed here are expected to relate to the largest annual bank exposure durations that would be experienced at each study site.

**Table 2.3.** Bed-material and transport characteristics.

Site Reference No.	Bed Material					Substrate					Bed-load Rating			
	D <sub>16</sub> (mm)	D <sub>25</sub> (mm)	D <sub>50</sub> (mm)	D <sub>75</sub> (mm)	D <sub>84</sub> (mm)	D <sub>16</sub> (mm)	D <sub>25</sub> (mm)	D <sub>50</sub> (mm)	D <sub>75</sub> (mm)	D <sub>84</sub> (mm)	Coeffi- cient	Expo- nent	r <sup>2</sup>	Q <sub>eff</sub> (m <sup>3</sup> /s)
1	7.4	20.3	30.4	36.8	39.5	1.5	2.9	6.7	21.0	27.0	0.1063	1.0831	0.89	10.0
2	5.9	17.8	30.4	47.4	60.6	1.5	3.0	7.4	31.9	40.2	0.0569	2.3034	0.75	15.3
3	42.2	51.8	92.5	195.7	276.7	1.9	2.8	5.8	18.1	24.3	0.0022	1.8554	0.87	42.7
4	21.1	26.7	36.8	50.3	56.4	0.9	1.5	5.3	17.5	21.3	0.0112	3.4257	0.67	6.2
5	4.2	5.5	19.0	28.8	33.3	1.4	2.9	6.2	18.5	20.8	0.1489	1.8054	0.80	11.3
6	20.4	27.3	36.3	51.4	63.9	1.5	4.4	6.2	8.7	20.0	0.0521	1.2033	0.58	10.5
7	4.7	6.3	25.1	40.2	45.4	1.4	2.7	5.9	19.1	24.7	0.3910	1.1326	0.88	17.6
8	18.2	29.2	47.3	160.9	244.1	1.4	2.1	5.6	19.0	25.4	0.4303	1.0512	0.91	21.0
9	20.5	25.6	34.9	66.1	83.9	1.5	2.7	5.8	18.7	22.7	0.0023	1.6698	0.81	18.6
10	33.4	40.0	51.8	91.1	118.2	1.4	2.8	5.7	8.3	20.3	0.1124	1.1649	0.68	11.2
11	4.5	5.4	18.7	33.8	39.9	0.4	0.7	4.4	6.8	7.9	0.1282	2.4232	0.79	4.1
12	4.5	5.4	18.7	33.8	39.9	0.4	0.7	4.4	6.8	7.9	0.1630	0.8591	0.85	0.8



**Table 2.4.** Channel bank characteristics.

Site Reference No.	Bank Characteristics			
	Surficial Geology†	Average Bank Angle, $\square$	Hydraulic Shear Torvane (Pa)	Hydraulic Shear Penetrometer (Pa)
1	Clay Till	37	54.4 (22.4)	39.7 (10.7)
2	Clay Till	28	59.7 (27.1)	30.5 (19.6)
3	Clay Till	59	59.7 (23.2)	29.5 (21.7)
4	Clay Till	26	40.6 (19.3)	17.7 (4.4)
5	Clay Till	49	30.7 (12.1)	15.9 (13.4)
6	Spillway Deposits	40	41.6 (12.1)	25.1 (14.7)
7	Clay Till	48	59.7 (27.1)	30.5 (19.6)
8	Clay Till	42	38.7 (22.9)	21.7 (12.3)
9	Clay Till	44	44.3 (10.0)	26.6 (10.1)
10	Clay Till	60	60.2 (24.4)	53.8 (30.1)
11	Clay Till	35	47.9 (17.8)	32.9 (15.2)
12	Sand Plain	53	44.3 (15.1)	27.3 (10.4)

Notes: † Chapman and Putnam (1966, 2007). (Parentheses = standard deviation)

There were no correlations between the annual percent shear stress exceedance of the critical shear of the bed-material median ( $F_{\text{Bed}50}$ ) or the 84<sup>th</sup>-percentile ( $F_{\text{Bed}84}$ ) particle sizes nor critical bank shear ( $F_{\text{Bk}}$ ) (using hydraulic shear values converted from the pocket penetrometer measurements) versus effective catchment area or urban land-use percentage. A direct comparison was undertaken between  $F_{\text{Bk}}$  versus  $F_{\text{Bed}50}$  (Figure 2.6a) and  $F_{\text{Bed}84}$  (Figure 2.6b). With the exception of Sites 3 and 10,  $F_{\text{Bk}}$  was greater than  $F_{\text{Bed}50}$  (Figure 2.6a). Therefore, the median and smaller bed particle sizes are more mobile and susceptible to bed denudation relative to the side boundary materials. Conversely,  $F_{\text{Bed}84}$  was commonly equal to or less than  $F_{\text{Bk}}$  (Figure 2.6b). The annual percent duration exceeding  $\tau_{\text{C}84}$  was never greater, on average, than 1.98% (7.2 days) in any given year. These results support the common observation that the coarser material

is armouring the beds of channels in urban-stream reaches, leading to the banks becoming more susceptible to erosion and widening.

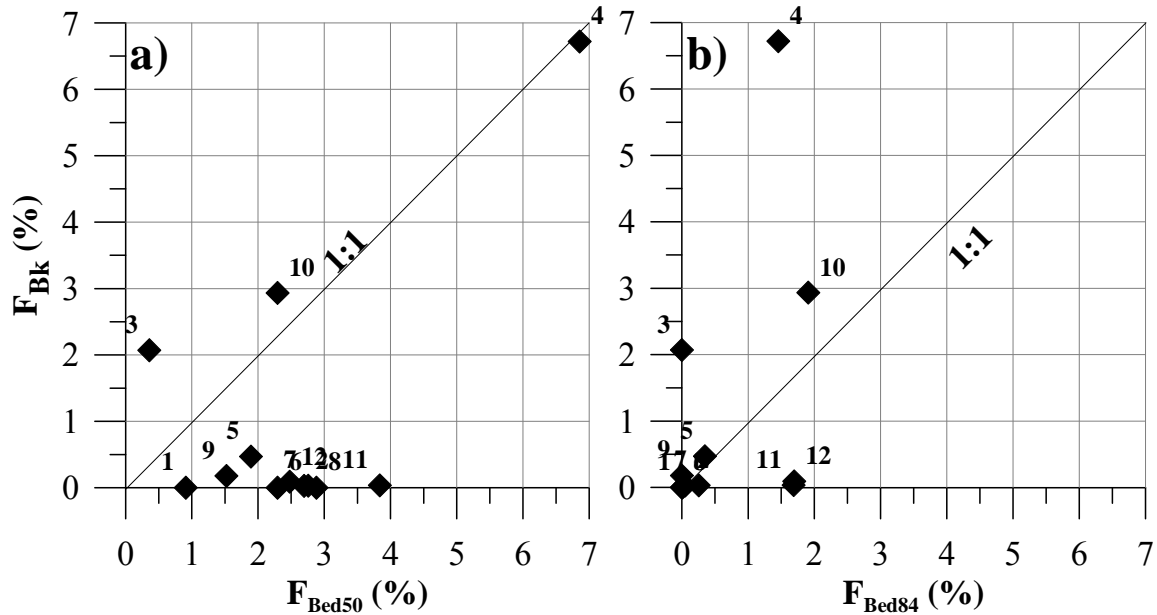


**Figure 2.6.** Annual duration flow exceeding critical bank shear stress ( $F_{Bk}$ ) versus the annual percent shear stress exceeding critical shear of the a) median bed material ( $F_{Bed50}$ ), and b) the 84<sup>th</sup>-percentile bed material ( $F_{Bed84}$ ).

Given that channel widening is not occurring in the urban study reaches (when compared to the rural study reaches), the hydraulic geometry must be in a state of quasi-equilibrium between channel slope, hydraulic radius, and sediment continuity to maintain the channel form. Eleven of the twelve urban-stream channels are riffle-pool dominated channel morphologies and the consistency in annual duration exceeding critical bed shear ranges between bed material  $D_{50}$  and  $D_{84}$  and bank shear, floodplain connectivity must be contributing to maintaining low hydraulic radii and shear stress, thus arresting downcutting. Sufficient bed-material supply and transport must also be occurring to maintain the existing channel morphology. Riparian vegetative control is undoubtedly further contributing to bank stability in all of the cases, as has been previously reported

elsewhere (Zimmerman *et al.*, 1967; Keller and Swanson, 1979; Hickin, 1984; Hey and Thorne 1986; Thorne, 1990). Field evidence consistently identified successional growth in over story species with trees further away from the channel banks being more mature, which may suggest that bank accretion and channel narrowing is actually occurring on a time scale greater than that of the current study and also in response to channel in-filling following the largest flood observed in the systematic record (Hurricane Hazel in 1954).

### **2.3.2 Hydrology**

Allowing for the inherent geological complexity and varying relief in watersheds, effective catchment area is the axiomatic scale for bankfull discharge (Wolman and Miller, 1960; Ashmore and Day, 1988). There is a bivariate relationship between bankfull discharge and the effective catchment area for both the urban and rural sites in this study that has also been detected in various other study reaches across the world (Figure 2.7). The rural or wilderness data used in Figure 2.7 utilized bankfull discharge wherever available; however in some instances, only maximum annual discharge data were available. The 2-year return period calculated by Gingras *et al.* (1994) for the same hydrophysiographic region of southern Ontario (Region 7) shows a trend parallel to the field-observed and calibrated bankfull discharges of the urban and rural studies here, demonstrating consistency in the regional climatic responses. The variability in bankfull discharge for a given effective catchment area in Figure 2.7 reflects influences of the drainage area, drainage basin topography and geology, spatial and temporal trends of precipitation, and nature of the sediment load (Ashmore and Day, 1988).

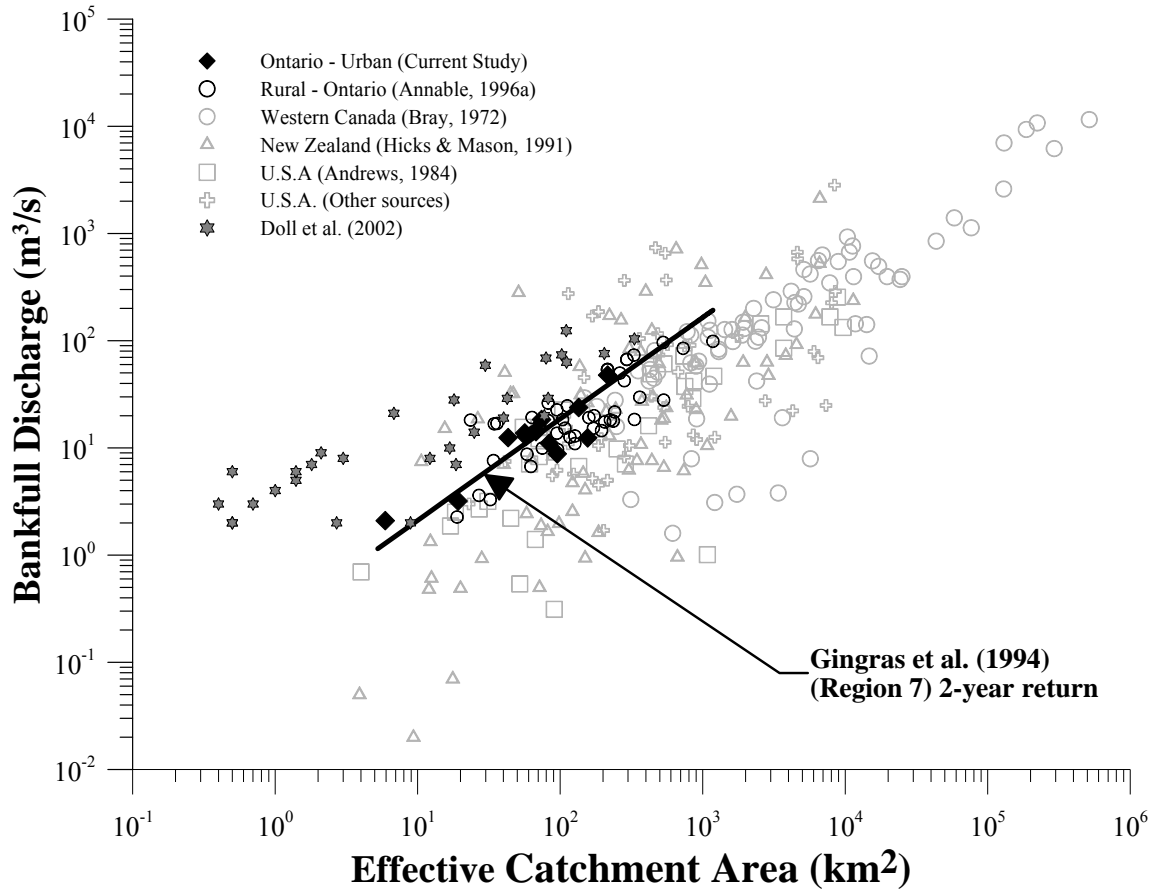


**Figure 2.7.** Bankfull discharge ( $Q_{bf}$ ) versus effective catchment area ( $A_{eff}$ ).

The rural and urban data sets were found to be coincident ( $p = 0.18$ ) with the other data sets from around the world, shown in Figure 2.7. The only exception is a data set by Doll *et al.* (2002) for urban or urbanizing streams in North Carolina. It is not found to be coincident with the observations in southern Ontario and elsewhere ( $p = 0.00$ ). Doll *et al.* (2002) reported that “cross sections were surveyed at a representative stable riffle or run that was not suffering from severe active erosion” but the survey limits were significantly shorter than those of the current study. The field protocol used by Doll *et al.* (2002) may suggest that their study reaches were not entirely in a state of quasi-equilibrium; the reaches may have been in an incised condition where bankfull estimation

methods are problematic or not applicable (U. S. Department of Agriculture, Forest Service (USDAFS), 2003) and, therefore, overestimated.

The annual number of observed events equal to or exceeding bankfull discharge ( $N_e$ ) versus percent urban land use of each effective catchment area are evaluated for the water years 1969 to 2008 (Figure 2.8). Each box-and-whisker plot in Figure 2.8 represents the maximum, 75<sup>th</sup>-percentile, average, 25<sup>th</sup>-percentile, and minimum bankfull events observed in any given year. Consistent with findings in other rural or wilderness watershed studies, the one frequency of rural bankfull discharge was typically less than one event per year and so places in the lower left region of the plot. The frequency of bankfull discharge in the urban streams was consistently equal to or greater than once per year but varied greatly between years. In many cases, bankfull frequency ranged between four to eight events per year. Sites 4 and 10 are the least-developed watersheds (13% and 9% urban land use, respectively) and their hydrologic response is similar to the rural watersheds. Site 6 is downstream of two seasonally-operated on-line reservoirs, which attenuate flows in the summer convective storm months, leading to a reduction in flood events. The increased frequency of shorter return periods in the urban watersheds is consistent with observations by Leopold (1968), Hammer (1972), and Booth (1990). These results demonstrate that the return frequency of bankfull discharge in increasingly-urbanized watersheds is highly variable; however, no predictive trend based upon either effective catchment area or urban land use was apparent. Increasing watershed complexity with increasing stream order, spatial placement of storm-water management facilities on lower order stream channels, outfall locations of combined sewers and/or

storm sewers, and the relative location of hydrometric monitoring stations create too much complexity for statistically-significant bivariate relationships to emerge.

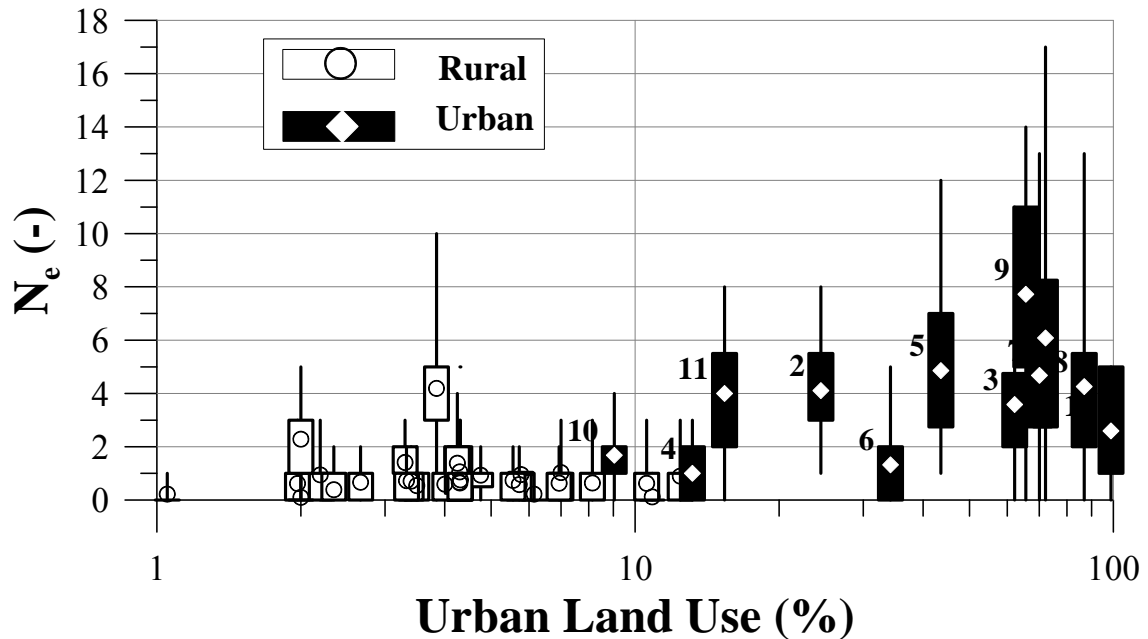


**Figure 2.8.** Annual frequency of bankfull discharge events ( $N_e$ ) versus percent urban land use.

The annual return frequency of bankfull discharge at the rural sites is typically greater than 1.0 (Figure 2.9a). Return frequency outliers below 1.0 occur in a series of rural watersheds principally comprised of over-consolidated clay tills, where antecedent moisture conditions are quickly achieved causing increased rates of overland runoff, which can increase the frequency of smaller flood events. On average, there is a 1.6-year bankfull return period in the rural watersheds in the region (Annable, 1996b), which is consistent with the findings in other rural or wilderness watersheds (e.g., Leopold *et al.* (1964) and Hicks and Mason (1991)). When the Log-Pearson III method is employed to estimate bankfull discharge, similar rural return frequencies are obtained, exceeding a 1-year return (Figure 2.9b). Conversely, the majority of the urban streams have

significantly lower annual return periods based upon the observed cumulative annual events (Figure 2.9a). There is a contradiction in the prediction of urban bankfull return frequencies when employing the annual series Log-Pearson III method (Figure 2.9b); it consistently over-predicts the discharge frequency by virtue of a solution method using yearly instantaneous peak discharges (USGS, 1982; Sweet and Geratz, 2003). Thus from the predictive standpoint, employing any method which uses peak annual time-series data to predict bankfull discharge return frequencies in urban watershed cases will lead to over-prediction of the channel-forming flow if consistent with bankfull discharge.

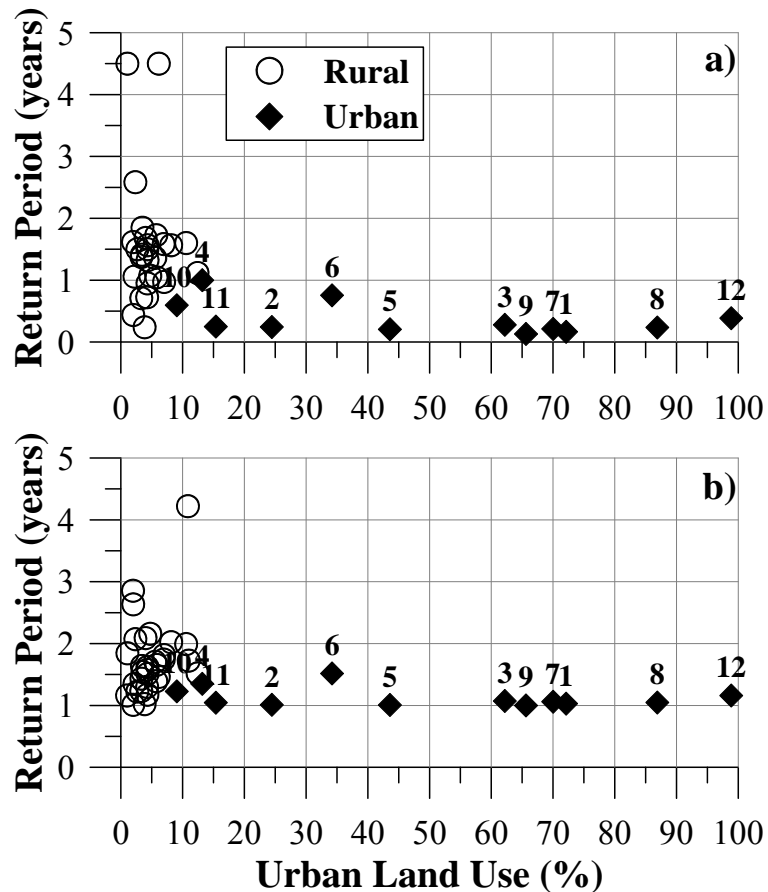


**Figure 2.9.** Annual return period of bankfull discharge using: a) annual frequency of bankfull discharge events ( $1/N_e$ ), and b) maximum annual instantaneous discharge data.

The maximum annual intensity of events versus effective catchment area are evaluated in Figure 2.10a. Statistical analysis of the urban and rural event intensities identified a nominally coincident state ( $p = 0.05$ ). However, when Sites 4 and 10 were removed from the urban analysis (the least urbanized sites, responding hydrologically quite like the rural study sites), the urban and rural data sets were not found to be coincident ( $p = 0.00$ ). These results are consistent with observations by Packman (1979) and Henshaw and Booth (2000). Detailed inspection of the time-series data identified a pattern of very short duration urban watershed events (compared to the rural streams) followed by extended durations at lower or base-flow conditions. Conversely, rural streams exhibited extended duration on the falling limbs of the hydrographs with significantly longer durations between base flow and bankfull discharge.

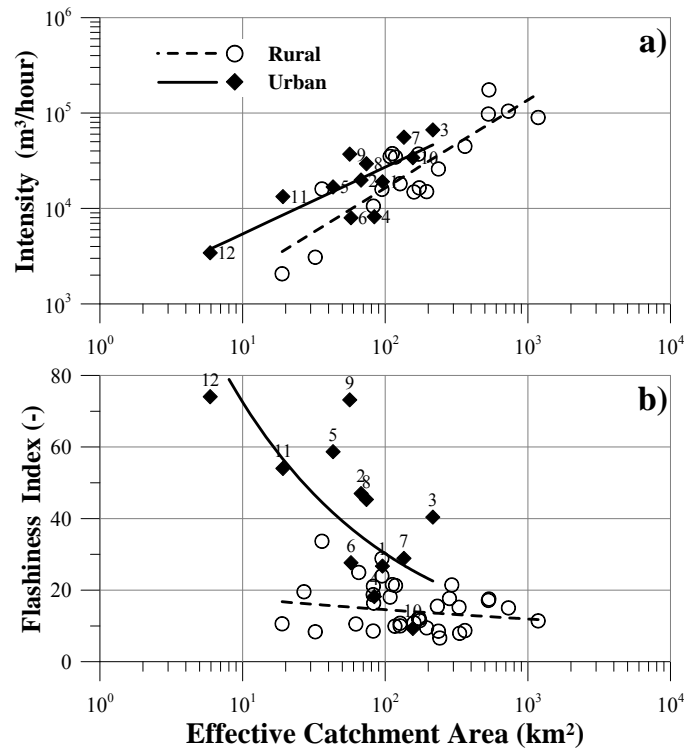


**Figure 2.10.** a) flood intensity and b) flashiness index versus effective catchment area ( $A_{\text{eff}}$ ).



Applying the flashiness index versus effective catchment area, the urban and rural reaches (Figure 2.10b) were found not to be coincident ( $p = 0.00$ ). The more urbanized watersheds plot higher on the ordinate axis compared to the rural streams or the urban streams with lower urban land use (Sites 4, 6, and 10). Results observed here are consistent with several other studies (Hollis and Luckett, 1976; Packman, 1979; Urbonas and Roesner, 1993). The flashiness index decreases in both the urban and rural sites with increasing effective catchment area because the increases of source storage and routing complexity lead to decreased flashiness. The more dramatic decrease in flashiness index with increasing effective catchment area in the urban-stream sites, which tends towards the slope of the rural sites, further expresses the hydrologic complexity and cumulative hydraulic controls arising from increasing watershed scale that results in attenuated hydrographic peaks and extended flood durations.

Annual cumulative volume of flow ( $V_{\text{tot}}$ ) for each watershed versus effective catchment area shows no distinguishable differences between the rural and urban watersheds studied (Figure 2.11); the data sets are coincident ( $p = 0.43$ ). Similar findings have been described by Leopold (1968), the American Society of Civil Engineers (ASCE, 1975), and Konrad and Booth (2002) throughout the United States. These results also support the assertion of Gingras *et al.* (1994) that this region of southern Ontario exhibits uniform hydrophysiographic conditions.

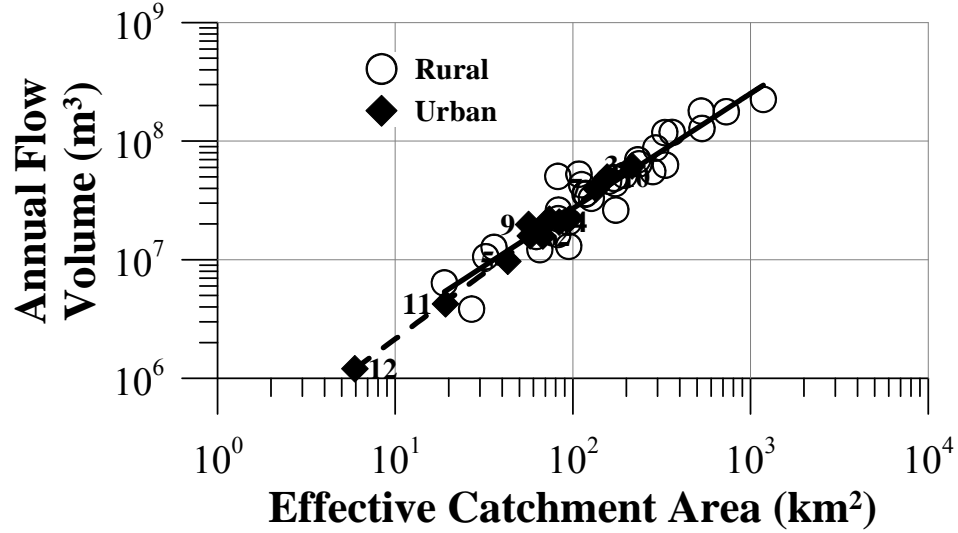


**Figure 2.11.** Annual flow volume ( $V_{\text{tot}}$ ) versus effective catchment area ( $A_{\text{eff}}$ ).

Figure 2.12a shows the annual cumulative volume of events where bankfull discharge was exceeded ( $V_{\text{ae}}$ ), based upon the event criteria of Figure 2.3, versus effective catchment area. There was no significant difference between  $V_{\text{ae}}$  derived from the shorter duration, multiple events of the urban watersheds and the less frequent but longer duration events of the rural sites; rural and urban study sites were found to be coincident ( $p = 0.46$ ). A general increase in the percent annual fraction duration of discharge events where bankfull discharge was exceeded ( $T_{\text{ae}}$ ) was identified as a function of increasing effective catchment area (Figure 2.12b). However, the variance in ( $T_{\text{ae}}$ ) within both the urban and rural data sets was too large to discriminate statistically-significant trends between the urban and rural watersheds. Detailed inspection of annual hydrographs determined that the duration and related volume of flows between  $\bar{Q} \leq Q \leq Q_{\text{bf}}$  of the rural study sites were significantly longer and larger compared to the urban settings, as indicated by the flashiness index of Figure 2.10b. The banks of urban channels are exposed to more frequent wetting and drying cycles than those in the rural

settings whereas there is a larger, often single, annual bank inundation period in rural watersheds. An annual increase in the frequency of wetting and drying cycles may contribute to increased rates of bank erosion observed in many settings where channel incision has occurred. MacRae and Rowney (1992), studying several lower order regulated urban-stream channels in the same region of Ontario, found that if storm-water facilities were designed in a manner that increased the duration of flows at or near bankfull discharge, there would be longer duration of excess shear, leading to increased rates of channel erosion. Therefore, the flashy responses of the urban-stream channels studied here, together with ready access to adjoining floodplains of low hydraulic radii, are a complementary combination leading to minimizing channel erosion.

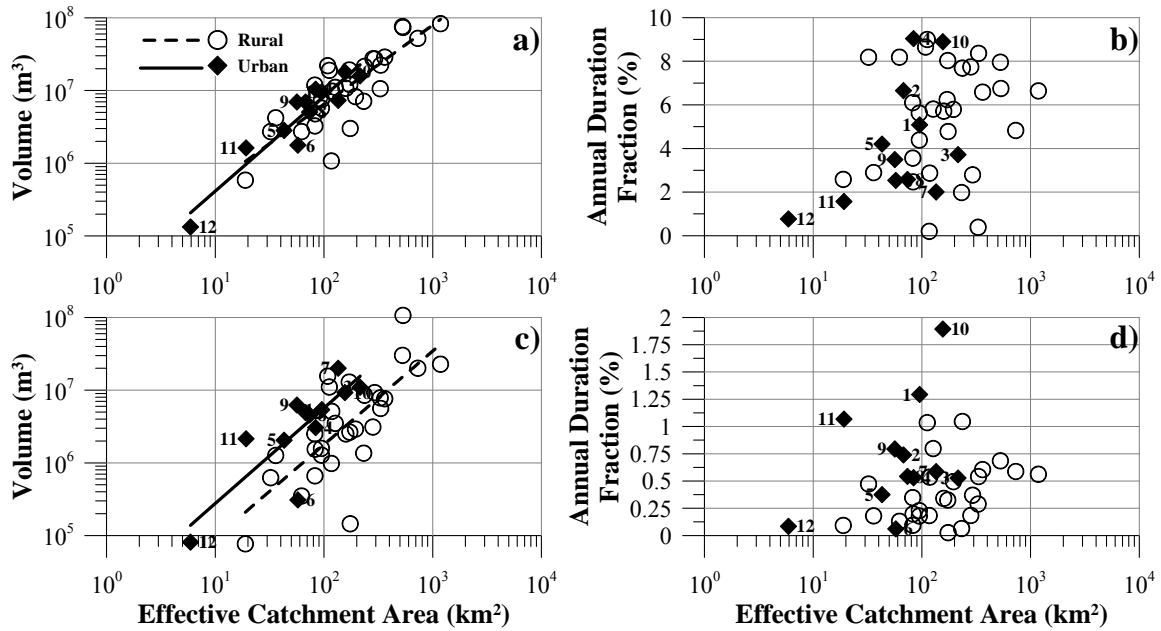


**Figure 2.12.** Annual cumulative a) volume ( $V_{ae}$ ) and b) duration ( $T_{ae}$ ) of events where bankfull discharge has been equaled or exceeded; and, annual cumulative c) volume ( $V_{abf}$ ) and d) duration ( $T_{abf}$ ) of discharge exclusively exceeding bankfull discharge versus effective catchment area ( $A_{eff}$ ).

The annual cumulative flow volume exclusively exceeding bankfull discharge ( $V_{abf}$ ) is compared to the effective catchment area in Figure 2.12c, again employing the criteria of Figure 2.3. Regression analysis shows the urban and rural data sets behaving parallel, with a greater volume of flow exclusively exceeding bankfull discharge in the urban settings. The two data sets were not coincident ( $p = 0.02$ ) and, therefore, statistically different between the rural and urban watersheds. These findings demonstrate that the urban streams cumulatively inundate their floodplains more frequently and with larger volumes of water compared to the rural study reaches. As with results of Figure 2.12b, there are no statistically-significant relationships between the annual flow-duration fraction that exclusively exceeded bankfull discharge ( $T_{abf}$ ) and the effective catchment area (Figure 2.12d). However, Figure 2.12d does show that there is an approximate order of magnitude decrease in the average duration of flow exceeding bankfull discharge compared to the entire annual event volume durations (Figure 2.12b).

### **2.3.3 Bed-material Characteristics**

The annual bed-material transport characteristics were evaluated using the at-a-station hydraulic geometry. Two different methods were evaluated: 1) field observations from gauge stations (Equation (2.3)), and 2) those from representative channel morphology sections from calibrated HEC-RAS models (Equation (2.4)), both using the same systematic 15-minute discharge interval data. The analysis did not detect any discernible relationships between the bed-material transport equations employed and either the effective catchment area or percent urban land use in the urban and rural study sites. The bed-material yield using the Meyer-Peter Müller (Wong and Parker, 2006), Einstein-Brown (Brown, 1950), and Wilcock and Kenworthy (2002) equations versus

effective catchment area were found to be coincident in each case ( $p = 0.85$ ,  $p = 0.84$ ,  $p = 0.13$ , respectively). Figure 2.13 illustrates the average annual yield results for gravel-bed urban and rural streams using the Einstein-Brown equation. Bed-material yield was commonly one order of magnitude larger when the modified Meyer-Peter Müller equation was employed, whereas the Wilcock and Kenworthy equation typically predicted a lesser yield (commonly between 1 and 2 orders of magnitude).

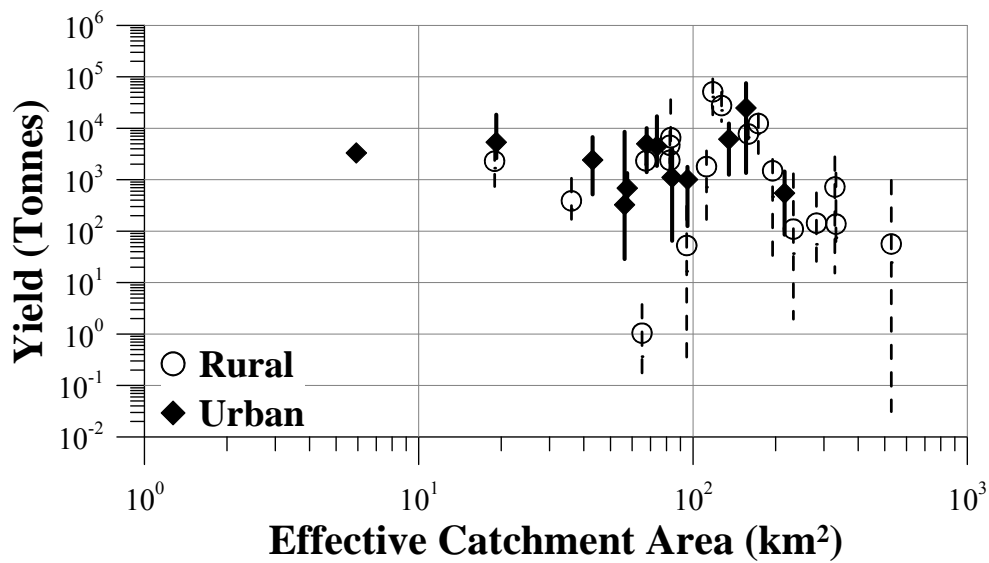


**Figure 2.13.** Annual bed-load transport yield capacity versus effective catchment area ( $A_{\text{eff}}$ ) using Einstein-Brown equation (Brown, 1950). *Note: Whisker extents represent the maximum and minimum yield for the period of record.*

A complementary evaluation of the suspended-sediment data that was available and/or collected over the study period was undertaken with an annual framework similar to that outlined in Equation (2.11). Although channel evolution in gravel-bed streams is not largely influenced by suspended-sediment concentrations (Schumm *et al.*, 1984), the analysis was undertaken to determine if there were any particular differences between the urban and rural study reaches. In this case, power-function coefficients and exponents

were best fit to instantaneous suspended-sediment discharge observations versus instantaneous discharge. The results of this analysis (not shown) identified a monotonically increasing relationship of suspended sediment with increasing effective catchment area and that the rural and urban data sets were coincident. Visual inspection of the results indicated that the average annual yield from the urban watersheds was usually larger than the rural watersheds, which is a consistent observation with the findings of Wolman (1967), Wolman and Schick (1967), Lee *et al.* (2002), and Lawler *et al.* (2006); however, the data sets were identified as coincident.

#### **2.3.4 Channel Bed-material Transport Capacity**

Bed-load sampling took place over a 15-year period, lengthy enough for data to be captured during large flood events. Figure 2.14 illustrates the bed-material transport relationships established for the twelve urban study sites. Bed-load sampling was not included in the 1996 study of rural streams in the same region (Annable, 1996a) and it was also beyond the scope of the current research to include it. Power-function regression analyses of the measured instantaneous bed-load discharge rates versus observed discharge are illustrated in Figure 2.14 and their coefficients of determination listed in Table 2.3; the bed-load transport relationships are organized in decreasing order of urbanization (left to right and top to bottom) in the figure. The coefficients of determination of power-fit regression analysis ranged between  $0.58 \leq r^2 \leq 0.91$ . During the bed-load sampling program, it was commonly observed that sizeable quantities of anthropogenic material (asphalt, glass, metal, road sand, etc.) were also present.

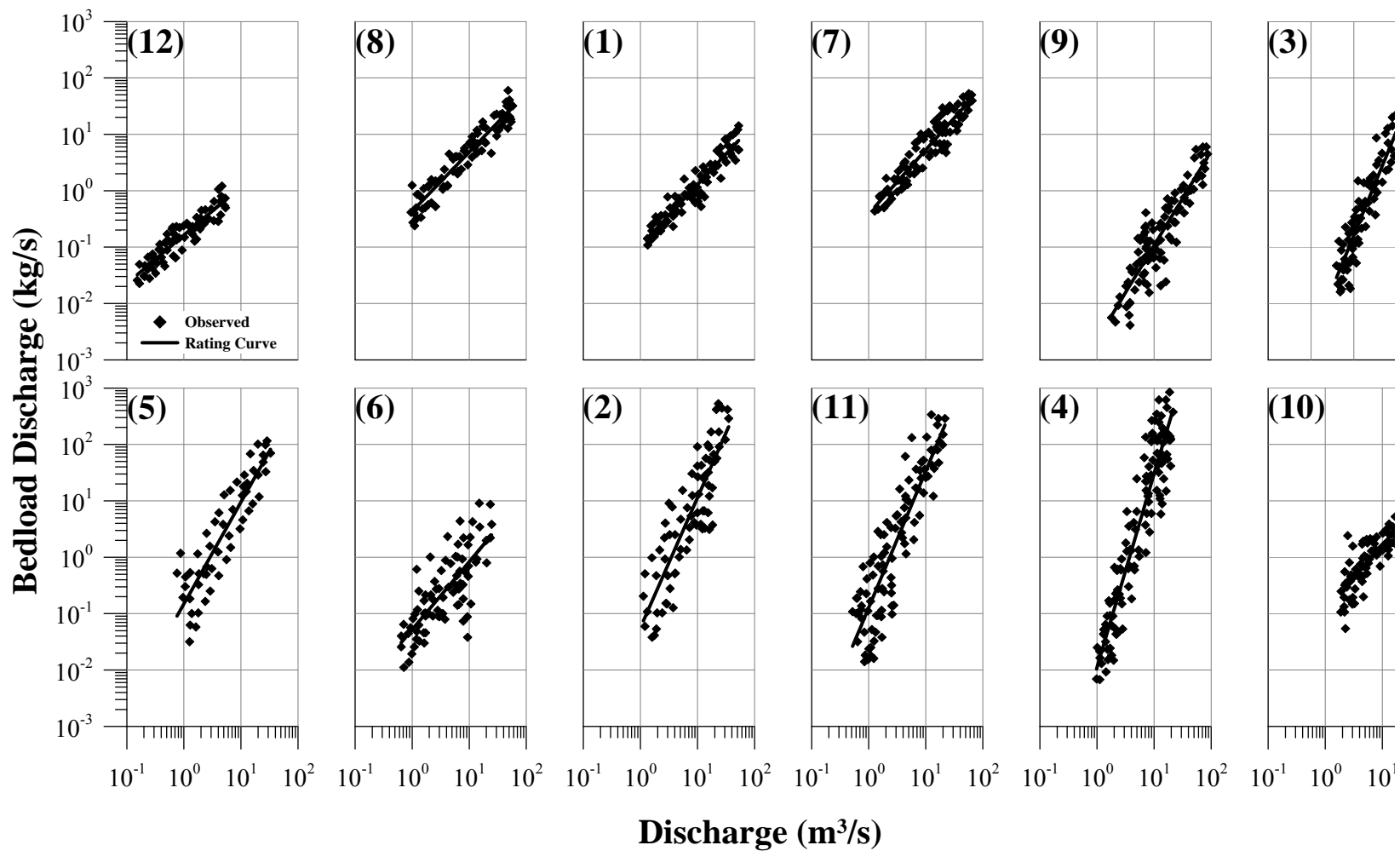


**Figure 2.14.** Bed-load rating curves. *Note: Sites are organized by decreasing urban land use from left to right and top to bottom.*

The power regression exponents of the best-fit analysis of Figure 2.14 and Table 2.3, which describe the bed-material transport rate as a function of instantaneous discharge, are compared with percent urban land use in Figure 2.15a. There is a monotonically decreasing material transport rate as the percent urban land use increases;  $r^2 = 0.42$ . In addition, it can be observed that with increasing urbanization (Figure 2.12, Table 2.3), the  $r^2$  values of the bed-load rating curves commonly increased from 0.68 to 0.91 in discord with the downward trend observed in Figure 2.15a. It is acknowledged that there can be significant spatial and temporal variability in bed-load sampling that is related to the limitations of the sampling procedures (Emmett, 1980; Edwards and Glysson, 1988; Emmett and Wolman, 2001) and hysteresis (Nanson and Young, 1981). Nevertheless, in increasingly urbanized watersheds, there is often an increase in in-stream channel works, storm-water ponds, works to mitigate site-specific erosion, and protect bridges and sewers, which may alter the longitudinal spatial distribution of bed-material supply to a given stream. Possibly, the anthropogenic erosion management of river channel lengths in urban watercourses leads to a more longitudinally evenly-distributed bed-material supply and thus a higher coefficient of determination rather than the often site-specific discontinuous spatial pattern of supply (a subset of bends for example) found in rural watercourses (Wolman, 1967; Leopold, 1973; Graf, 1975). The increased hydrologic efficiency of overland runoff and transport in urban watersheds may also contribute to more consistent (but smaller quantity) bed-material transport.

Bed-material transport yield was evaluated using Equation (2.14) and the average annual transport yield was compared with the effective catchment area (Figure 2.15b). The results show a weak monotonically increasing bed-material yield with increasing



effective catchment area. Figure 2.15b also shows that the effective catchment areas with lower percent urban land use (represented by smaller circles circumscribing the average annual bed-material yields) have larger bed-material yields and more effective urbanized catchment areas.

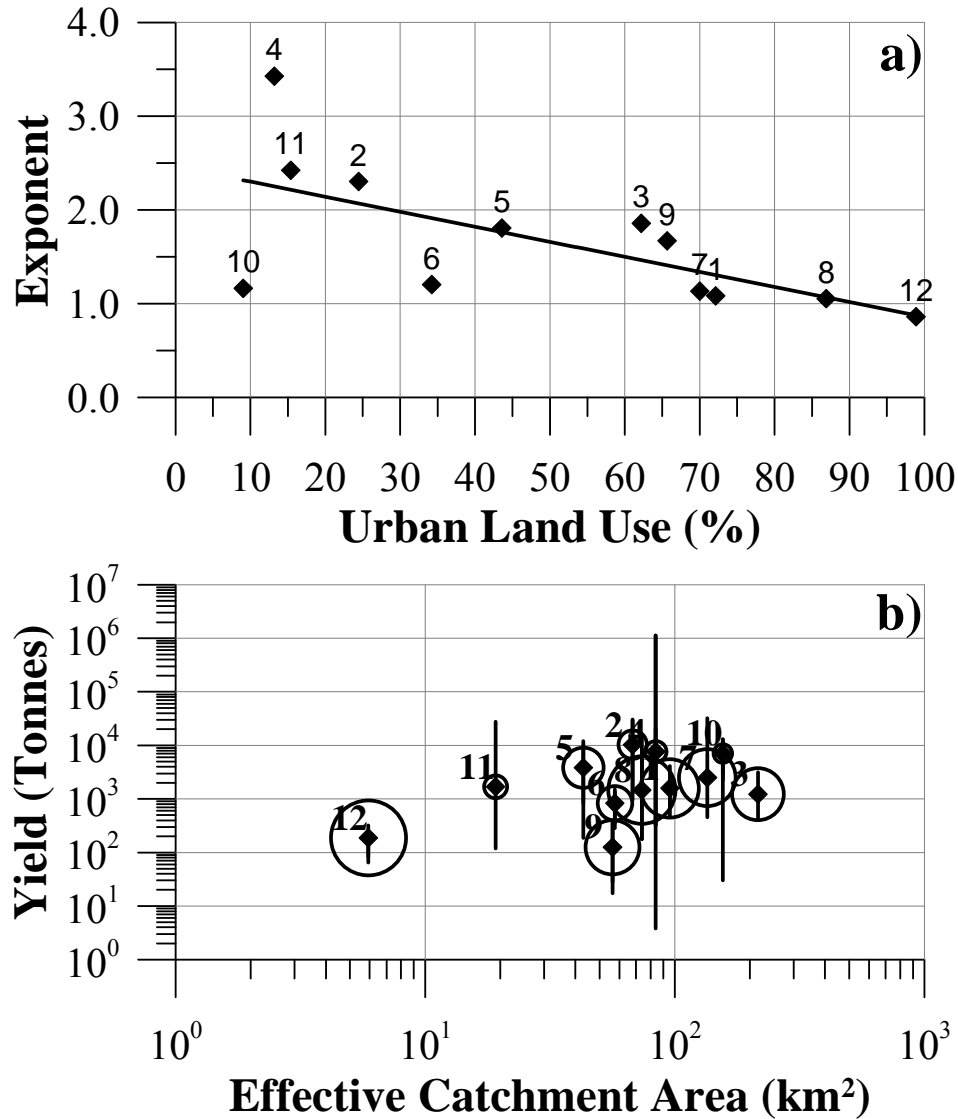


**Figure 2.15.** Urban reach a) bed-load rating curve exponents ( $\beta_s$ ) versus percent urban land use, and b) annual bed-load yields versus effective catchment area ( $A_{\text{eff}}$ ). *Note: Whisker extents represent the maximum and minimum yield for the period of record. Increasing circle diameters represents increasing percent urban land use.*

The cumulative annual duration fraction of flow events where bankfull discharge has been exceeded (1% to 9% of the year; Figure 2.12b) is similar to the annual duration of flows where critical shear stress is exceeded (0.2% to 7% of the year; Figure 2.6). Correspondingly, the cumulative annual duration fraction of flows exclusively exceeding bankfull discharge (0.1% to 1.28% of the year; Figure 2.12d) is similar in annual duration fraction to flows exceeding the critical shear stress of the average 84<sup>th</sup>-percentile bed material (0.08% to 1.97% of the year): which is approximately half of the annual amount of time where flows exceed the critical shear stress of the median bed-material particle size (0.21% to 3.93%). The similarity in annual percent fraction of flows exceeding bankfull discharge and critical shear stress of both bed and bank materials also supports the proposition that, in cases of riffle-pool dominated channels, the bankfull discharge and effective discharge are both representative of the morphology-forming flow (Emmett and Wolman, 2001). A comparison between effective discharge and bankfull discharge (Figure 2.16) shows a very strong correspondence ( $r^2 = 0.97$ ) between these two geomorphological metrics, further supporting the field observations that the urban study reaches are in a state of quasi-equilibrium between hydraulic geometry, geotechnical stability, and sediment-supply continuity.

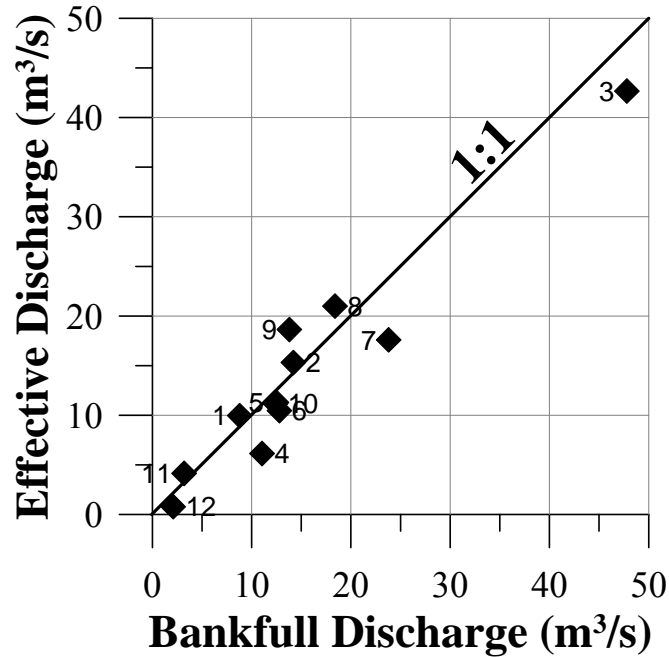


**Figure 2.16.** Effective discharge ( $Q_{eff}$ ) versus bankfull discharge ( $Q_{bf}$ ).

## 2.4 DISCUSSION

In general, the observations from this study have shown that the annual frequency of bankfull discharge occurrences in the urban-stream channels is significantly higher than in the rural less-developed watersheds in the same physiographic region. The cumulative annual volume of water derived from urban and rural watersheds as a function of effective catchment area are very similar in addition to the cumulative annual discharge of all flood events and duration of events exceeding bankfull discharge. Larger annual volumes of water were observed to inundate the floodplains of the urban-stream channels compared to the rural watersheds studied. Bed-material transport was observed to decrease with increasing urban land use in each urban site that was imposing limits (artificial works) on the supply of new bed material; however, channel degradation was not observed. Finally, the cross-sectional geometry of bankfull width and depth of the

urban channels was statistically identical as a function of bankfull discharge to the rural streams studied by Annable (1996a), which were also found to be in a state of quasi-equilibrium.

The results of this study can be summarized using the constitutive relationships offered by Schumm (1969), who studied the morphological changes to alluvial channels in the mid-western United States and Australia related to human activities such as reservoirs, water taking, and in-stream gravel mining. He proposed the following relationships that generalized the morphological responses due to single-state variable changes of increased discharge ( $Q^+$ ), increased bed-material load ( $Q_s^+$ ), and decreased bed-material load ( $Q_s^-$ ):

$$Q^+ \approx \frac{W^+ D^+ \lambda^+}{S_o^-}, Q_s^+ \approx \frac{W^+ \lambda^+ S_o^+}{D^- \Omega^-}, Q_s^- \approx \frac{W^- \lambda^- S_o^-}{D^+ \Omega^+} \quad (2.17 \text{ a – c})$$

where the + or - signs represent increases or decreases of various parameters, respectively,  $\lambda$  is the meander wave length,  $\Omega$  is the channel sinuosity, and  $\bar{\omega}$  is the width/depth ratio of the bankfull channel. Schumm (1969) also offered two additional relationships where increases in discharge and either increases or decreases in the percent of bed-material load ( $Q_T$ ) occur:

$$Q^+ Q_T^+ \approx \frac{W^+ \lambda^+ \bar{\omega}^+}{\Omega^-} S_o^\pm D^\pm, Q^+ Q_T^- \approx \frac{D^+ \Omega^+}{S_o^- \bar{\omega}^-} W^\pm \lambda^\pm \quad (2.18 \text{ a – b})$$

A common observation in urban-stream channels correlates an increase in discharge with increasing channel width and depth, and an accompanying decrease in channel slope by lateral migration extension if unimpeded from anthropogenic

influences. When the effects of increased discharge and increased bed-material supply during the early stages of urbanization occur, a similar trend is observed but is further altered by decreased sinuosity with increased bed-material supply and increased width/depth ratio, which is consistent with many other studies (Wolman, 1967; Hammer, 1972; Booth, 1990) and is reflective of Equation (2.18a). The results of the present study showed that there was an increased average annual cumulative volume of flow exclusively exceeding bankfull discharge but that the average annual bed-material supply in the increasingly urbanized watersheds decreased. The channel responses to both increased discharge and decreased bed-material supply observed are consistent with Equation (2.18b).

A similar downstream reduction in channel width and width/depth ratio was observed by Nanson and Young (1981) downstream of urbanized portions of watersheds in southeastern Australia. They found that the reduced bed-material supply with increased urbanization resulted in decrease in channel width. The trend was similar to reaches downstream and distal to reservoirs beyond the dis-equilibrium reach associated with channel scour, where decreases in channel width and width/depth ratio have commonly been observed (Schumm, 1969).

The combined effects of decreased bed-load supply and larger volumes of water per annum accessing the floodplain in this study result in a cross-sectional profile that is similar to the channel widths and depths found in surrounding rural river studies. The effect of increasing the frequency of bankfull events and increased frequency and volume of floodplain inundation tend to offset the influence of a reduced sediment rating curve exponent (Wolman and Miller, 1960; Andrews, 1980). It is possible that the urban

reaches studied were not entirely in a state of quasi-equilibrium, and if the reductions in bed-material supply continued over time, it may be expected that there will be further reductions in the channel width and width/depth ratio, an expectation that is consistent with the successional vegetation patterns observed in the field. It is the intent of future research to re-survey each urban research site on a decadal basis at the permanent cross section to continue to study its evolution.

## **2.5 SUMMARY**

This study investigating the quasi-equilibrium characteristics of urban gravel-bed stream channels in southern Ontario, Canada, has been conducted over the past 15 years and its findings compared to rural gravel-bed stream channels of the same hydrophysiographic region. Urban channel morphology studied here did not respond in the commonly observed fashion of increases in channel width and depth with increasing urbanization. Results show no statistically-significant differences of bankfull width or depth and bankfull discharge between the urban and rural study sites. The field observations were also compared with a larger international data base of gravel-bed streams, finding consistency in the population observations of hydraulic geometry versus dimensionless discharge.

The frequency of bankfull and larger discharge events increased with increasing urbanization within the study watersheds, with corresponding increases in flashiness index and the number of shorter duration events, as has been seen in several other studies. The interactions between storm sewers, combined sewers, storm-water quantity ponds and other infrastructure resulted in complex watershed responses that made detection of

predictive trends between urban land use and bankfull frequency return periods elusive. Analyses comparing partial duration series data and annual series data found a discrepancy in the prediction of bankfull return period that results in significant over-prediction of the morphological forming flow where peak annual return methods are employed to predict bankfull return periods. Using peak annual series data to estimate bankfull discharge in stream restoration projects then may also lead to significant over-estimates of channel-forming flows resulting in the production of incised channels rather than floodplain-dominated channel morphologies.

Annual discharge volumes derived from each effective catchment area identified no statistical difference in total flow. Similarly, the annual volume summations of all bankfull or larger events in urban streams were indistinguishable from the less frequent but longer duration events recorded in the rural study sites. However, the annual volume summation exclusively exceeding bankfull discharge was larger in the urban-stream channels whereas a larger volume of flow occurred between the low flow and bankfull stages in the rural study reaches. The annual duration of flows onto the floodplains in the urban study sites was similar to the annual duration of flows exceeding either the critical bank shear or critical bed shear of the median bed-material particle sizes.

Volumes of bed material transported were found to decrease with increasing per cent urban land use, indicating a reduction in supply with increasing urbanization. Downcutting was not observed in any of the urban study reaches; however, which suggests that the reduction in bed-material supply is offset by ease of access to floodplains during flood events, thus maintaining low hydraulic radii and the reduced channel width contrary to most urbanizing stream responses. In each urban study reach,

the median ( $D_{50}$ ) bed particle size was found to be mobile between 0.14% and 6.8% of the year but the 84<sup>th</sup>-percentile particles were only mobile under the largest flood events, indicating a mobile but armoured bed.

The ready spill onto floodplains and the reduced velocities there appear to function as a strong buffer against any channel degradation due to the increase in flood intensities and volumes but reduced flood durations in urban settings. The combined urban and rural findings in this study are consistent with the anthropogenic responses identified by Schumm (1969), namely that reductions in the percent bed-material supply and increased discharge result in smaller rather than larger bankfull geometry proportions, with the proviso that adequate adjacent floodplain access be maintained. This study is one of a very small suite of studies attempting to identify the quasi-equilibrium conditions of urban-stream channels rather than investigating the degradational responses. The implications of this study for urban-stream rehabilitation are that smaller bankfull channel geometries may be the design end-point rather than larger channel geometries, to balance the reduction in bed-material supply. The increase in the magnitude and frequency of flood discharges is offset by allowing overspill greater access to continuous floodplains in order to maintain low hydraulic radii and thus shear stress to enhance the channel stability.



# **CHAPTER 3**

## **PLANFORM AND BED MORPHOLOGY**

### **CHARACTERISTICS**

#### **3.1 INTRODUCTION**

Chapter 2 determined that the annual frequency of bankfull discharge was greater in the urban streams, commonly averaging between four to eight times per year compared to an average rural frequency of 0.6. Multi-year bed-load sampling established a trend of decreasing bed-material supply with increasing percent urbanization. There were no statistical differences in bankfull width nor depth between the urban and rural study reaches as a function of effective catchment area.

During the course of the study, it was observed that there were changes in bed morphology that were unlike those in the local rural watercourses and elsewhere (Annable, 1996a; Leopold and Wolman, 1960; Williams, 1986). Many reaches developed multiple pools and riffles along the cross-overs between bends rather than the commonly observed single riffle between bends and pools on the outsides of bends in single-thread channels (Leopold and Wolman, 1960). Further, frequent field sediment sampling under high-flow conditions found patterns of standing waves at the majority of sites (Figure 3.1), which may be surface expressions of bedform development as a means

of both grain and bedform energy dissipation, similar to that reported by Simons and Richardson (1963) in sand-bed channels. Alternatively, the changes in bed morphology may be the result of larger clasts pulsing through the river systems due to the more frequent but brief discharge events creating more frequent keystone and armouring points.

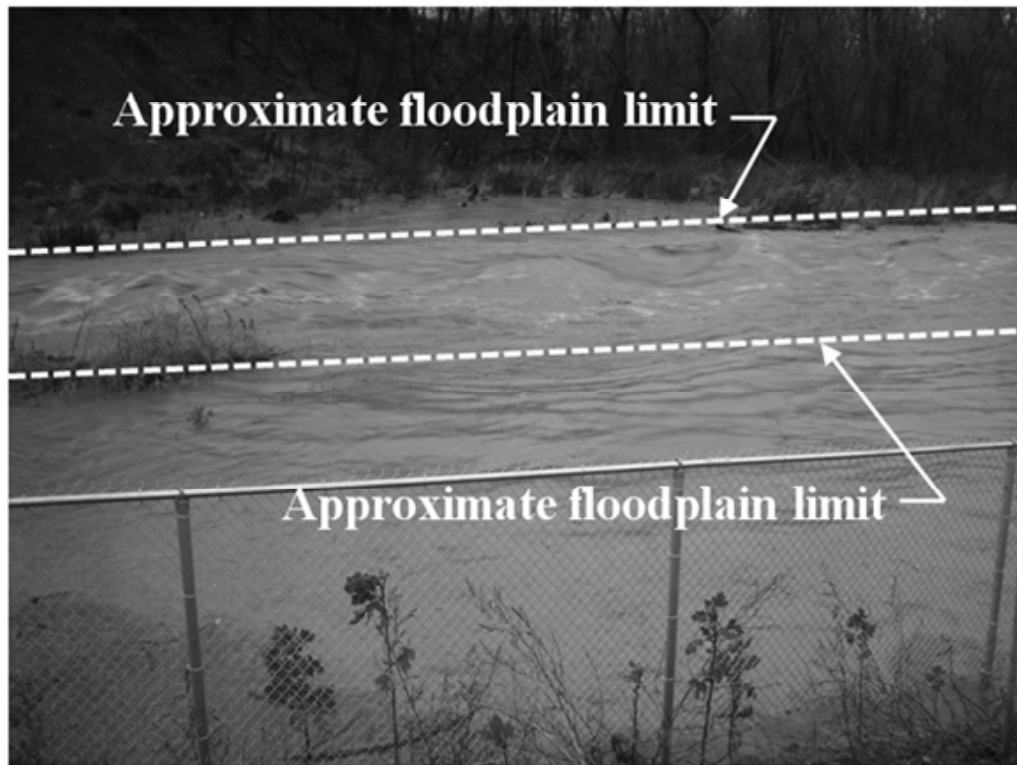


**Figure 3.1.** Standing wave pattern in Little Etobicoke Creek at York Mills (Site 7) at  $32.4 \text{ m}^3/\text{s}$ . Bankfull discharge is  $23.8 \text{ m}^3/\text{s}$ .

Here, the results of a study of both the urban gravel-bed channel planforms and their bed morphologies is presented. Where applicable, results are compared to rural gravel-bed channels in the same hydrophysiographic region (Annable, 1996a). Techniques in large clast particle tracking are employed to investigate the pulsing of particles and the development of keystone and armour layers throughout each reach.

Calibrated one-dimensional models are also developed for each site to examine the flow regimes under a range in discharge conditions to relate energy dissipation to bedforms.

## 3.2 BACKGROUND

The characteristic planforms of alluvial and bedrock rivers have been well studied for many decades finding striking similarities between channel pattern and bankfull width and axiomatically discharge (Horton, 1945; Leliavsky, 1955; Leopold and Wolman, 1960; Brice, 1984; Williams, 1986). Many have attempted to stratify channels into statistically-distinct taxonomies in order to address the specific channel forms and processes unique to certain channel morphologies (Simons and Richardson, 1963; Kellerhals *et al.*, 1972; Rosgen, 1996; Montgomery and Buffington, 1997; Wohl and Merritt, 2008). Common metrics used to stratify channels into various morphologies include: valley form, cross-sectional relief, bed-material size and supply, flow regime, sediment-transport relationships, fluid-mechanics parameters, and channel slope.

Similarity in river-meander patterns has been expressed quantitatively through empirical relationships relating the geometric properties of meanders to one another such as:

$$\lambda \propto W_{bf}, \Gamma \propto W_{bf}, A_p \propto W_{bf}, R_C \propto W_{bf} \quad (3.1a - d)$$

where  $\lambda$  is the meander wave length,  $\Gamma$  is the meander belt width,  $A_p$  is the meander amplitude, and  $R_C$  is the radii of curvature as measured along the centre line of the bankfull channel. Belt width and meander amplitude are measured normal to the valley trend (Brice, 1973; Annable, 1996b) whereas meander wave length is measured parallel

to the valley trend. The majority of studies have related the proportionalities in Equation (3.1) to power-function forms by regression analysis. Summaries of planform-meander geometry relationships from several sources can be found in FISRWG (1998) and Biedenharn *et al.* (2008).

### **3.2.1 Bed Morphology**

Bed-material supply in step-pool channels is principally derived from colluvial sources (keystones) plus alluvial material from bed and bank erosion. The entrainment, transport, and deposition of the larger keystones has been observed to occur only in larger magnitude flood events, typically exceeding a 30-year return period (Grant *et al.*, 1990; Chin, 1999; D'Agostino and Lenzi, 1997; Curran and Wilcock, 2005). Energy dissipation in these environments is due to a combination of grain roughness, bedform roughness, turbulence, and frequent hydraulic jumps. Several studies have related the step height ( $H_{RP}$ ) and length ( $L_{RP}$ ) from step crest to downstream pool invert to channel bed slope and have suggested that the flow regime is deterministic in the frequency of step-pool formations (Abrahams *et al.*, 1995; D'Agostino and Lenzi, 1998; Grant and Mizuyama, 1991; Kennedy, 1963).

Channels with lower slope transitions to run-pool dominated morphologies derive the majority of their bed material from bend and bank erosion and throughput. Run-pool morphology as defined here is consistent with the plane-bed definition of Montgomery and Buffington (1997) but it has been labeled differently to avoid confusion with the kind of plane-bed form associated with a particular flow regime in sand-bed channels (Simons and Richardson, 1963). Although there can be large erratics within the run-pool

dominated morphologies, most of the bed material is entrained at notably lower return periods than the keystone grains associated with step-pool channels (Montgomery and Buffington, 1997). Energy dissipation per unit length occurs from grain roughness, turbulence, and secondary flow in bends (Rozovskii, 1957; Wohl and Merritt, 2008).

Lower gradient single-thread streams derive the majority of their sediment from throughput, bank erosion, and bed erosion, with the majority of bed-load transport occurring at flows exceeding effective discharge. One caveat is that if the channel beds are significantly coarsened by armoring, larger return periods are required to mobilize their material. Madej (2001) noted that in addition to bed armouring, imbrication, and packing, the magnitude and duration of flows able to mobilize bed material can have a significant impact on channel stability and form. Madej (2001) further suggests that bedforms can be buried during such discharges and sediment pulses but later re-form through scour and deposition returning to self-organized heterogeneous channels with regularly-spaced bedforms. Energy dissipation per unit length occurs from grain roughness, turbulence, secondary flow in bends, and floodplain form roughness during flood flow conditions.

Rhythmic spacing and origin of pools and riffles are characteristic of many low-gradient single-thread alluvial channels (Leopold and Wolman, 1960; Keller, 1971; Montgomery and Buffington, 1997) with pool-pool spacing ( $L_{IP}$ ) by bankfull width typically ranging between  $3 \leq L_{IP}/W_{bf} \leq 9$  and averaging  $L_{IP}/W_{bf} \approx 5.5$  (Keller and Melhorn, 1978). There are many theories to explain the formation of pool-riffle sequences, relating them to the: time rate of energy expenditure (Yang, 1971), velocity and shear reversals from low- to high-discharge events (Keller, 1971; Hey, 1976), and

macro-turbulent eddies generated at the boundaries of straight uniform channels that produce alternating regions of acceleration and deceleration of flow leading to pool-riffle formations (Yalin, 1971). Hey (1976), based upon field evidence, suggested that the spacing of riffles should typically be observed as a function of channel width spaced by  $2\pi W_{bf}$ .

### 3.3 METHODS

Chapter 2 provides details of the land-use conditions and effective catchment delineations for both the urban and rural watercourses studied here. Effective catchment areas rather than topographic boundaries are used to allow for changes in the limits of contributing basin areas due to alterations in storm-sewer networks, basin capture, etc. (Leopold, 1968; Booth *et al.*, 2004; Jordan *et al.*, 2009). Table 2.1 listed general reach characteristics, channel morphology, and adjacent land use. Figure 3.2 illustrates typical reach characteristics at each site.

Longitudinal profiles and series of cross sections at the upper third of riffles and runs were surveyed along each reach, using a total station and geo-referenced with a 1<sup>st</sup>-order differential GPS. Bankfull stage was placed at the top of the convex (inside) bend on point bars for riffle-pool dominated channel morphologies (Wolman and Leopold, 1957) and at the stage of the minimum-width depth ratio in the case of the run-pool channel (Wolman, 1955). Bankfull discharge ( $Q_{bf}$ ) was field-verified during flood events at each reach and the timing reconciled with the instantaneous discharge ( $Q_i$ ) at each gauge station. Further details of bankfull calibration in urban environments can be found in Chapter 4.

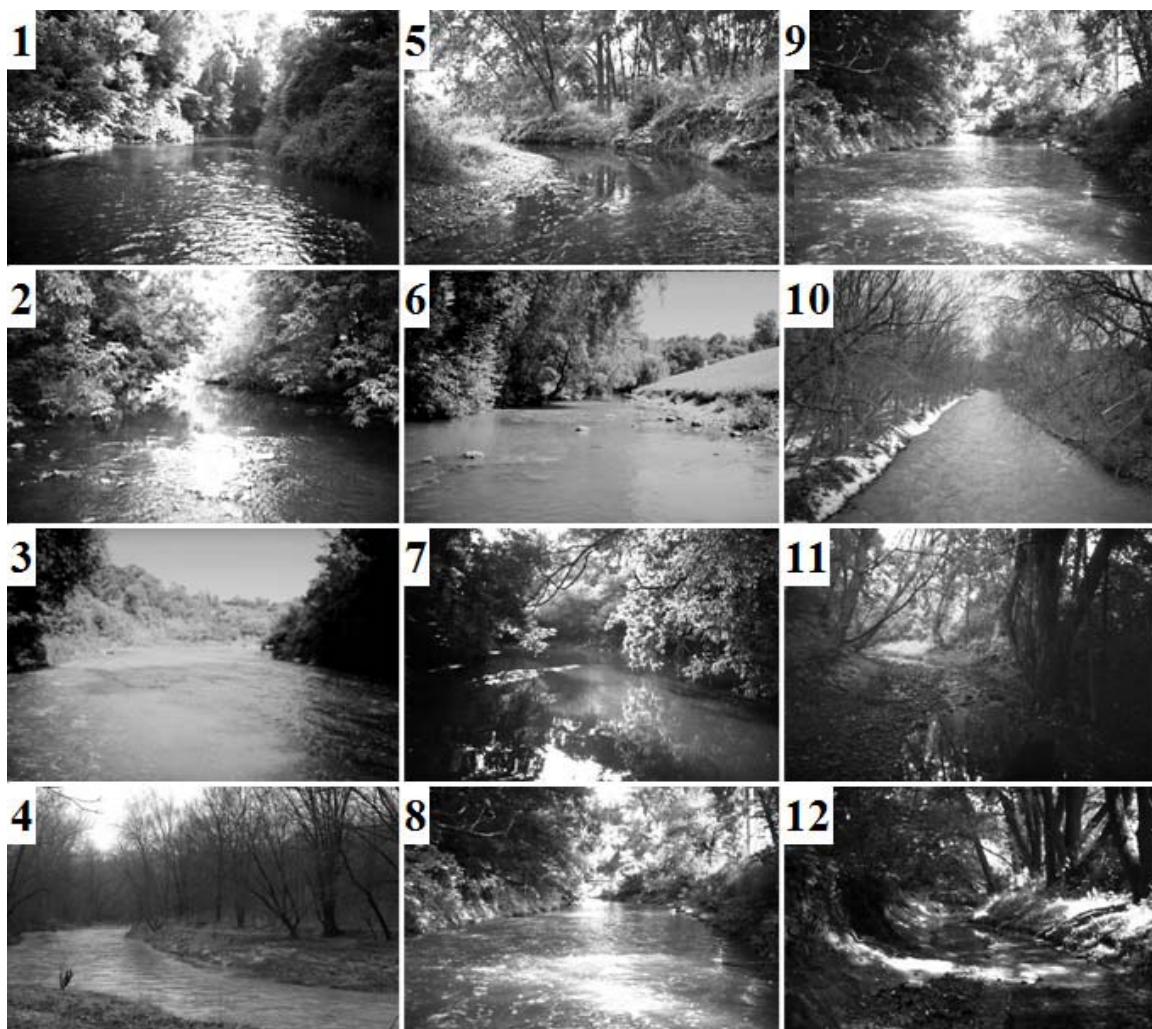


**Figure 3.2.** Study reach images. *Note: Numbers denote the site reference numbers listed in Table 2.1.*

Channel features mapped included crests and bottoms of riffles and runs, pool inverts, and any other notable changes in channel bed slope or geomorphic features (Figure 3.3). Cross sections detailed the bankfull channel limits, terraces, and floodplain features meeting the parameterization requirements of HEC-RAS 4b (USACE, 2004) for developing one-dimensional hydraulic models. Parameters at each cross-section and longitudinal profile included: bankfull width, bankfull depth ( $D_{bf}$ ), and bank-slope angles ( $\phi$ ), pool depth ( $D_P$ ) relative to bankfull stage, change in elevation ( $H_R$ ) along each riffle

length ( $L_R$ ), net elevation change ( $H_{RP}$ ) and distance ( $L_{RP}$ ) between the crest of a riffle and the immediate downstream pool invert, and the inter-pool length between two adjacent pools ( $L_{IP}$ ). Streamwise distances were measured relative to the bankfull channel centre line. The metrics identified in Figure 3.3 are consistent with those used by Grant *et al.* (1990), Chin (1999), D'Agostino and Lenzi (1997), and Curran and Wilcock (2005), which have been used to interpret morphological spacings in step-pool channels.

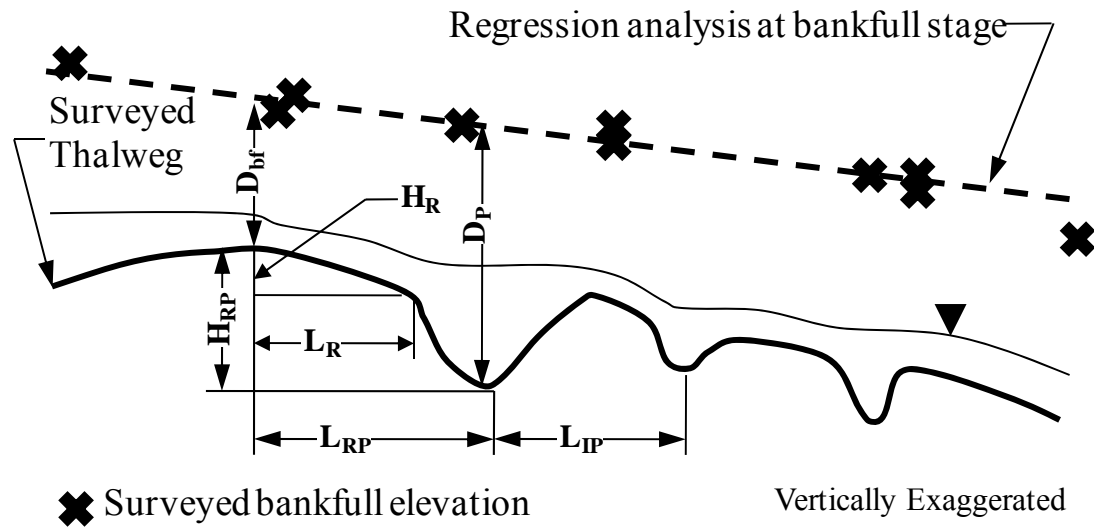


**Figure 3.3.** Typical measurements of longitudinal profile.

### 3.3.1 Bed Material

To investigate the effects of discharge pulsing on bed-material movement, particle tracking of large clasts was undertaken. Particles larger than the  $D_{75}$  of the bed material were commonly selected as they form along the crests of riffles, providing grade control and keystone positioning. Particles were pressure washed *in-situ* if imbedded at low-flow conditions, allowed to dry and then painted: poor water quality often created algae layers that required cleaning prior to painting. Particle tracking was not attempted at Site 12



because the largest particle sizes were too small to be effectively painted. Different paint colours were used on different riffles to increase tracking capabilities. Travel distances were measured using either a total station or GPS. Particles were repeatedly painted over a 5-year period to track clast-transport distances. Radio frequency identification (RFID) tags were in their infancy of application at the time of the study and beyond the financial limits of the study.

Bed-material (pavement) samples were also obtained on series of riffles and runs at each study reach following the methods of Klingeman and Emmett (1982), Church *et al.* (1987), Annable (1996b), and Bunte and Abt (2001). Four to six samples were obtained on each morphological feature resulting in eighteen to twenty-four bed-material samples per site. Samples were subject to grain-size analysis using dry sieving methods at 0.5-phi intervals (Friedman and Sanders, 1978).

The discharge ( $Q_C$ ), annual frequency of events ( $N_C$ ), and cumulative annual duration ( $T_C$ ) exceeding critical shear of reach for averaged  $D_{50}$  and  $D_{84}$  bed-material grain sizes at each site were determined employing the dimensionless Shields parameter ( $\tau_i^*$ ) to investigate the effects of discharge pulsing on bedforms.  $\tau_i^*$  for a given grain size  $D_i$  is defined as  $\tau_i^* = \rho u_*^2 / (\gamma_s - \gamma) D_i$ , where  $\rho$  is the fluid density,  $\gamma_s$  is the specific weight of the solid, and  $\gamma$  is the specific weight of the fluid. Shear velocity ( $u_*$ ) is defined by  $u_* = \sqrt{\tau_b / \rho}$  where bed shear ( $\tau_b$ ) is defined as  $\tau_b = \gamma R_h S_0$  where  $S_0$  is the channel bed slope and  $R_h$  is the hydraulic radius for a given discharge ( $Q_i$ ). The dimensionless critical Shields parameter  $\tau_{sCi}^*$  was determined using a modified form of Brownlie's (1981) curve as outlined by Parker *et al.* (2007) of the form:

$$\tau_{\text{Sci}}^* = \frac{1}{2} \left[ 0.22 \text{Re}_{\text{pi}}^{-0.6} + 0.06 \times 10^{\left(-7.7 \text{Re}_{\text{pi}}^{-0.6}\right)} \right] \quad (3.2)$$

The dimensionless particle Reynolds number ( $\text{Re}_{\text{pi}}$ ) used in Equation (3.2) is defined as (Parker *et al.*, 2007):

$$\text{Re}_{\text{pi}} = \frac{\sqrt{(G-1)gD_i D_i}}{\nu} \quad (3.3)$$

where  $g$  is gravitational acceleration and  $\nu$  is the kinematic viscosity. Equation (3.2) was used rather than that offered by Brownlie (1981) as Parker *et al.* (2007) identified that Equation (3.2), based upon the analysis of incipient-motion data by Montgomery and Buffington (1997), represents the lower range in critical Shields number rather than the average value of critical Shields number offered by Brownlie (1981).

At-a-station hydraulic geometry developed from the historical field records at each gauge station could be used to calculate the hydraulic radius ( $R_h$ ) needed in the shear-stress calculations above. However, Chapter 4 identifies shortcomings in the representativeness of these data as the hydraulic geometry reflected conditions of the gauge site (commonly occurring at bridges) rather than the natural channel morphology. Rather, one-dimensional HEC-RAS (USACE, 2004) models were developed and calibrated for each site to produce at-a-station hydraulic geometry of the channels and floodplain relief at each surveyed cross section on riffles or runs of the form:

$$W = \text{fn}(Q_i), D = \text{fn}(Q_i), \bar{V} = \text{fn}(Q_i), V_{\text{mc}} = \text{fn}(Q_i), R_h = \text{fn}(Q_i) \quad (3.4 \text{ a - e})$$

where  $W$  is the flow top width,  $D$  is the average flow depth,  $\bar{V}$  is the average channel velocity,  $V_{mc}$  is the main channel velocity, and  $R_h$  is the hydraulic radius. Relationships were developed for Equation (3.4) for flows ranging from  $0 < Q \leq Q_{100}$ , where  $Q_{100}$  is the 100-year return period based on a Log Pearson III analysis (USGS *Bulletin 17B*, 1982). Each calibrated model simulated one-hundred discrete discharge events evenly distributed between  $Q_{min} \leq Q \leq Q_{100}$  to produce geometry discharge relationships.

Reach-based channel roughness, used in the calibration of the one-dimensional models, was estimated employing the Wolman (1954) pebble-count method at a series of riffles, pools, and runs appropriate to each study site. Grain-size distribution results from each riffle were used to estimate the Manning's roughness coefficient ( $n$ ), employing Chow's (1959) form of the Strickler (1923) equation as defined by  $n = 0.0417 D_{50P}^{1/6}$ , where  $D_{50P}$  is defined as the log-normal median grain size of the pebble-count grain-size distribution.

The continuous instantaneous discharge records ( $Q_i$ ) from each site were then entered into Equation (3.4) developed for each site to calculate the various parameters of interest. It is noted that all discharge values used throughout the analysis utilized systematic 15-minute interval discharge data for the period 1969 to 2008 unless a shorter period of record was available.

### 3.4 RESULTS

Bivariate meander geometry relationships were derived for reach belt width ( $\Gamma$ ), average meander wave length ( $\bar{\lambda}$ ), and average radius of curvature ( $\bar{R}_c$ ) versus bankfull width ( $\bar{W}_{bf}$ ) for both the urban and rural reaches (Figure 3.4). The urban and rural data

sets were found to be coincident for  $\Gamma$ , but not coincident for either  $\bar{\lambda}$ , or  $\bar{R}_C$  as a function of  $\bar{W}_{bf}$  ( $p = 0.08$ ,  $p = 0.03$ ,  $p = 0$ , respectively). The urban and rural data sets were also compared to other data sets across North America (Leopold and Wolman, 1960; Williams, 1986) for  $\Gamma$ ,  $\bar{\lambda}$ , and  $\bar{R}_C$  as a function of  $\bar{W}_{bf}$  (Figure 3.5) which were not found to be coincident for  $\Gamma$  ( $p = 0.008$ ), and coincident for  $\bar{\lambda}$  and  $\bar{R}_C$  ( $p = 0.11$ ,  $p = 0.68$ , respectively). The variability in planform geometry has previously been attributed to valley confinement, variability and heterogeneity in geology, and controls in riparian vegetation (Zimmerman *et al.*, 1967; Schumm, 1969; Schumm *et al.*, 1984; Hickin, 1984; Thorne, 1990).

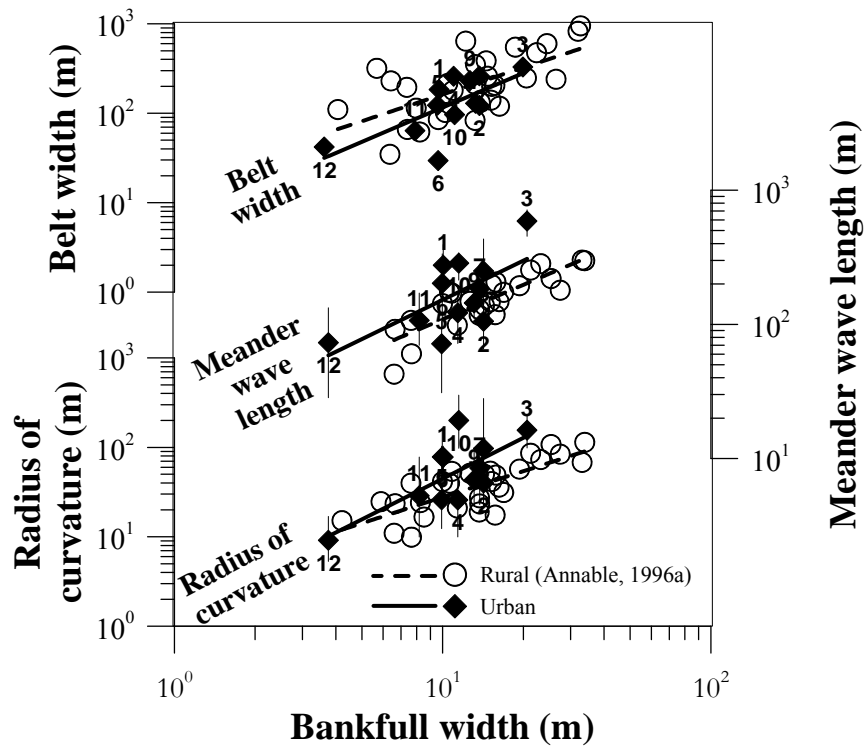


**Figure 3.4.** Belt width, meander wave length, and radius of curvature ( $R_C$ ) versus average bankfull width for urban and rural streams in the same hydrophysiographic province. *Note: Whisker extents represent the maximum to minimum range in parameters measured.*

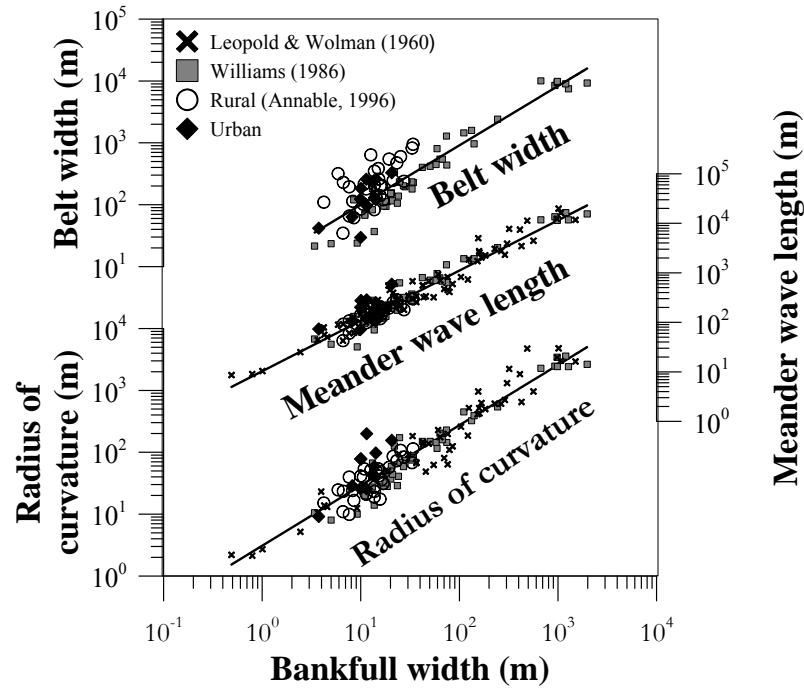


**Figure 3.5.** Belt width, meander wave length, and radius of curvature ( $R_C$ ) versus average bankfull width for urban and rural Ontario streams (Leopold and Wolman, 1960; Williams, 1986).

Power-fit regression analysis of each metric against average bankfull channel width shows that there is a modest decrease in belt width (although statistically not significant), increase in average meander wave length, and increase in average radius of curvature as a function of average bankfull width (Figure 3.4). These responses are common to underfit valleys where lateral channel migration is limited by the valley walls or in the case of urban areas by surrounding development and infrastructure. The increased meander wave length is also in accordance with constituent relationships offered by Schumm (1969) where meander wave length may increase with increases in discharge and decreases in bed-material load as is observed in these study reaches (Equation (2.18)).

Changes in the urban channel meander geometry may also be related to the changes in effective flows in the urban settings. Carlston (1965) suggested that flows responsible for the transport of sediment, processes related to point-bar deposition, and outer bank erosion, shape and form the dimensions of unconstrained meanders leading to stream-wise migration. Chapter 2 observed significant increases in the annual frequencies of bankfull discharge (a 1:1 correspondence ( $r^2 = 0.97$ ) between bankfull discharge and effective discharge was also observed) as the percent urban land use increased. The effects of discharge pulsing are discussed below in further detail.

### 3.4.1 Bed Morphology

Inter-pool spacing was evaluated by comparing reach  $\bar{\lambda}/\bar{W}_{bf}$  versus  $\bar{L}_{ip}/\bar{W}_{bf}$  (Figure 3.6a). The urban and rural data sets were found to be weakly coincident ( $p = 0.13$ ), but both parallel trend and intercept tests were not significant ( $p = 0.05$ ;  $p = 0.05$ , respectively). The rural reaches of Annable (1996a) closely follow a 2:1 trend where the invert of pools are found on the outside of bends (Leopold *et al.*, 1964; Hey, 1976). Conversely, in the urban reaches, meander wave lengths increased, relative to bankfull width and pools were found to occur on a similar frequency commonly ranging between  $5 \leq W_{bf} \leq 8$ . The urban pool spacing shows a trend independent of meander wave length, which closely relates to distance between successive pools ( $2\pi W_{bf}$ ) as suggested by Hey (1976) and Thorne (1997) who assumed that the maximum flow-structure eddies occupy half of the channel width. Observations here also corroborate Wolman and Leopold (1957; Leopold and Wolman, 1960) who proposed that the flow structure is responsible

for complementary matching waveforms in bed topography and planform of meandering channels.

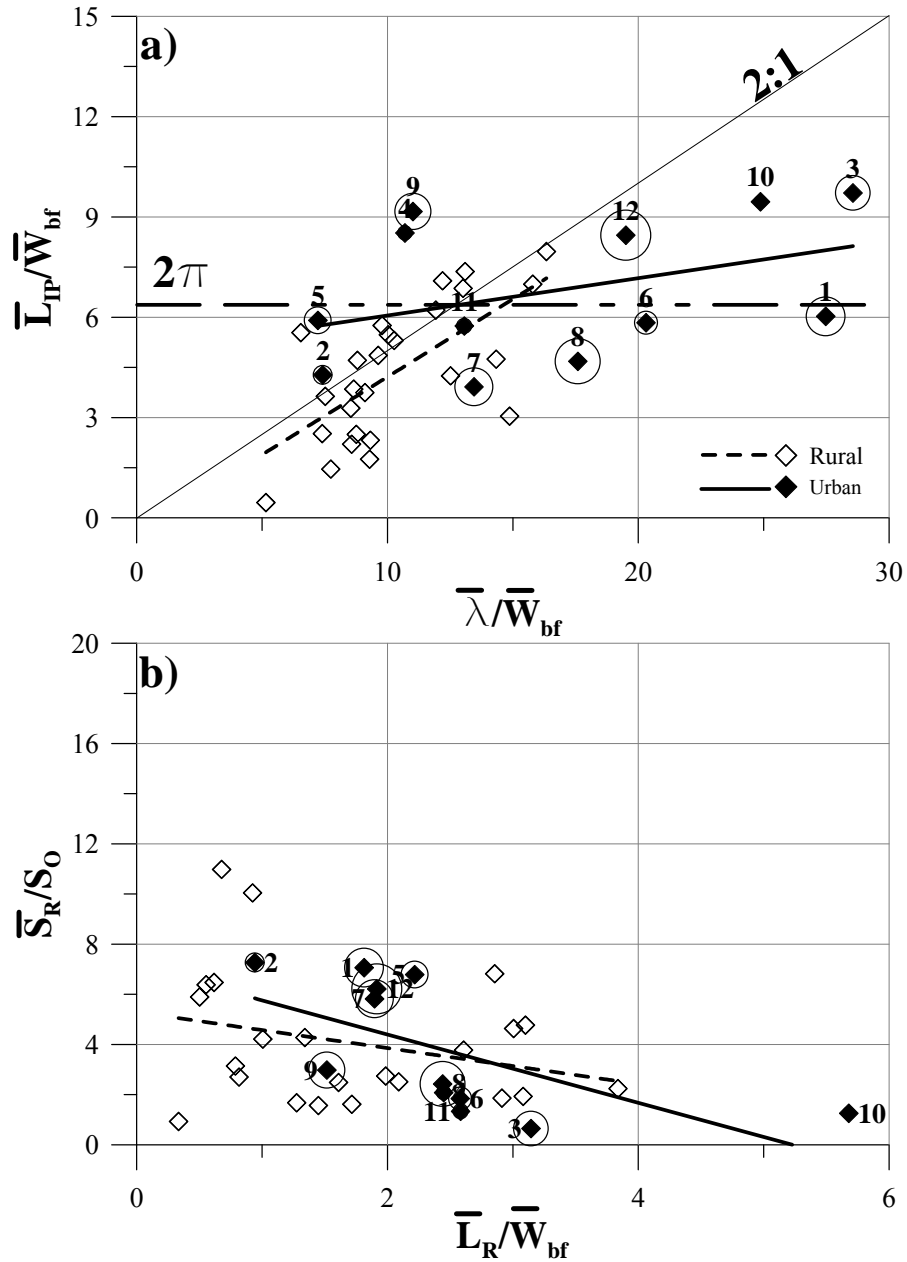


**Figure 3.6.** a) inter-pool length ( $\bar{L}_{IP}$ ) by bankfull width ( $\bar{W}_{bf}$ ) versus meander wave length ( $\bar{\lambda}$ ) by  $\bar{W}_{bf}$  and b) riffle slope ( $\bar{S}_R$ ) by bed slope ( $S_o$ ) versus riffle length ( $\bar{L}_R$ ) by bankfull width ( $\bar{W}_{bf}$ ). *Note: Increasing circle sizes represent increasing percentage of urban land use in each watershed.*

Average reach riffle slopes ( $\bar{S}_R$ ) normalized by channel bed slopes ( $S_0$ ) were compared against average riffle length ( $\bar{L}_R$ ) normalized by bankfull width ( $\bar{W}_{bf}$ ) (Figure 3.6b). The urban and rural data sets were found to be coincident ( $p = 0.80$ ) with the rural data set from Annable (1996a). Inspection of Figure 3.6b shows that in the majority of reaches where larger percentages of urban land use occur (larger circumscribed circles) riffle slopes were often steeper than in lower percentages of urban land use (smaller circumscribed circles). Steeper riffles reflect limited bed-load supply (Chapter 2) and ongoing armouring resulting from anthropogenic inputs of coarser material – such as riprap and debris from failed channel works.

The characteristics of pool depths measured between inverts and bankfull stage ( $D_p$ ) normalized by average bankfull depth measured at riffles and runs ( $\bar{D}_{bf}$ ) versus  $R_C/\bar{W}_{bf}$  were inventoried (Figure 3.7). For pool depths on bends (Figure 3.7a), results produce an envelope that is similar to lateral channel mobility envelopes reported by Hickin and Nanson (1975), Chang (1988), and Julien (2002). These studies indicate that the maximum likelihood of lateral mobility occurs when  $R_C/\bar{W}_{bf} \approx 2.0$ , which is related to the greatest intensity in secondary flow (Rozovskii, 1957) resulting from centripetal forces (helical flow). Bagnold (1960) suggested that a meander bend with  $2 \leq R_C/W \leq 3$  is associated with minimization of energy losses due to asymmetry in the flow distribution. Values of  $R_C/\bar{W}_{bf} > 10.0$  relate to the run-pool morphology of Site 10, where the radii of curvature are relatively large compared to the bankfull width. As  $R_C/\bar{W}_{bf} \rightarrow 2.0$ , the intensity of the secondary flow increases in flood stage, relative to sharper or more subtle bends. A common field observation correlated deeper pools on



bends with significant bank vegetation, which was inhibiting lateral erosion resulting in deeper pools.

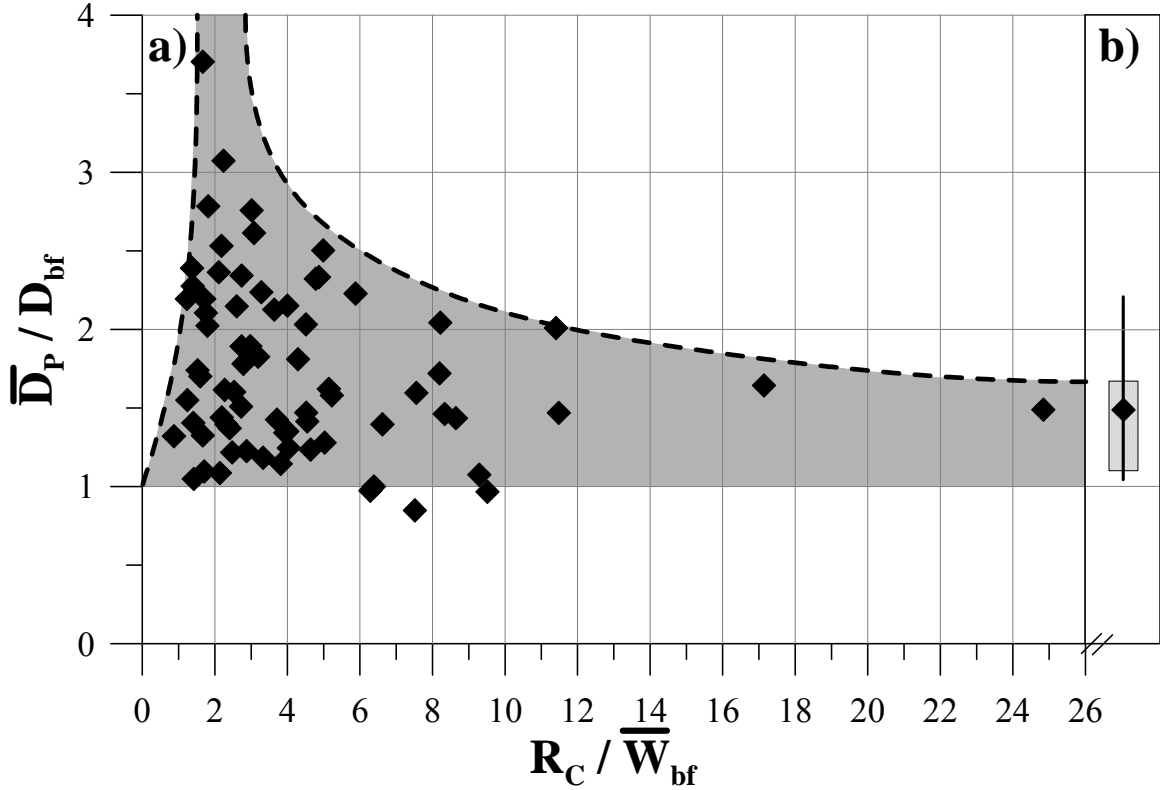


**Figure 3.7.** Pool depths ( $D_P$ ) at bankfull stage by average reach bankfull depth ( $\bar{D}_{bf}$ ) versus radius of curvature ( $R_C$ ) by average reach bankfull width ( $\bar{W}_{bf}$ ) for a) bend pools and b) box-and-whisker plot for in-line pools.

Pools between bends, hereinafter referred to as in-line pools, were found to be much shallower. Figure 3.7b consolidates all of the measured in-line pools from all study sites into a single box-and-whisker plot. The 25<sup>th</sup> and 75<sup>th</sup> in-line pool depths were found to range between  $1.17 \leq D_P / \bar{D}_{bf} \leq 1.73$  and averaged  $1.58 \bar{D}_P / \bar{D}_{bf}$ .

Average spacing of pools in the urban sites closely approximates  $2\pi W_{bf}$ , which was the assertion of Wolman and Leopold (1957; Leopold and Wolman, 1960) for the flow structure responsible for complementary wave forms producing bed and planform

structure. Standing waves during flood events (Figure 3.1) merited investigation into the possible manifestation of pool (and riffle) frequencies as a bedform resistance response that dissipates additional energy in the urban watercourses (similar to Simons and Richardson (1963) and Van Rijn (1984) in sand-bed streams). The riffle-crest to pool-depth height ( $H_{RP}$ ) versus inter-pool distance ( $L_{IP}$ ) were compared to the relationships developed by Van Rijn (1984) for the wave length and amplitude of dunes and ripples in the sub-critical flow regime where he found that  $L_{IP} \approx 7.3 H_{RP}$ : this relationship was also close to the theoretical value offered by Yalin (1964) of  $L_{IP} \approx 2\pi H_{RP}$ . A regression analysis between the riffle-crest height to pool invert ( $H_{RP}$ ) versus inter-pool distance ( $L_{IP}$ ) was developed (not shown) which found that  $L_{IP} \approx 73H_{RP}$ , which is significantly larger than the ratio obtained by either Van Rijn (1984) or Yalin (1964).

Wohl and Merritt (2008), analyzing an international data base of 335 step-pool, run-pool, and riffle-pool channel reaches in gravel and courser-grained material, identified a continuum of transformations between steep to gentle slopes in a manner that minimizes variance in hydraulic roughness, maximizes flow resistance, minimizes downstream variability in energy expenditure and, where bedforms are present, renders hydraulic radius and bedform amplitude ( $H_{LR}$ ) interdependent. Assuming that energy is proportional to both  $Q_i$  and  $S_o$ , they also found that bedform frequency evolves to maximize flow resistance. The ratio of  $H_{LR}/L_{RP}$  versus  $S_o$  are compared for the urban sites and steeper channels in Figure 3.8. The continuum of bedform dimensions as a function of slope (and thus energy) supports the contention of Wohl and Merritt (2008) that the frequency and spacing of bedforms maximize resistance to discharge. Chapter 2 found increased annual volumes of flow exceeding bankfull discharge that spilled onto

the adjacent floodplains. The increased volume and frequency of flood flows (and thus of energy) and the observed increase in frequency of pools in the urban sites supports the assertion that manifestations in the channel beds are reach responses to maximize flow resistance. Analysis of calibrated one-dimensional site modelled flows between  $0 < Q_i \leq Q_{100}$  found maximum Froude numbers ( $F_r$ ) within the bankfull channel limits to range between  $0.62 \leq F_r \leq 0.84$ , but never approach the critical flow regime where a plane-bed channel develops standing wave patterns. The sub-critical flow regime coupled with field observations of standing waves are consistent with the presence of dune forms similar to those observed in sand-bed streams (Simons and Richardson, 1963).

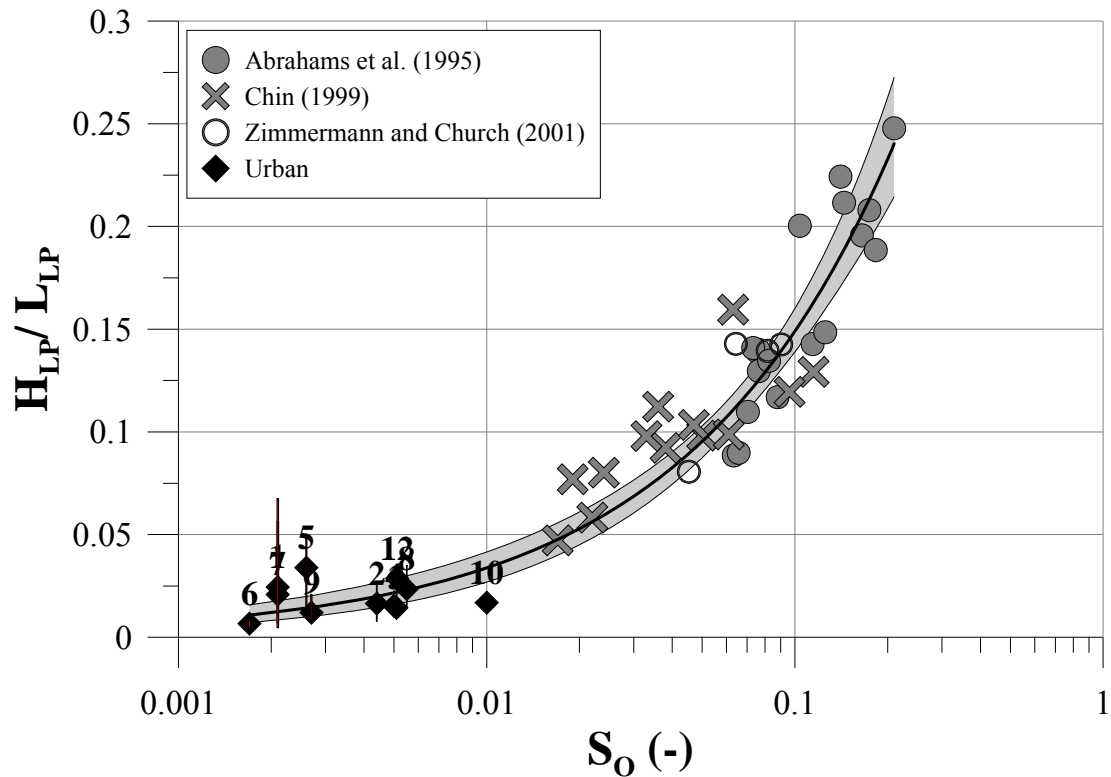


**Figure 3.8.** Riffle crest to pool invert height ( $H_{LP}$ ) by length of crest of riffle to pool invert ( $L_{LP}$ ). *Note: Whisker extents represent the maximum to minimum range in ratios of each study reach. Grey envelope represents the predicted 95<sup>th</sup>-percentile confidence limits.*

### 3.4.2 Discharge Pulsing

The graph of average annual discharge events where  $\tau_{C50}$  and  $\tau_{C84}$  of the bed material were exceeded is shown in Figure 3.9. On average, discharges in rural streams where  $D_{50}$  particles were mobilized commonly occurred less than one to three times and for  $D_{84}$  particles less than once per year. In a few cases, the average annual number of discharge events mobilizing both  $D_{50}$  and  $D_{84}$  grain sizes was greater than 1.0 but only in medium gravel and smaller substrates where the standard deviation between the  $D_{50}$  and  $D_{84}$  grain sizes was small.

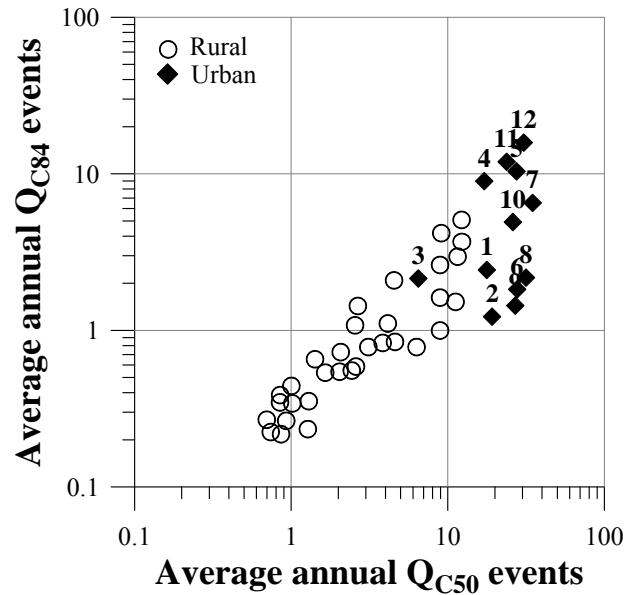


**Figure 3.9.** Average annual number of observed discharge events where critical shear of  $D_{50}$  particle grain sizes ( $Q_{C50}$ ) versus  $D_{84}$  particle grain sizes ( $Q_{C84}$ ) are exceeded.

Discharge event frequencies where both  $\tau_{C50}$  and  $\tau_{C84}$  of the bed material were exceeded were much greater for the urban streams (Figure 3.9). Commonly there were twenty to thirty events per year that mobilized the  $D_{50}$  grain sizes and one to fifteen events for the  $D_{84}$  grain sizes, resulting in active mobile armour layers. There was less

frequent mobilization of  $D_{50}$  and  $D_{84}$  grain sizes at Site 3, which has the largest grain sizes and also very angular clast shapes (Table 3.1 – Magalhaes and Chau (1983)).

**Table 3.1.** Reach geometry and bed-material characteristics.

Bankfull Channel Characteristics					Bed Material				
Site Reference No.	Bed Slope (m/m)	Discharge ( $m^3/s$ )	Average Width (m)	Average Depth (m)	$D_{16}$ (mm)	$D_{25}$ (mm)	$D_{50}$ (mm)	$D_{75}$ (mm)	$D_{84}$ (mm)
1	2.1E-03	8.8	14.9	0.93	7.4	20.3	30.4	36.8	39.5
2	4.4E-03	14.2	13.0	0.43	5.9	17.8	30.4	47.4	60.6
3	5.1E-03	47.8	19.1	0.83	42.2	51.8	92.5	195.7	276.7
4	5.0E-03	11.1	11.7	0.47	21.1	26.7	36.8	50.3	56.4
5	2.6E-03	12.5	9.7	0.77	4.2	5.5	19.0	28.8	33.3
6	1.7E-03	12.8	10.2	0.81	20.4	27.3	36.3	51.4	63.9
7	2.1E-03	23.8	14.1	1.10	4.7	6.3	25.1	40.2	45.4
8	5.5E-03	18.4	11.7	1.15	18.2	29.2	47.3	160.9	244.1
9	2.7E-03	13.8	13.1	0.57	20.5	25.6	34.9	66.1	83.9
10	1.0E-02	12.4	10.8	0.71	33.4	40.0	51.8	91.1	118.2
11	1.0E-02	3.2	8.7	0.76	4.5	5.4	18.7	33.8	39.9
12	5.1E-03	2.1	3.8	0.82	4.5	5.4	18.7	33.8	39.9

Changes in the urban hydrology regimes have resulted in annual increases in average cumulative duration of flows exceeding both  $\tau_{C50}$  and  $\tau_{C84}$ , compared to the rural watersheds (Figure 3.10). Commonly, the cumulative annual duration of flows exceeding  $\tau_{C50}$  was greater than 2% (7.3 days), while the cumulative annual duration of flows exceeding  $\tau_{C84}$  was less than 2% for the urban sites studied. The rural sites were below these ranges. Implicit within a decreased duration of annual flows exceeding critical shear values in the rural streams is a decreased frequency of channel-forming flows and even less frequent longer duration flows that are able to move the larger grain sizes (Leopold *et al.*, 1964; Chang, 1988; Parker *et al.*, 2007).

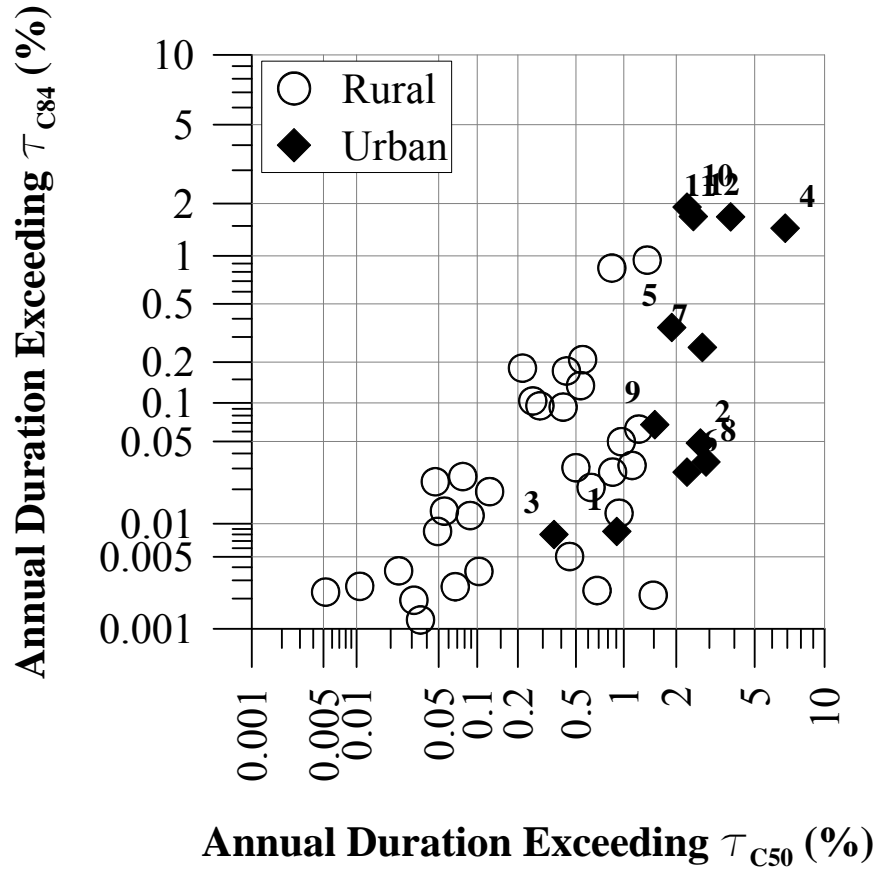


**Figure 3.10.** Average annual duration of time exceeding thresholds of  $\tau_{C84}$  versus  $\tau_{C50}$ .

In the urban sites, the increased cumulative annual duration of flows exceeding both  $\tau_{C50}$  and  $\tau_{C84}$  and the increased frequency of discharge events exceeding critical thresholds results in many brief events mobilizing the bed material and producing sediment pulses. Typically, events exceeding critical shear conditions for  $D_{84}$  values lasted between 1 to 5 hours each and events exceeding the  $D_{50}$  threshold averaged 4 to 8 hours each. There were longer duration events exceeding either  $\tau_{C50}$  or  $\tau_{C84}$  during the spring freshet when the stream beds were commonly mobile between 2 to 5 days, including common diurnal fluctuations across the critical shear thresholds. In the rural stream channels, typically only zero to two events mobilized the  $D_{50}$  bed material, dominated by spring freshets of 5- to 9-day durations.

Over a 5-year period, the pulsing of the bed material was evaluated by field particle tracking in all but the smallest urban-stream channel (Site 12). As is common to particle tracking using the methods described above, losses were between 63% and 78% of the initial complement. Losses were attributed to burial, abrasion, transport to distances beyond the inventoried limits, and in this study, some deliberate removals to build artistic piles on the adjacent floodplains. Particle travel distances ( $L_{\square}$ ) were normalized relative to the bankfull channel width and classed into  $2L_{\square}/W_{bf}$  categories.

The results show that the majority of the particles travelled less than two bankfull channel widths downstream in any given one event (Figure 3.11). The primary exception to this observation occurred on bends where particles were either transported through the bends or were deposited on the point bars. Clast-transport distances dramatically decreased after twelve bankfull widths downstream of the original source location. The short travel distances of the larger clasts in each study reach further demonstrate that short pulses of sediment are occurring for given events. Inventories of clast-transport distances showed that travel distances increased with increased duration above critical flow conditions.

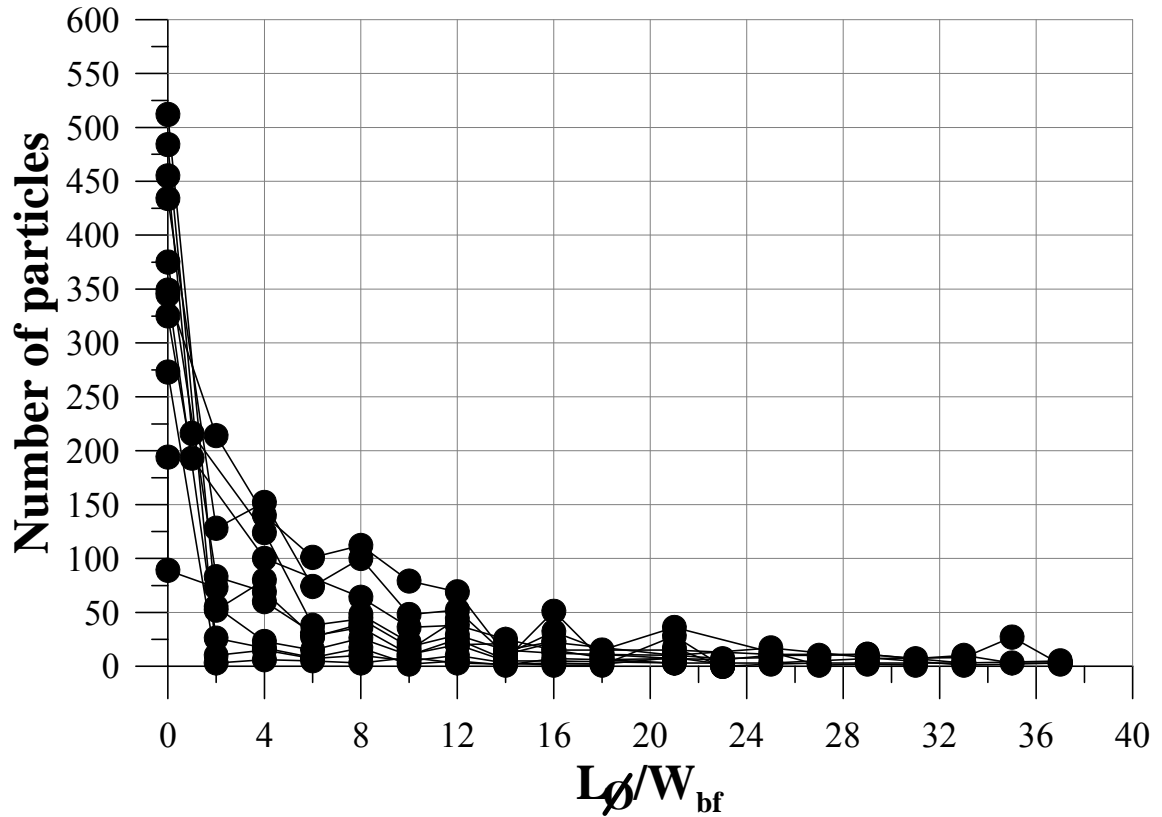


**Figure 3.11.** Number of observed clast particles versus clast-travel distance ( $L_0$ ) by average bankfull width.

### 3.5 SUMMARY

Manifestations in channel planform and bedform are responses in a river system to maximizing the flow resistance, while minimizing variability in energy expenditure in a downstream direction. Increases in meander wave length and radii of curvature of urban-stream channels, compared to rural watercourses in the same hydrophysiographic region, are surface expressions of increased flood frequency (pulsing) and volume but decreased bed-load supply.

Increased frequency of pools (and riffles) between adjoining bends in the urban channels is caused by both sediment pulsing of larger clasts and the creation of ‘dune-



*like*' bedforms to maximize flow resistance. The short travel distances of larger clasts within each reach result from the flashy convective storm events observed in the region combined with changes in land-use and overland routing characteristics. The short travel distances allow keystones to be placed (commonly they are coarse anthropogenic material) that serve as frequent grade-control positions along each watercourse resulting in riffles as the hydrographs recede with shallower pools (compared to bends) between the riffle crests.

The frequency of riffle crests (and pools), field observations of standing waves during flood flows, and observed increase in flood flows above bankfull stage (thus energy) also support previous observations that bedforms may be developing as an alternative means of dissipating the increased stream energy external to the reaches by maximizing flow resistance. Distances between pool depths is much greater ( $L_{IP} \approx 73H_{RP}$ ) than those observed in sand-bed streams ( $L_{IP} \approx (2\pi \text{ to } 7.3) H_{RP}$ ) and in other gravel-bed dune formations observed by the author. Here, the likelihood is that both bedform development and sediment pulsing are synergistically complementary in the development of the urban channel bedforms.

# **CHAPTER 4**

## **ESTIMATING CHANNEL-FORMING DISCHARGE IN URBAN WATERCOURSES**

### **4.1 INTRODUCTION**

The concept that there is a channel morphology-forming discharge; which determines the quasi-equilibrium shape and size of a channel for a given slope, valley form, bed-material supply, and grain-size distribution, while maintaining sediment continuity; has been studied for over two centuries (Hutton, 1788; Lindley, 1919; Lacey, 1930; Inglis, 1949; Lane, 1955; Leopold *et al.*, 1964; Andrews, 1980; Emmett and Wolman, 2001). Given the global variety in hydrophysiographic regions, vegetational communities, and geologic properties, a standard definition or means of identifying this channel-forming (or ‘dominant’) flow is rare. Instead, a range in potential measures may be proposed (Andrews, 1980; Williams, 1978; Parker *et al.*, 2007). Identifying or defining the channel-forming discharge in ephemeral rivers or in degrading reaches is further complicated by the frequent absence of consistent field indicators and by issues related to the transient nature of a channel in disequilibrium (Stevens *et al.*, 1975; Baker, 1977; Schumm *et al.*, 1984; USDAFS, 2003). Urban-stream channels have problems akin to all of the above conditions plus further complications caused by anthropogenic

modifications of the basin morphology, insertion of infrastructure that alter valley and channel form, and the non-stationarity that may be introduced into any long-term flow records.

Channel-forming flow has frequently been defined as that at bankfull discharge (Wolman and Leopold, 1957). Methods of field identification of the bankfull stage and the associated discharge in natural channels have been well documented and summarized (Wolman and Leopold, 1957; Leopold *et al.*, 1964; Williams, 1978; Johnson and Heil, 1996; USDAFS videos 1995, 2003). The methods identify geomorphic features that may be commensurate with bankfull stage include: sedimentary surfaces of floodplains, the stage when water just begins to encroach upon the floodplain, or evidently relict benches above flood level, plus waterline boundary features such as the lower limit of perennial vegetation, and cross-sectional geometric positions such as the elevation where the width/depth ratio is a minimum (the stage corresponding to the first maximum of the Riley (1972) bench), and to the changes in the relationship between channel cross-sectional area and discharge top width. Other research has sought to relate bankfull discharge to watershed-based parameters such as effective catchment area (Carter, 1961; Leopold, 1968; Anderson, 1970; Packman, 1979; Kibler *et al.*, 1981; Sauer *et al.*, 1982), mean annual discharge (Carter, 1961; Anderson, 1970; Packman, 1979), and mean annual flood (Carter, 1961; Anderson, 1970; Packman, 1979) amongst other metrics. Statistical frequencies have also been correlated with bankfull discharge in various hydrophysiographic regions (Leopold *et al.*, 1964; Woodyer, 1968; McGilchrist and Woodyer, 1968; Kellerhals *et al.*, 1972; Hicks and Mason, 1991; Annable, 1996b). In the majority of cases involving such statistical estimates, the authors stress that published

values represent the ensemble mean averages of frequency return periods and that there can be significant spatial variation due to specific watershed characteristics.

An alternative approach in estimating channel-forming flow is based upon the analytical calculation of effective discharge (Wolman and Miller, 1960), which cannot be validated in the field. This method employs systematic flow records and sediment-transport equations (Wolman and Miller, 1960; Andrews, 1980; Biedenharn *et al.*, 2000) or field-measured sediment rating curves (Emmett and Wolman, 2001), and seeks to determine which discharge class (volume of flow) transports the largest amount of sediment over a long period of time. However, as identified by Emmett and Wolman (2001), the majority of these studies have utilized suspended-sediment equations or rating curves rather than bed-load data as the latter are seldom available. The use of suspended-sediment rating curves in effective discharge estimates can lead to significant estimation bias since, in the case of coarser-bed channels, suspended sediment does not define the channel morphology.

Many of these methods are ineffective or inappropriate where the natural channel has been modified by urban works. Sanitary and storm sewers are frequently constructed within river valleys, often resulting in channel crossings or realignments and floodplain re-grading that may alter the channel form and destabilize its quasi-equilibrium condition. The introduction of maintenance roads or levees adjacent to river corridors further alters cross-section profiles and thus may change the relationship of different terrace elevations to the bankfull stage. Changes in hydrology often lead to vegetation migration inside the bankfull channel limits, changing the significance of vegetational waterline features. Changes in urban hydrology commonly alter the frequency of lower magnitude flood

returns (Chapter 2; Leopold, 1968; Packman, 1979; USGS, 1982; Sweet and Geratz, 2003) resulting in a situation where there is no means of estimating bankfull discharge that is statistically consistent. Moreover, the introduction of storm-water management facilities that extend the duration of flow above critical shear conditions (MacRae and Rowney, 1992) begin to alter depositional benches in urban channels also leading to the improper field identification of bankfull stage.

The placement of gauge stations in urban environments is often adjacent to bridges for ease of access and to facilitate discharge measurement and sediment sampling. A consequence of such selection is that the at-a-station hydraulic geometry reflects the bridge structure rather than that of the channel morphology (Williams, 1978). Estimating bankfull discharge is then biased by the hydraulics of the constricted flow conditions at the bridge structure. Effective discharge estimates may also be prone to similar errors based upon imposed hydraulic geometry inconsistent with the channel morphology.

For the past 15 years, an intensive field program has been undertaken on twelve quasi-equilibrium (Langbein and Leopold, 1964) urban-stream channels in southern Ontario, Canada. Eleven of the channels studied have pool-riffle dominated morphologies and the remaining channel has a steeper run-pool, semi-confined form (Table 4.1). A variety of the methods outlined above were tested to estimate the channel-forming flows in these settings. Many of them had to be abandoned due to anthropogenic modifications to the floodplain regions or existing infrastructure, while others had to be adapted for conditions specific to each study reach. This chapter describes many of the limitations

**Table 4.1.** General urban site characteristics and channel-forming flow metrics.

Site Reference Number	Station ID	Station Name	Period of Record	Morphology	Cross-sectional Relief	Effective Catchment Area (km <sup>2</sup> )	Urban Land Use (%)	Field Observed Bankfull Discharge (m <sup>3</sup> /s)	Effective Discharge (m <sup>3</sup> /s)	Average Annual Return Period (yrs)	Log-Pearson III Return Period (yrs)
1	02HC005	Don River at York Mills	1945 - 2009	Riffle-pool	Semi-confined	95.5	72	8.8	10.0	0.16	1.0306
2	02HC017	Etobicoke Creek at Brampton	1957 - 2009	Riffle-pool	Unconfined	67.7	24	14.2	15.3	0.24	1.0095
3	02HC030	Etobicoke Creek below QEW	1966 - 2009	Riffle-pool	Unconfined	215.4	62	47.8	42.7	0.28	1.0734
4	O2HB012	Grindstone Creek near Aldershot	1965 - 2009	Riffle-pool	Unconfined	83.9	13	11.05	6.2	1.00	1.3491
5	02HD013	Harmony Creek at Oshawa	1980 - 2009	Riffle-pool	Unconfined	43.0	44	12.5	11.3	0.21	1.0079
6	02GA024	Laurel Creek at Waterloo	1959 - 2009	Riffle-pool	Unconfined	57.5	34	12.8	10.5	0.76	1.5183
7	02HC029	Little Don River at Don Mills	1964 - 1966	Riffle-pool	Unconfined	135.1	70	23.8	17.6	0.21	1.0609
8	02HC033	Mimico Creek at Islington	1965 - 2009	Riffle-pool	Unconfined	73.8	87	18.4	21.0	0.23	1.0475
9	02HA014	Redhill Creek at Hamilton	1977 - 2004	Riffle-pool	Unconfined	56.3	66	13.8	18.6	0.13	1.0001
10	O2HB007	Spencer Creek at Dundas	1959 - 2009	Run-pool	Semi-confined	156.0	9	12.4	11.2	0.59	1.2274
11	02HA022	Stoney Creek at Stoney Creek	1989 - 2009	Riffle-pool	Unconfined	19.2	15	3.2	4.1	0.25	1.0448
12	02HA027	Walker Creek at St. Catherines	1991 - 1994	Riffle-pool	Unconfined	5.9	99	2.1	0.8	0.38	1.1612

identified during the field program that can result in poor estimates of channel-forming flow, and offers alternatives found to be successful in the urban conditions.

## **4.2 FIELD METHODS**

Longitudinal profiles and a series of cross sections were surveyed at each site using a total station and geo-referenced using a 1<sup>st</sup>-order differential GPS. The study reaches ranged between  $52 \leq W_{bf} \leq 77$  in length, where  $W_{bf}$  is defined as the average bankfull-channel width: this typically translated to five to seven meander wave lengths per survey. Attributes acquired included the thalweg (at approximately every bankfull-width spacing), maximum invert of pools, and any other notable changes in channel bed slope. Cross sections were surveyed perpendicular to the channel and located at the upper third of a series of riffles or runs. Each cross section included discrete survey points demarcating the top and bottom of channel banks, thalweg, floodplain attributes, and any notable changes in slope. Typically, fifty to sixty discrete points were surveyed at each irregular cross section. Additional cross sections were taken where there was infrastructure. All data obtained were consistent with the data parameter population requirements of HEC-RAS 4b (USACE, 2004).

Bankfull stage was identified on all of the riffle-pool dominated stream morphologies as the maximum stage occurring on the convex bank (top of point bar), when water just begins to encroach upon the floodplain (Wolman and Leopold, 1957); this was, for the most part, commensurate with the existing valley flat (Woodyer, 1968; Kellerhals *et al.*, 1972). Bankfull stage was also identified at each riffle cross section using linear (quasi-horizontal) boundary features such as the valley flat, vegetation, or

benches where applicable. Bankfull stage on the steeper run-pool morphology was identified as the stage where the lowest width/depth ratio was observed (Wolman, 1955) or at the upper limit of point bars (USDAFS, 2003). Most ‘waterline’ boundary features at gauge stations were ineffective estimators of bankfull stage because cross sections and benches had frequently been re-graded to conform to bridge configurations rather than to the channel morphology. Moreover, heavy pedestrian traffic along channel banks further altered any terracette detail and vegetation boundaries, causing additional challenges in estimating bankfull stage. Typically, bankfull stage at gauge stations was demarcated by identifying any remnant bench, vegetation, or rock-staining indicators, and by extrapolation of the other surveyed locations within the study reach by a best-fit regression analysis projected to the gauge station (Leopold *et al.*, 1964; Sweet and Geratz, 2003; USDAFS, 2003) as illustrated in Figure 4.1. The rating curve at each gauge station was then used to relate the identified bankfull stage to the associated rating discharge.

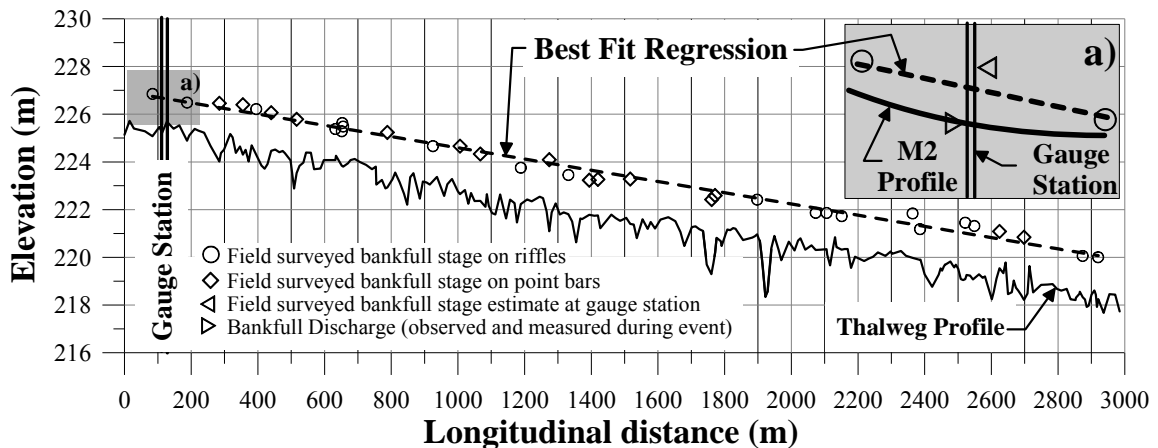


**Figure 4.1.** Longitudinal thalweg profile bankfull stage regression. *Note: Inset illustrates the differences in stage estimation from regression analysis and field observation at a gauge station.*



During the several years of bed-load and suspended-sediment sampling undertaken at each study site, each site was walked and its bankfull stage observed during high-flow conditions. The instantaneous bankfull discharge was then reconciled with the 15-minute stage-discharge observations at each gauge station to corroborate bankfull discharge. The field-observed discharges were then considered the correct values to represent bankfull discharge. Discrepancies were noted between the field-identified bankfull stage at the gauge station and those stages identified and corroborated in the field during high-flow conditions, as illustrated in Figure 4.2. Linear regression analysis of the data in Figure 4.2 identified a deviation from unity of 0.882 ( $r^2 = 0.92$ ). The majority of discrepancies occurred where gauge stations were either located on the downstream side of bridges or culverts, where closed footing culverts or bridges were present, or where weir control structures were installed to enhance accuracy in flow measurements. The presence of any of these structural conditions created channel constrictions in various forms, leading to an M2 profile (Henderson, 1966) at the structure openings and at the gauge stations (as illustrated in Figure 4.1a). The change in water-surface profile then leads to discrepancies between bankfull discharge observed in the field and the stage associated with bankfull discharge at the gauge station where waterline boundary features are used at the latter. Figure 4.1a illustrates the best-fit correlation of bankfull stage along a reach to that at a gauge station, plus the difference between that stage as defined by regression analysis and the field-identified bankfull stage using waterline boundary features, and the field-observed bankfull discharge (Figure 4.1a). These discrepancies were common for all of the urban-stream channels studied with the exception of Site 10, where the bridge span and gauge station cross

section conformed to the channel morphology. The use of waterline boundary features or longitudinal regression analysis in estimating bankfull stage where gauge stations are in close proximity to bridges should be carefully scrutinized when assessing this stage.

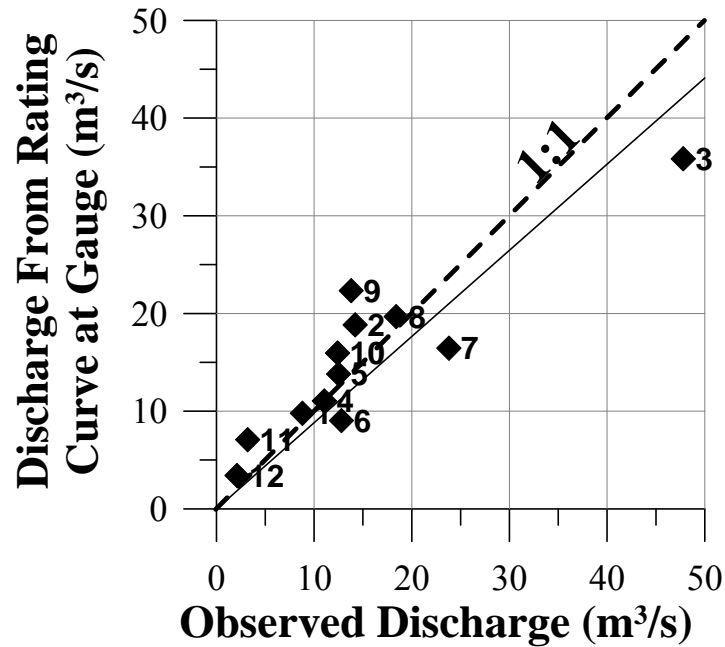


**Figure 4.2.** Discharge from bankfull stage estimate at gauge station versus observed bankfull discharge at top of point bars during flood event.

### 4.3 INDEPENDENT CALIBRATION

The 15-year duration of the study presented opportunities to further examine the various methods of estimating channel-forming flow, to investigate the variability in estimation made by different individuals, and to minimize bias. Eleven experienced practitioners participated in field investigations over the study period, in particular to corroborate the quasi-equilibrium characteristics of each reach and to identify channel-forming flow by whatever methods each participant deemed appropriate. Contributions

were disregarded if they explicitly related bankfull discharge to the putative 1.5-year return period, as will be discussed below.

The participants came from seven different countries on three different continents, often with experience in significantly-different geologic and hydrophysiographic regions. The participants had between 10 and 43 years of experience. Whenever possible, no two individuals had trained at the same institution or with the same instructor, so minimizing bias. Only six of the participants were able to visit all twelve study sites, the others visiting a sub-set of the reaches based upon availability and time.

At a study reach, each participant was given an aerial photograph of the area and walked (or, preferably, waded) the reach to become acquainted with the channel morphology. During the return walk, the participant then identified bankfull stage wherever he/she chose, and was also asked to identify bankfull stage at the gauge station. A consistent choice among all of the participants was the upper limit of the point bar on the convex (inside) curve of river bends. At riffles, many of the participants used either vegetation or small terrace indicators because the valley flat was not always commensurate with bankfull stage. The discharge stages identified by each practitioner were then tied to geodetically-referenced benchmarks located along each of the study sites.

To relate field-estimated stages from each participant to discharges, one pressure transducer was installed on the inside of a bend where all of the participants had identified bankfull stage, and a second on a riffle or run where all had also identified it. The bankfull stages of the participants were then related to the geodetic elevations of the pressure transducers. The role of the pressure transducers was not to relate stage and

discharge at a given location but, rather, to reconcile time at a given location where a participant had identified a bankfull stage marker with the observation time at the gauge station. The instantaneous discharge (to the closest 15-minute observation interval) at the gauge station was then considered to be the same as at the identified bankfull stage location. Continuity of discharge was valid in all cases between the gauge station and the field location where bankfull stage was identified. The pressure transducers were left in place for sufficient time for a flow event of large magnitude to inundate the floodplain, giving data which could be related to all participants' observations. The pressure transducers were then moved to other streams and the calibration process repeated.

The results of this independent field calibration are presented in Figure 4.3. Where bankfull stage was identified at the top of the point bars on the convex curve of bends, there was very little discrepancy between observers and bankfull discharge during flood conditions identified in the initial surveys of this project (Figure 4.3a). A power-function fit ( $r^2 = 0.99$ ) of the mean estimated discharge from each observer produced a coefficient and exponent of 0.99 and 0.98, respectively. Box-and-whiskers in Figure 4.3 represent the maximum, 75<sup>th</sup>-quartile, 25<sup>th</sup>-quartile, and minimum values and symbols represent average values of all observers. When participants attempted to identify bankfull stage at the riffles, many used the height of the valley flat (Woodyer, 1968; Kellerhals *et al.*, 1972), and others relied upon boundary features such as vegetation markers (Schumm, 1960; USDAFS, 2003) because they speculated that a small amount of incision might have occurred along these sections. Figure 4.3b illustrates the discharge results where pressure transducers were installed on riffles where all participants had identified bankfull positions. A power-function fit ( $r^2 = 0.94$ ) of the

mean estimated discharge from each observer produced a coefficient and an exponent of 1.06 and 0.97, respectively. There was a greater degree of variation between the practitioners, which is consistent with the more subjective methods of estimation using vegetation boundary features and the potential discrepancies where individuals believed that a minor amount of channel incision had occurred. In this particular study, the vegetation indicators typically under-predicted bankfull stage, whereas those participants using the height of the valley flat as the marker typically over-predicted it and the related discharge compared the results of Figure 4.3a.

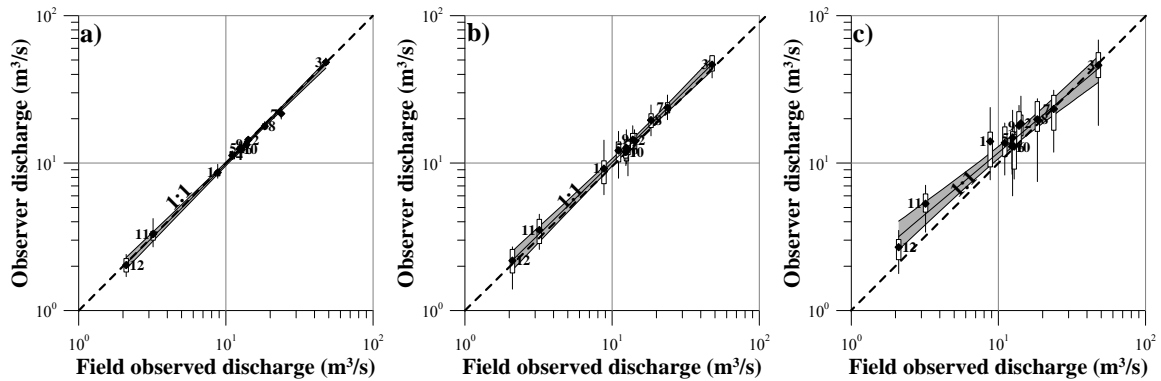


**Figure 4.3.** Independent evaluation of bankfull stage versus field observed bankfull discharge during flood events at a) upper-limits of point bars on the convex arc of bends, b) riffles, and c) gauge station. *Note: Grey envelope represents the 95<sup>th</sup>-percentile limits.*

In most cases, participants acknowledged that identifying bankfull stage at gauge stations was the most difficult location due to: 1) cross-section modifications by infrastructure, 2) use of materials such as concrete, gabion baskets, etc., 3) constructed benches for maintenance access, and 4) erosion of benches or vegetation indicators by pedestrian traffic. Of the three methods used to identify bankfull stage and the corresponding discharge, those undertaken at the gauge stations showed the largest variability, as illustrated in Figure 4.3c. A power-function fit ( $r^2 = 0.79$ ) of the mean

estimated discharge from each observer produced a coefficient and an exponent of 1.70 and 0.84, respectively. Due to the absence of valley-flat stages or benches at most gauge stations, the majority of participants used supposed waterline features or rock staining in attempts to estimate bankfull stage. The two exceptions where most participants consistently identified the same bankfull stage at gauge stations were Sites 4 and 10, the only sites where the gauge is located away from bridges (Site 4) or on the run-pool semi-confined channel morphology where the bridge conformed to the cross-sectional profile of the channel (Site 10). There was one boundary feature that did provide a consistent means of identifying bankfull stage: in the winter season with sufficient snowfall, if a discharge event occurred that was relatively recent to bankfull discharge, the upper limit of the melted snow on the convex arc of bends at the top of point bars and the same snowfall boundary limit at a gauge station provided a consistent linear field identifier of bankfull stage (Figure 4.4). It is noted, however, that this method of identification should only be used if the duration between the discharge event and the field observation is relatively short to ensure that no other events could have generated the waterline feature.

The results of this independent field calibration experiment further emphasize that great care should be taken in identifying bankfull stage in the field. In particular, bankfull-stage estimates at gauge stations where significant alterations to the cross-sectional geometry or boundary materials have been made should be carefully scrutinized. The most consistent method of identifying bankfull stage and the associated discharge is during a flood event when flow begins to encroach upon the floodplain (for floodplain-dominated channel morphologies) and then reconciling the instantaneous

discharge from the rating curve at the gauge station with the stage in the quasi-equilibrium channel section.



**Figure 4.4.** Field-identified bankfull stage using snow-melt limit where  $Q_{bf}$  is the stage associated with bankfull discharge (Redhill Creek at Hamilton).

#### 4.4 EFFECTIVE DISCHARGE

Employing the effective-discharge method to estimate channel-forming flow requires systematic discharge records over a sufficient time span, and a means of estimating the sediment transport (Wolman and Miller, 1960; Andrews, 1980; Biedenharn *et al.*, 2000; Emmett and Wolman, 2001). This study determined that significant errors in effective-discharge estimates can occur if the hydraulic geometry at the gauge station is significantly different from that of most of the channel, for the reasons identified above. Figure 4.5a illustrates the differences in discharge versus

channel top width and main-channel depth by comparing power-function relationships developed from field observations at one of the southern Ontario urban gauge stations with those from a representative surveyed cross section (representative channel morphology location) based upon a calibrated one-dimensional HEC-RAS hydraulic model of the same reach. The corresponding wetted perimeter ( $P$ ) and hydraulic radius ( $R_h$ ) for a given discharge, which are used to calculate shear stress ( $\tau_b$ ) used in the majority of bed-load transport equations, will also vary significantly based upon the differences in channel cross-sectional geometry.

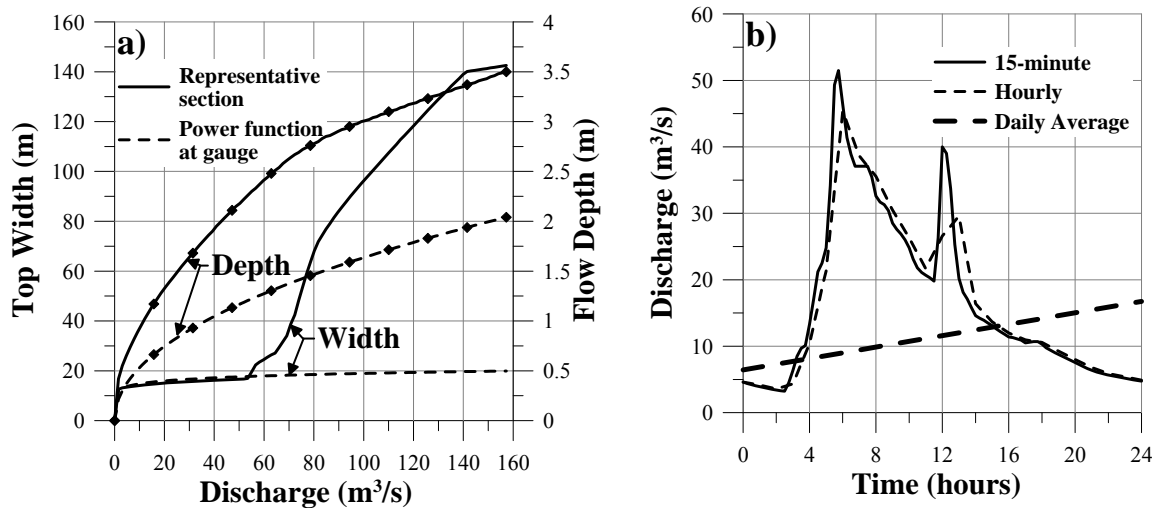


**Figure 4.5.** Flow conditions used in effective-discharge estimate from the Little Don River and Don Mills sites for a) hydraulic geometry observed at gauge station and representative cross section versus discharge and b) discharge versus time for different systematic time observation intervals.

The selection of the appropriate stage-discharge observation interval can also lead to errors in effective-discharge estimates, as identified by Biedenharn *et al.* (2000). Although the daily mean stream flow is a satisfactory observation interval for many stream channels in rural and wilderness settings, the change in overland flow-routing characteristics in urban watersheds results in flashier discharge responses, which are not



adequately captured in daily mean stream-flow observations (Figure 4.5b). The resolution in stage-discharge observation intervals can then alter the partial and cumulative discharge-distribution functions over the period of record, which can result in different discharge magnitude classes being associated with the effective discharge.

At-a-station power-function relationships were developed at each of the twelve gauge stations in the form:

$$W = c_1 Q^{e_1} , D = c_2 Q^{e_2} , A = c_3 Q^{e_3} , \bar{V} = c_4 Q^{e_4} \quad (4.1 \text{ a – d})$$

where  $Q$ ,  $W$ ,  $D$ ,  $A$ , and  $\bar{V}$  are the field-measured discharge, channel top width, main-channel depth, cross-sectional area, and discharge velocity ( $Q/A$  as opposed to the main channel velocity), respectively; and the coefficients  $c_1 - c_4$  and exponents  $e_1 - e_4$  result from the best-fit power-function regression analysis of each relationship, respectively. The coefficient of determination ( $r^2$ ) for all twelve urban streams exceeded  $r^2 > 0.84$ , and in nine of the twelve streams exceeded  $r^2 > 0.92$ . The wetted perimeter ( $P$ ) and hydraulic radius ( $R_h$ ) as a function of discharge were developed from Equations (4.1) through using a stepwise function (organized in ascending discharge order) of the form:

$$P = c_5 Q^{e_5} , R_h = c_6 Q^{e_6} \quad (4.2 \text{ a – b})$$

where the coefficients  $c_5 - c_6$  and exponents  $e_5 - e_6$  result from best-fit power-function regression analysis of each relationship.

One-dimensional models using HEC-RAS 4b (USACE, 2004) were developed for each of the twelve study sites using the field survey data and calibrated to the stage-discharge rating curves at each gauge station. Reach-based channel roughness ( $n$ ) was

estimated using the Strickler equation in the form  $n = 0.0417 D_{50}^{1/6}$  (Chow, 1959), where  $D_{50}$  is the median particle diameter of a log-normal distribution based upon a Wolman (1954) pebble count of each reach. Each calibrated model simulated one-hundred discrete discharge events that were evenly distributed between  $Q_{\min} \leq Q \leq Q_{100}$ , where  $Q_{\min}$  and  $Q_{100}$  are the minimum observed discharge and the 100-year return period (based upon USGS (1982) methods), respectively. Hydraulic-geometry relationships were then developed for representative cross sections of each reach of the form:

$$W = \text{fn}(Q) , D = \text{fn}(Q) , \bar{V} = \text{fn}(Q) , A = \text{fn}(Q) , R_h = \text{fn}(Q) \quad \textbf{(4.3 a - e)}$$

Effective-discharge calculations were made using the two-fraction bed-material model offered by Wilcock and Kenworthy (2002) for hydraulic geometry at each gauge station (Equation (4.1)), and at representative cross sections (Equation (4.2)) of each reach, using the 15-minute interval discharge data. Effective-discharge calculations were also conducted for each representative cross section using hourly data to compare it with the 15-minute observation results. Daily mean flow data were not considered in the analysis because the majority of events were not adequately captured using an interval of such low resolution.

A suite of analyses were conducted on the number of discharge classes needed to adequately evaluate the cumulative- and partial-distribution functions for different observation intervals. Biedenharn *et al.* (2000) showed that there is no absolute selection criterion for the number of discharge classes to be designated. It is largely the user's choice to achieve a relatively continuous distribution of the sediment-load histogram. A series of analyses were conducted on the urban-stream channels using between twenty

and one-hundred discharge classes. Higher resolution analyses produced a number of discharge classes with only one observation in them: these were associated with flashiness and peak discharges over a series of flood events, leading to discontinuous discharge frequency distributions. The majority of streams in this study were dominated by base-flow discharge classes and displayed very short duration, high-intensity, flashy events, which were not adequately captured when few discharge classes, typically less than thirty, were assigned (Chapter 2). The analysis determined that a selection of between thirty-five and fifty-five discharge classes were best suited for adequately representing the frequency distribution of flows.

The results from three of the urban study reaches are presented in Figure 4.6 to show the typical differences identified in effective-discharge estimates for all twelve of the study reaches. Given the typically prismatic cross section at gauge stations, too high shear values were calculated for the lower discharge classes there. The result was consistent under-prediction of the discharge class, which transported the greatest volume of bed load over time, when compared to the irregular channel cross sections that were more accordant with the channel morphodynamics. Selection of either hourly or 15-minute discharge observation intervals did not have a significant impact on the discharge class associated with effective discharge. In most cases, differences in effective-discharge estimates using hourly flow data typically varied by one to two discharge classes compared to the 15-minute observation intervals. However, no specific bias towards underestimation or overestimation was identified in the hourly discharge class; the estimates varied with each site studied.

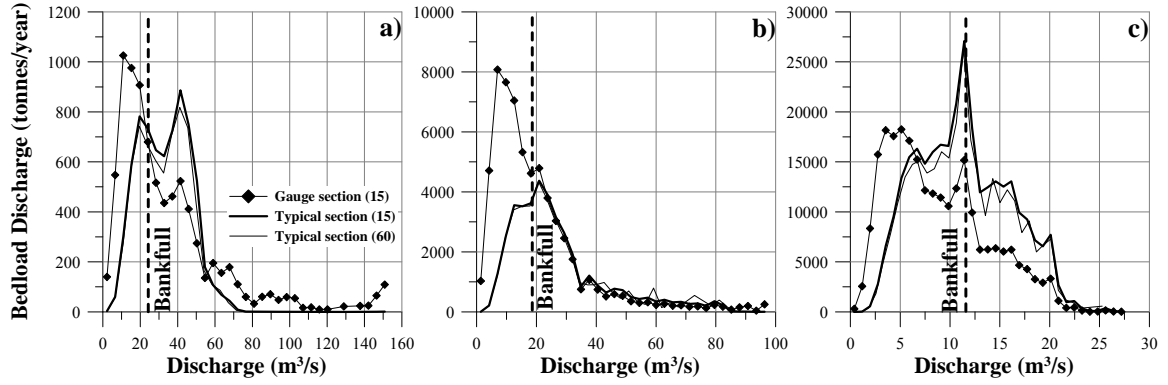


**Figure 4.6.** Effective-discharge analysis using Wilcock and Kenworthy (2002). Bedload discharge versus discharge for 15-minute flow observation data at gauge station cross section (15), representative cross section (15), and hourly data (60) at representative cross sections for a) Little Don River at Don Mills (Site 7), b) Mimico Creek at Islington (Site 8), and c) Spencer Creek at Dundas (Site 10).

## 4.5 HYDRO-GEOMORPHIC METHODS

The development of calibrated, one-dimensional hydraulic models afforded the opportunity to evaluate many of the cross-sectional hydraulic conditions that may be used to estimate channel-forming flow. Figure 4.7 illustrates the results of one-hundred discrete simulations evenly distributed between  $Q_{\min} \leq Q \leq Q_{100}$  for a representative cross section for one of the urban streams, using a series of hydraulic metrics. The discharge associated with the first local minimum of the width/depth ratio has often been used to identify bankfull discharge in floodplain-dominated channel morphologies (Wolman, 1955). The specific stream power ( $\hat{P}$ ) as defined by:

$$\hat{P} = \frac{\gamma Q S_f}{W} \quad (4.4)$$

where  $\gamma$  is the specific weight of water and  $S_f$  is the channel bed slope, is used in sediment-transport equations (Yang, 1979, 1984), and the maximum specific stream

power value over a wide range of flows in floodplain-dominated channel morphologies can also be associated with bankfull discharge, which is often commensurate with the valley flat. Correspondingly, the first local maximum of total channel shear ( $\tau_o = \gamma R_h S_f$ ), where the entire wetted perimeter is considered, can also correspond to the discharge associated with channel-forming flow at the stage of inundation of the valley flat. The maxima associated with discharge velocity ( $Q/A$ ) can also represent the discharge consistent with the stage of the valley flat because at flows that exceed bankfull stage the discharge velocity decreases due to floodplain roughness and increase in the wetted perimeter.

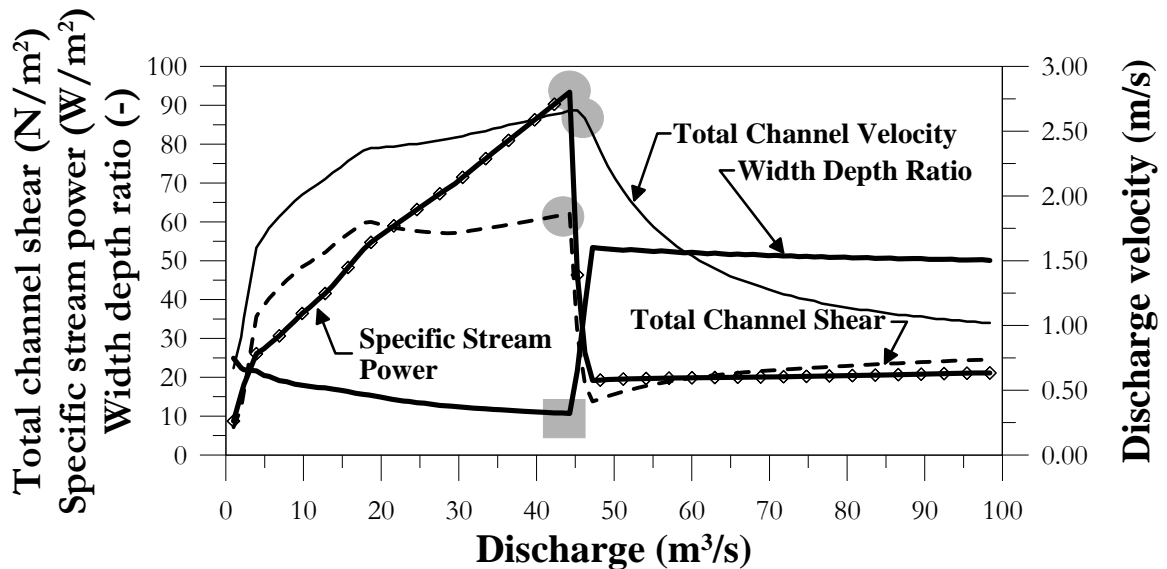


**Figure 4.7.** Total channel shear, specific stream power, width/depth ratio, and discharge velocity versus discharge for a representative cross section. One-hundred discrete evenly-distributed discharge simulation events between  $Q_{\min} \leq Q \leq Q_{100}$ . *Note: Shaded areas represent the locations of the first local maximum or minimum for the various relationships identified for floodplain-dominated channel morphologies in quasi-equilibrium.*

Each of the hydraulic metrics illustrated in Figure 4.7 can be further condensed into a single box-and-whisker plot to represent a given cross section for the one-hundred

discrete simulations between  $Q_{\min} \leq Q \leq Q_{100}$ . The analysis of a series of cross sections can then be evaluated longitudinally along a reach to calculate these metrics, as illustrated in Figure 4.8a and Figure 4.8b for discharge velocity and width/depth ratio, respectively. Each box-and-whisker in Figure 4.8 represents one-hundred discrete evenly-distributed discharge simulations between  $Q_{\min} \leq Q \leq Q_{100}$ , where the maximum and minimum values at each cross section are represented by the extents of each line, boxes the standard deviations of each metric, and symbols the average metric values. The bankfull velocity and width/depth ratio associated with bankfull discharge is represented by the dashed line. It is seen in Figure 4.8a that bankfull discharge is often correlated with the maximum discharge velocity observed at a series of cross sections along a river reach of interest. There are also a series of cross sections where the maximum discharge velocity does not occur at bankfull discharge; these are sections associated with bridge structures or where the river passes between higher banks associated with artificial fill or with terraces. Plots similar to Figure 4.8a can be produced for specific stream power and total channel shear.

Figure 4.8b illustrates the range in width/depth ratios. It is the inverse of Figure 4.8a, wherein the width/depth ratio at bankfull stage is typically the lowest value of the metric. In the cases of semi-confined, run-pool dominated channel morphologies, the local minima of width/depth ratios can be used to determine discharge that may be associated with bankfull discharge. However, the metrics where local maxima were used in floodplain-dominated riffle-pool morphologies were not applicable in the semi-confined channel morphologies. In these cases, breaks in slope observable by eye

(particular when the ordinate axis in Figure 4.8 is log-transformed) were often consistent with bankfull discharge.

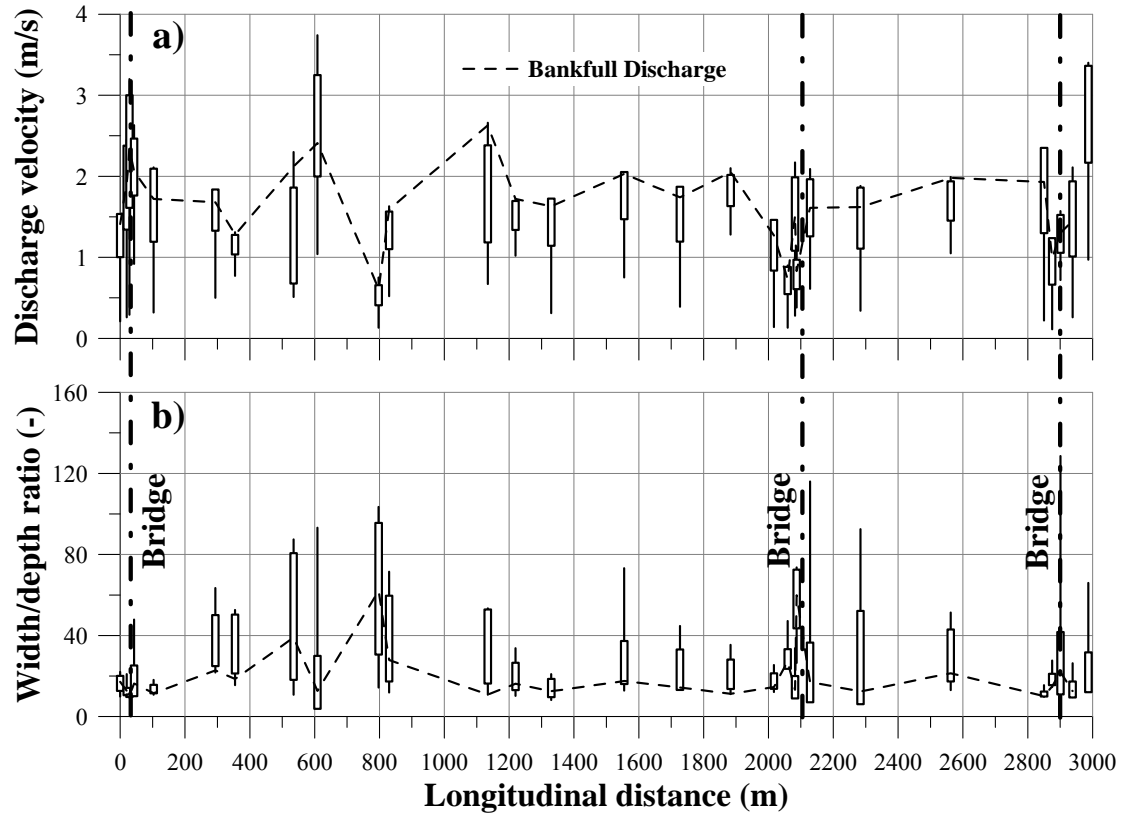


**Figure 4.8.** a) discharge velocity, and b) width/depth ratio versus longitudinal distance. *Note: The maximum and minimum values at each cross section are represented by the extents of each line, boxes the standard deviations of each metric, and symbols the average metric values.*

The results of the maxima observations of each study reach with respect to discharge velocity, total channel shear, and specific stream power extracted from each modeled cross section (similar to Figure 4.8) are illustrated in Figures 4.9a through 9c, respectively. The corresponding observations for the minima in width/depth ratios are illustrated in Figure 4.9d. In Figure 4.9, whiskers represent the maximum and minimum metric values. It should be noted that cross sections associated with bridges or other

infrastructure were removed from the analysis. The results show that there is a relatively strong relationship between field-observed bankfull discharge and the average of each hydraulic metric. There is notably significant variability within each study reach, however, represented by the maximum and minimum limits of each whisker that were determined using the defining conditions identified above. Based upon power-function regression analysis the relationships of total average channel velocity, total channel shear, specific stream power, and minimum width/depth ratio differ from unity by 1.251 ( $r^2 = 0.96$ ), 0.977 ( $r^2 = 0.97$ ), 1.05 ( $r^2 = 0.96$ ), and 1.035 ( $r^2 = 0.96$ ), respectively. Notwithstanding, the hydraulic methods evaluated here can be seen to provide an additional tool for determining the range of discharges that are associated with channel-forming flow.

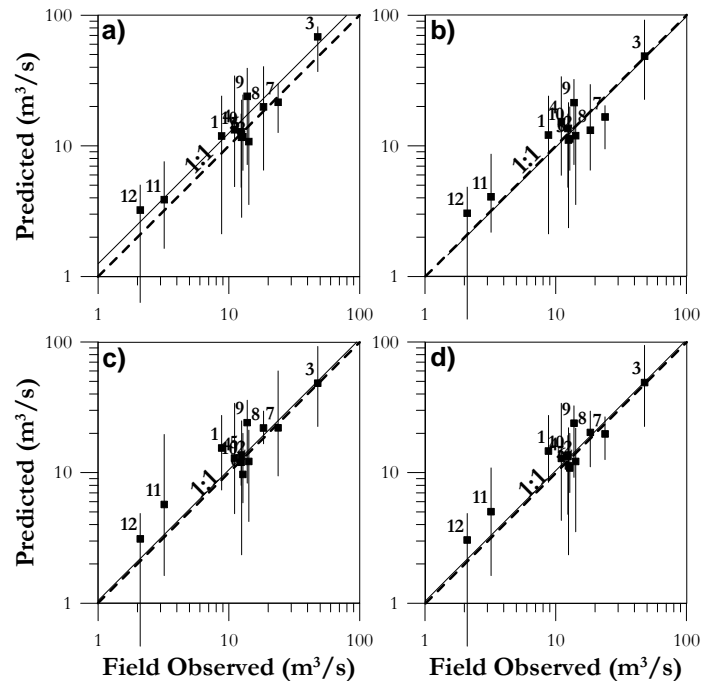


**Figure 4.9.** Field-observed bankfull discharge versus predicted channel-forming flow from one-dimensional model analysis using local maxima values of a) discharge velocity, b) total channel shear, c) specific stream power, and d) width/depth ratio. *Note: Whisker extents represent maximum and minimum calculated values.*



The technique discussed here should not be employed where topographic maps or DEMs are used to establish the cross sections. In this study, one-dimensional hydraulic models were also developed using the available 1.0-m or 5.0-m DEM data, the cross sections were extracted and the hydraulic metrics outlined above were re-evaluated with them. In all cases, there were significant differences in the discharges predicted for channel-forming flow when compared to those of field-surveyed cross sections. In many cases, the model average discharge values associated with the various metrics differed by two to eight times from those that used the detailed cross sections.

A corollary to applications of Figure 4.8 lies in the evaluation of proposed river-rehabilitation projects. I have also found over many years of evaluating rehabilitation projects that the production of plots like Figure 4.8, and similar plots of specific stream power and total channel shear, provide a very effective means of evaluating the hydraulic characteristics of a channel and floodplain function. If a proposed project intends to produce a single-thread channel within a floodplain-dominated channel morphology, plots similar to Figure 4.8 should arise from the design. If the bankfull discharge is not quite closely consistent with either the maxima or minima of the applicable metrics, the proposed channel morphology will be inconsistent with the hydraulics and the validity of the project should be re-evaluated.

## **4.6 FLOW-FREQUENCY METHODS**

Many investigations such as those by Carter (1961), Espey *et al.* (1966), Leopold (1968), Stankowski (1974), and Sauer *et al.* (1982) have related various return periods ( $Q_X$ ), where X represents the probabilistic return period of years of interest, to bankfull

discharge. As identified by USGS (1982), National Research Council (NRC, 1999), and Sweet and Geratz (2003), the use of peak annual series flow records to predict smaller floods can generate considerable bias because the multiple peaks in one given year in a basin may be larger than the single peak in some other year. The USGS (1982), NRC (1999), and Sweet and Geratz (2003) identify divergence in frequency-return periods based upon annual peak series data versus those using partial duration series analysis of continuous time-series data (Figure 4.10), for frequency returns typically less than 5-year return periods. Further, land-use changes in urban watersheds invalidates the assumption of stationarity in the land-use signal used in the calculation of frequency-return periods with peak annual series data. Although attempts have been made to adjust the land-use signal to account for the drift attributable to urbanization (Beighley and Moglen, 2003), the spatial variability of precipitation within any given watershed is sufficiently great that a reliable, method of land-use signal correction has not yet been attained.

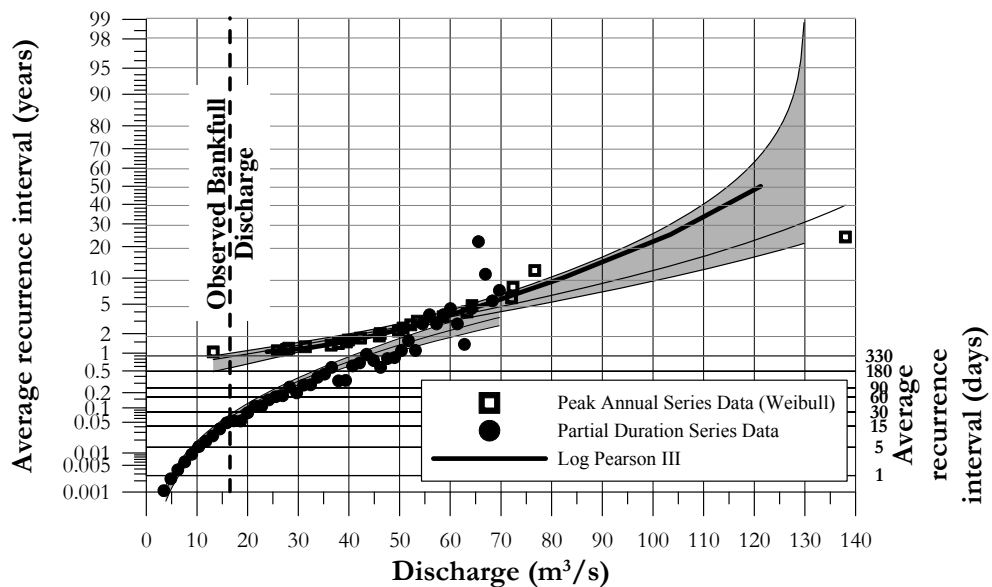


**Figure 4.10.** Recurrence interval versus discharge (Red Hill Creek at Hamilton (Site 9)).  
*Note: The grey envelopes represent the predicted 95<sup>th</sup>-percentile confidence limits.*

In the twelve streams studied, urban land use ranged from 9% to 99% of the catchment area. Effective catchment areas ( $A_{\text{eff}}$ ) (Leopold, 1968; Booth *et al.*, 2004) were defined by combining the topographic limits of each watershed defined by 1.0-m DEMs with storm-sewer networks and combined-sewer networks, in GIS. Bankfull discharge was observed to occur at least once and, in most instances, several times in any given year, commonly ranging between four and eight events per year (and in one extreme case seventeen times in a single year). The commonly used frequency return of 1.5 years was evaluated for each gauge station with the Weibull plotting position method and Log-Pearson III analysis consistent with *Bulletin 17B* (USGS, 1982), using the annual instantaneous peak-discharge observations for each gauge station's period of record. Based upon a linear regression analysis, the results show (Figure 4.11) that there are significant differences in most study reaches between the field-observed bankfull discharge and that predicted by either the Weibull method (Figure 4.11a) or the Log-Pearson III analysis (Figure 4.11b), as they vary from unity by 1.620 ( $r^2 = 0.97$ ) and 1.635 ( $r^2 = 0.95$ ), respectively. Results, as outlined in Table 4.1, are consistent with those identified by Leopold (1994) for urban streams where he noted that the bankfull-discharge return period in urban settings was commonly much lower than the 1.5-year return period and was frequently around 1.05 years or lower. Return frequencies are also similar to those observed by Sweet and Geratz (2003) studying urbanizing watersheds in the eastern United States. It should be noted that the period of record for Site 12 is insufficient for an annual frequency analysis; given the small watershed size and amount of urbanization within the effective catchment area, annual frequency return periods were calculated for the sake of completeness, but should be considered qualitative only.

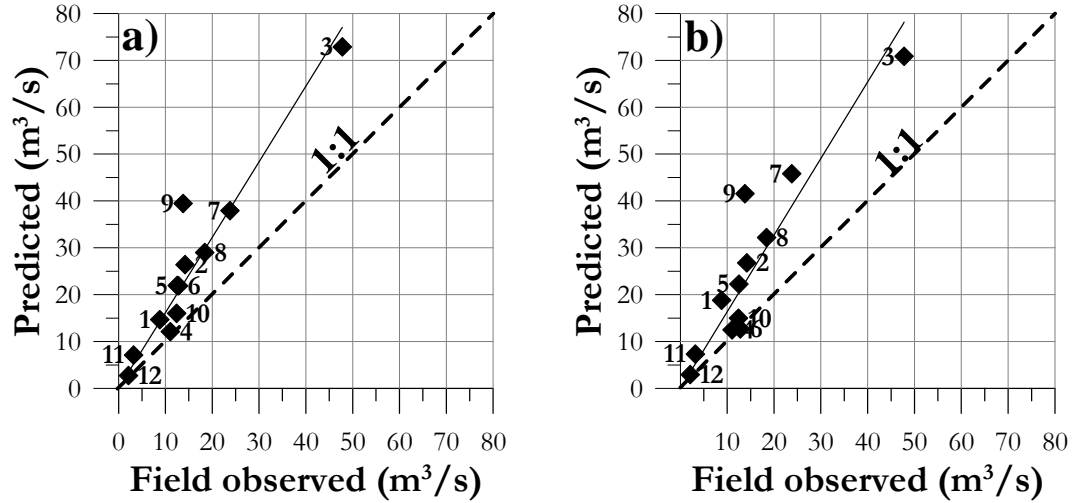


**Figure 4.11.** Predicted bankfull discharge for the 1.5-year return interval versus field-observed bankfull discharge for a) for Weibull analysis, and b) Log Pearson III analysis.

Notwithstanding these limitations, a series of return periods were used to evaluate trends in bankfull discharge as they relate to various return periods. For a comparison between urban and rural watersheds in the same hydrophysiographic region, a rural data set from Annable (1996a) was included in the analysis, in which bankfull discharge was also identified in the field. The results of dimensionless discharge (defined as  $Q_2/Q_{bf}$ ,  $Q_5/Q_{bf}$ , and  $Q_{10}/Q_{bf}$  versus effective drainage area ( $A_{eff}$ )) are illustrated in Figure 4.12. Based upon partial duration and annual series analysis of each urban gauge station, the 10-year return period showed consistent results in frequency return periods between the two methods of analysis, and was considered beyond the limits of divergence where an annual return period may be biased by the distribution in peak events as discussed above. The results show that the dimensionless discharges are consistently higher for the urban-stream channels than the rural rivers studied by Annable (1996a). Regardless of the return period used, no distinguishable trends were identified for the urban streams studied or when compared to rural streams of the same hydrophysiographic province.

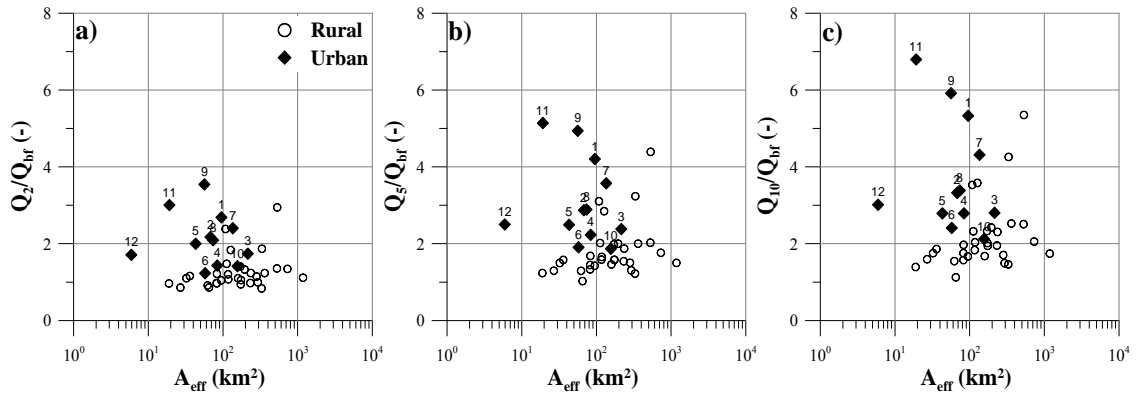


**Figure 4.12.** Discharge return period a)  $Q_2$ , b)  $Q_5$ , and c)  $Q_{10}$  by bankfull discharge ( $Q_{bf}$ ) versus effective catchment area ( $A_{eff}$ ) for urban streams and rural streams in the same hydrophysiographic region.

Dimensionless discharge was also evaluated by defining it as the ratio  $Q_{bf}/Q_{eff}$  versus  $Q_X/Q_{ma}$ , where  $X$  are the annual return periods as identified above and  $Q_{ma}$  is the mean annual discharge. Like the results of Figure 4.12, Figure 4.13 shows that the urban streams have higher dimensionless ratios along the abscissa at the various return periods when compared to the rural streams of Annable (1996a). If the Site 12 outlier is removed from the analysis, an apparent linear trend is evident in the urban-stream channels. Further, Sites 4 and 10 are the least urbanized watersheds studied (Table 4.1), and have frequency responses similar to the sample rural stream. However, recognizing that the majority of the urban streams studied were floodplain-dominated channel morphologies where bankfull and effective discharge are similar in value,  $Q_{bf}/Q_{eff} \approx 1$  (Emmett and Wolman, 2001), this trend is considered to be spurious, relating to the particular channel morphologies rather than to the urban hydrologic responses. No other correlations were identified using either annual series discharge return frequencies or mean annual discharge. A similar analysis was conducted with the mean annual flood discharge

(Carter, 1961; Espey *et al.*, 1966; Anderson, 1970; Packman, 1979) for both the rural and urban watersheds; the analysis did not yield any significant relationships.

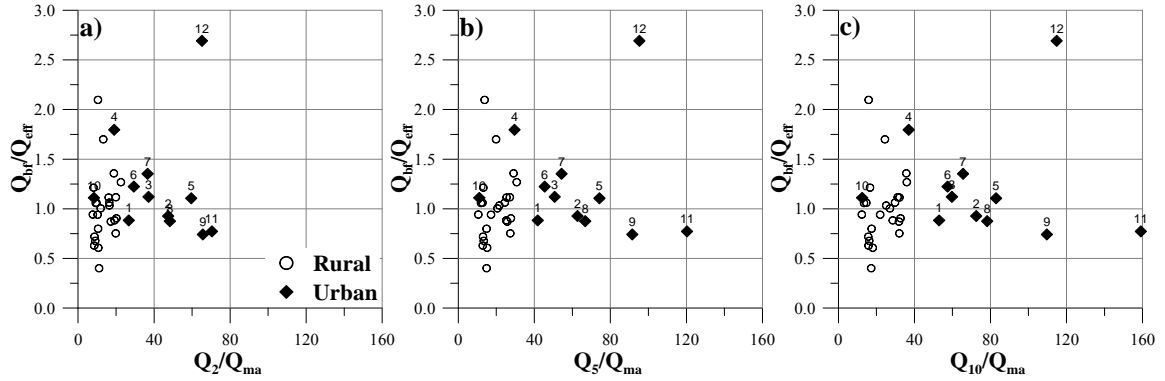


**Figure 4.13.** Bankfull discharge ( $Q_{bf}$ ) by effective discharge ( $Q_{eff}$ ) versus discharge return period a)  $Q_2$ , b)  $Q_5$ , and c)  $Q_{10}$  ( $Q_X$ ) by the annual average median discharge ( $Q_{ma}$ ) for urban streams and rural streams in the same hydrophysiographic region.

An evaluation of the bankfull-flow frequency based upon partial duration series analysis using systematic 15-minute stage-discharge data for the period of record, 1969 to 2005, was compared to watershed urban land use for both the urban streams and the rural streams studied by Annable (1996a). Figure 4.14 demonstrates the increasing frequency-return period with increasing watershed urban land use. Although an increasing return frequency trend is observed, the correlation is very poor as evidenced by the 95<sup>th</sup> percentile of the predicted regression limits. Conversely, with lower percentage urban land use, the discharge frequency-return period tends towards the average bankfull discharge frequency return value of 1.6 years observed by Annable (1996a) for rural streams in the same hydrophysiographic region: this is also consistent with average bankfull-frequency returns identified in other studies (Williams, 1978). Given the complexity of storm-sewer networks, their variability in size and location of outfalls, and the highly varied types of flow controls used in storm-water management facilities in

different watersheds, a predictable bankfull-frequency return for any given urban-channel reach with respect to urban land use should be considered only a qualitative metric.

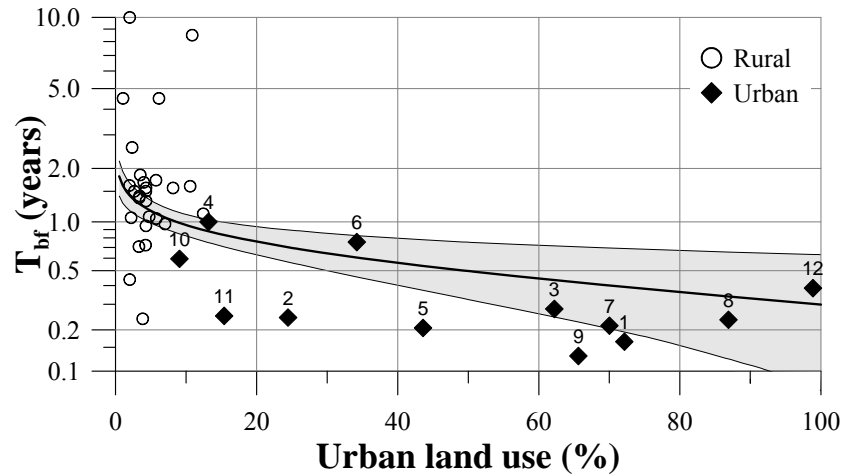


**Figure 4.14.** Bankfull discharge return period ( $T_{bf}$ ) versus watershed urban land use for urban streams and rural streams in the same hydrophysiographic region. *Note: The grey envelope represents the 95<sup>th</sup>-percentile confidence limits of the predicted trend line.*

## 4.7 CATCHMENT RELATIONSHIPS

Relationships of bankfull discharge to watershed-based metrics were investigated to identify common or contrasting trends in the urban and rural streams in the southern Ontario hydrophysiographic region. The topographic catchment areas used in defining the effective catchment areas for the rural study sites (Annable, 1996a) were delineated with 5.0-m DEMs rather than 1.0-m DEMs. As illustrated in Figure 4.15a, a relationship between bankfull discharge and effective catchment area exists, as in many other studies (Leopold *et al.*, 1964; Bray, 1972; Andrews, 1984; Hicks and Mason, 1991). No distinguishable difference was identified in bankfull discharge versus effective catchment area for the urban and rural streams from the same region. However, as indicated by the

95<sup>th</sup>-percentile confidence limits, estimation of bankfull discharge using the effective catchment area should be considered only a 1<sup>st</sup>-order approximation.

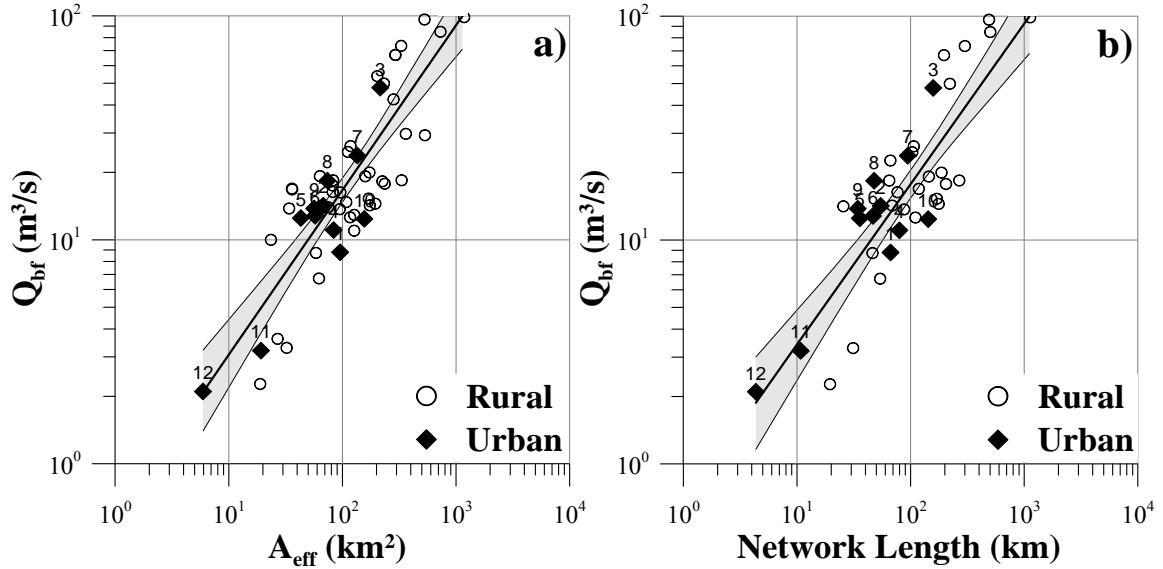


**Figure 4.15.** Bankfull discharge ( $Q_{bf}$ ) versus a) effective discharge, and b) stream-network length for urban streams and rural streams in the same hydrophysiographic region. *Note: The grey envelopes represent the 95<sup>th</sup>-percentile confidence limits.*

A comparison of total stream-network length to bankfull discharge yielded similar trends when compared to the effective catchment area, as illustrated in Figure 4.15b. Hydrology applications in GIS were utilized to identify each sub-catchment and its associated stream lengths, based upon the resolution of the available DEMs used in the rural and urban watersheds. As with the effective catchment area, no distinguishable trend was identified when contrasting the urban with the rural watershed settings. It is further noted that the use of GIS hydrology applications to identify stream channels, and thereby network lengths, were of limited use for identifying the smaller tributaries such as the 1<sup>st</sup>- and 2<sup>nd</sup>-order streams of Horton (1945). In urban settings, the definition of the



drainage swales and road-side ditches to be included in a drainage-network inventory can also be subjective and limited in extent.

## **4.8 SUMMARY**

Over the course of a multi-year study, a number of different methods were applied to estimate the channel-forming discharge in a selection of urban-stream channels. Results of independent evaluations by eleven different practitioners established that the most consistent estimation of channel-forming discharge was based upon stage at the upper limit of point bars along the convex arc (inside) of channel bends. The poorest field estimates of bankfull discharge by all of the independent evaluators were at gauge stations where the channel morphology had been modified to conform to the hydraulic geometry of bridge structures rather than the needs of stable channels. Further changes in cross-sectional profiles at gauges and changes in local roughness due to the construction materials in bridges, aprons, or weirs further constricted or altered the flow regime relative to quasi-equilibrium study reaches, typically leading to overestimates of bankfull stage and the corresponding discharge. Similar errors occurred when attempting to regress a water-surface slope at bankfull stage to the location of a gauge station. For these reasons, great care should be taken when identifying bankfull stage and the associated discharge in urban settings.

The changes in channel cross-section geometry at urban gauge stations further biased effective discharge-based predictions of channel-forming flow. Typically, effective discharge was underestimated where channel geometry conformed to the bridge or culvert span openings, when compared to a representative irregular cross section along

a quasi-equilibrium reach. Therefore, great care should be taken when estimating effective discharge to ensure that the cross-sectional geometry at a given gauge station is consistent with the channel morphology. Where there is significant divergence at a gauge station, it is recommended that a one-dimensional model be developed of the reach, calibrated to the stage-discharge rating curve and channel roughness, and effective discharge determined based upon the hydraulic geometry extracted from one or more representative cross sections within an adjoining study reach. It is further noted that as long as effective discharge is evaluated using either hourly or 15-minute stage-discharge observation intervals, there is not a significant difference in the final estimates of effective discharge. However, daily average discharge observations should be avoided in urban-stream channels because this interval does not adequately capture the resolution and response of the high-intensity short-duration events.

The use of calibrated one-dimensional models to estimate channel-forming flow based upon hydro-geomorphic metrics can provide a reasonable estimate of channel-forming discharge. Given the large variability in geometric irregularity amongst cross sections, to apply this method, several cross sections should be considered in the analysis and those related to urban infrastructure omitted. The use of DEMs or topographic maps to extrapolate cross sections for one-dimensional models typically will not provide sufficient definition or resolution of the hydraulic geometry of a given cross section for this method to be accurate.

The application of flow frequency-return periods based either on annual series peak maximum or continuous time-series data did not identify any quantifiable relationships between frequency-return periods and bankfull discharge. A general trend

of increasing frequency of bankfull return period was identified with the increasing imperviousness of urban surfaces; however, given the variability of storm-sewer networks and the complexity of different storm-water control facilities, a reliable method of prediction could not be identified. The results do show that the frequency return in all of the urban streams studied was less than a 1-year return period and often ranged between four to eight bankfull discharge events per year. The application of frequency-return analysis in estimating channel-forming discharge using annual series data should be seriously questioned in any urban setting.

Although the methods evaluated and presented here can be used at any hydrometric monitoring station to scrutinize the site conditions in estimating channel-forming discharge, they are particularly relevant to the urban-stream condition. It is further noted that the methods were applied to quasi-equilibrium urban-stream channels that were either riffle-pool or run-pool dominated morphologies. Several of the methods of estimating bankfull discharge may not be applicable when investigating incised river reaches. Finally, based upon all of the methods evaluated, there still remains no better means of identifying channel-forming discharge than field recognition of bankfull stage during a flood event that can then be related to the instantaneous discharge at the nearest gauge station.

## **CHAPTER 5**

### **CONCLUSIONS AND RECOMMENDATIONS**

One-hundred-and-sixty-eight gauged river reaches in southern Ontario, Canada, were assessed by land-use classifications, morphometric analysis, and field reconnaissance to identify if river reaches in a state of quasi-equilibrium existed in urban land-use settings. Twelve quasi-equilibrium reaches were identified ranging in length between fifty-two and seventy-seven bankfull channel widths and occurred within effective catchment areas ranging between 5.9 km<sup>2</sup> and 215.4 km<sup>2</sup> and where urban land-use assemblages varied between 9% and 99% of the total effective catchment areas. The reaches were studied over a 15-year period commencing in 1994 to characterize the hydraulic, hydrologic, sedimentological, and geomorphic conditions of quasi-equilibrium. These activities complete the first two of three objectives identified in this research program.

The third objective of the research program was to compare the characteristics of urban and rural streams identified to be in a state of quasi-equilibrium of the same hydrophysiographic region and identify their principal similarities and differences and conditions distinct to urban-stream stability. The following observations and comparisons were identified:

- Urban channels studied here did not respond in the commonly-observed fashion of increases in channel width and depth with increasing urbanization. Results show no statistically-significant differences of bankfull width or depth and bankfull discharge between the urban and rural study sites. The field observations were also compared with a larger international data base of gravel-bed streams, finding consistency in the population observations of hydraulic geometry versus dimensionless discharge.
- Manifestations in channel planform and bedform are responses in a river system to maximizing the flow resistance, while minimizing variability in energy expenditure in a downstream direction. Increases in meander wave length and radii of curvature of urban-stream channels, compared to rural watercourses in the same hydrophysiographic region, are surface expressions of increased flood frequency (pulsing) and volume but decreased bed-load supply.
- The frequency of bankfull and larger discharge events increased with increasing urbanization within the study watersheds, with corresponding increases in flashiness index and the number of shorter duration events, as has been seen in several other studies. The interactions between storm sewers, combined sewers, storm-water quantity ponds, and other infrastructure resulted in complex watershed responses that made detection of predictive trends between urban land use and bankfull frequency-return periods elusive.
- Annual discharge volumes derived from each effective catchment area identified no statistical difference in total flow. Similarly, the annual volume

summations of all bankfull or larger events in urban streams were indistinguishable from the less frequent but longer duration events recorded in the rural study sites. However, the annual volume summation exclusively exceeding bankfull discharge was larger in the urban-stream channels, whereas a larger volume of flow occurred between the low-flow and bankfull stages in the rural study reaches. The annual duration of flows onto the floodplains in the urban study sites was similar to the annual duration of flows exceeding either the critical bank shear or critical bed shear of the median bed-material particle sizes.

- Volumes of bed material transported were found to decrease with increasing percent urban land use, indicating a reduction in supply with increasing urbanization. Downcutting was not observed in any of the urban study reaches; however, which suggests that the reduction in bed-material supply is offset by ease of access to floodplains during flood events, thus maintaining low hydraulic radii and the reduced channel width contrary to most urbanizing stream responses.
- Increased frequency of pools (and riffles) between adjoining bends in the urban channels is caused by both sediment pulsing of larger clasts and the creation of ‘dune-like’ bedforms to maximize flow resistance. The short travel distances of larger clasts within each reach result from the flashy convective storm events observed in the region combined with changes in land-use and overland routing characteristics. The short travel distances allow keystone to be placed (commonly they are coarse anthropogenic material)

that serve as frequent grade-control positions along each watercourse resulting in riffles as the hydrographs recede with shallower pools (compared to bends) between the riffle crests.

- The frequency of riffle crests (and pools), field observations of standing waves during flood flows, and observed increase in flood flows above bankfull stage (thus energy) also support previous observations that bedforms may be developing as an alternative means of dissipating the increased stream energy external to the reaches by maximizing flow resistance. Distances between pool depths is much greater ( $L_{IP} \approx 73H_{RP}$ ) than those observed in sand-bed streams ( $L_{IP} \approx (2\pi \text{ to } 7.3) H_{RP}$ ) and in other gravel-bed dune formations observed by the author. Here, the likelihood is that both bedform development and sediment pulsing are synergistically complementary in the development of the urban channel bedforms.
- The application of flow frequency-return periods based either on annual series peak maximum or continuous time-series data did not identify any quantifiable relationships between frequency-return periods and bankfull discharge. A general trend of increasing frequency of bankfull return period was identified with the increasing imperviousness of urban surfaces; however, given the variability of storm-sewer networks and the complexity of different storm-water control facilities, a reliable method of prediction could not be identified. The results do show that the frequency return in all of the urban streams studied was less than a 1-year return period and often ranged between four to eight bankfull discharge events per year. The application of

frequency-return analysis in estimating channel-forming discharge using annual series data should be seriously questioned in any urban setting.

- The use of calibrated one-dimensional models to estimate channel-forming flow based upon hydro-geomorphic metrics can provide a reasonable estimate of channel-forming discharge. Given the large variability in geometric irregularity amongst cross sections, to apply this method, several cross sections should be considered in the analysis and those related to urban infrastructure omitted.
- Results of independent evaluations by eleven different practitioners established that the most consistent estimation of channel-forming discharge was based upon stage at the upper limit of point bars along the convex arc (inside) of channel bends. The poorest field estimates of bankfull discharge by all of the independent evaluators were at gauge stations where the channel morphology had been modified to conform to the hydraulic geometry of bridge structures rather than the needs of stable channels. Further changes in cross-sectional profiles at gauges and changes in local roughness due to the construction materials in bridges, aprons, or weirs further constricted or altered the flow regime relative to quasi-equilibrium study reaches, typically leading to overestimates of bankfull stage and the corresponding discharge. Similar errors occurred when attempting to regress a water-surface slope at bankfull stage to the location of a gauge station. For these reasons, great care should be taken when identifying bankfull stage and the associated discharge in urban settings.



The ready spill onto floodplains and the reduced velocities there appear to function as a strong buffer against any channel degradation due to the increase in flood intensities and volumes but reduced flood durations in urban settings. The combined urban and rural findings in this study are consistent with the anthropogenic responses identified by Schumm (1969), namely that reductions in the percent bed-material supply and increased discharge result in smaller rather than larger bankfull geometry proportions, with the proviso that adequate adjacent floodplain access be maintained. This study is one of a very small suite of studies attempting to identify the quasi-equilibrium conditions of urban-stream channels rather than investigating the degradational responses. The implications of this study for urban-stream rehabilitation are that smaller bankfull channel geometries may be the design end-point rather than larger channel geometries, to balance the reduction in bed-material supply. The increase in the magnitude and frequency of flood discharges is offset by allowing overspill greater access to continuous floodplains in order to maintain low hydraulic radii and thus shear stress to enhance the channel stability.

## **5.1 RECOMMENDATIONS**

Based upon the 15-year study of twelve urban-stream channels in southern Ontario, Canada, many additional research questions, project extensions, and adaptations were made. However, for the sake of brevity, only the major recommendations are enumerated here:

1. The most compelling observation made over the course of this study was the decrease in bed-material supply with increasing urbanization (particularly

towards build-out). This has been a very rare observation as most gauging stations across North America do not collect bed-load material (particularly gravel and larger grain sizes). Even a smaller subset of gauge stations or individuals collected bed-material load in urban watersheds. Although Wolman (1967) identified the potential for decreased suspended-sediment yield within a maturing urban watershed where a new watershed equilibrium condition would be achieved, suspended sediment does not have primacy over the formation of gravel and coarser-grained channels. If the observations made here are consistent for other urban-stream channels, significant value should be placed on the collection and transport characteristics of the bed-material load of urban and urbanizing stream channels to better understand the end-point state variable. Considering the significant financial investment allocated to urban restoration and rehabilitation projects, better establishing the bed-material supply and transport characteristics will reinforce and quantify the processes controlling the stability of many urban-river channels. Without this state parameter of Lane's (1955) proportionality adequately quantified, many rehabilitation efforts of urban stream could possibly suffer significant engineering and financial consequences over several years post-design and construction.

2. This study sought out what are believed to be quasi-equilibrium urban-stream channels from the best evidence possible. It is recognized that the majority of urban-stream channels studied here respond in a fashion contrary to most urban channels studied. The commonly-observed channel degradation

response to urbanization may, however, be partially spurious as the community interested in rivers and/or associated maintenance and/or recreation afford a great deal of time, effort, and financial resources to identifying problem reaches and prescriptions for rehabilitation or restoration rather than identifying stable channel reaches and researching the inherent characteristics of channel stability. Notwithstanding, many additional urban rivers should be studied that demonstrate quasi-equilibrium characteristics to elucidate their characteristics and to see if there is consistency with the results identified here. Further, streams should also be studied that have radically adjusted to the urban watershed conditions (without intervention) in new watershed land-use equilibrium conditions that have achieved a new quasi-equilibrium condition. Such studies may also identify other or different key river responses and metrics that further quantify the quasi-equilibrium urban state.

3. The field observations of standing waves in the relatively straight sections of many of the channels, where elongated meander wave lengths exist, alludes to a provocative analogy of riffle-pool bedforms (similar to dunes) developing in these regions to dissipate excess stream energy. Although field analysis of these observations are very challenging and problematic to obtain, laboratory-scale experiments in re-circulating flumes may garner considerable insight into the plausibility of such bedforms occurring.

## REFERENCES

- Abrahams AD, Li G, Atkinson JF. 1995. Step-pool streams: adjustment to maximum flow resistance. *Water Resources Research* 31: 2593–2602.
- Alexander JD. 1999. Little Etobicoke Creek – a natural channel design case study for urban streams. In: Proceedings of the Second International Conference on Natural Channel Systems, Niagara Falls, Ontario, Canada, March 1-4, Session 3, pp. 1–5.
- American Society of Civil Engineers (ASCE), Task Committee on the Effects of Urbanization on Low Flow, Total Runoff, Infiltration, and Groundwater Recharge. 1975. Aspects of hydrological effects of urbanization. *Journal of Hydraulic Division* 101(5): 449–468.
- Anderson DG. 1970. Effects of urban development on floods in northern Virginia. U. S. Geological Survey, Water Supply Paper 2001-C, 22 p.
- Andrews ED. 1980. Effective and bankfull discharges of streams in the Yampa River Basin, Colorado and Wyoming. *Journal of Hydrology* 46: 311–330.
- Andrews ED. 1984. Bed-material entrainment and hydraulic geometry of gravel-bed rivers in Colorado. *Geological Society of America Bulletin* 95: 371–378.
- Annable WK. 1996a. Database of Morphologic Characteristics of Watercourses in Southern Ontario. Ontario Ministry of Natural Resources, Queen's Printer for Ontario: Toronto, Ontario, ISBN # 0-7778-5112 -1, 212 p.
- Annable WK. 1996b. Morphological Relationships of Rural Watercourses in Southwestern Ontario and Selected Field Methods in Fluvial Geomorphology. Ontario Ministry of Natural Resources, Queen's Printer for Ontario: Toronto, Ontario, ISBN # 0-7778-5113-X, 92 p.
- Ashmore P, Church M. 2001. The Impact of Climate Change on Rivers and River Processes in Canada. Geological Survey of Canada Bulletin 555, Natural Resources Canada: Ottawa, Ontario.
- Ashmore PE, Day TJ. 1988. Effective discharge for sediment transport in streams of the Saskatchewan River basin. *Water Resources Research* 24(6): 864–870.

- Bagnold RA. 1960. Some Aspects on the Shape of River Meanders. U. S. Geological Survey, Professional Paper 282E, pp. 135–144.
- Baker VR. 1977. Stream-channel response to floods, with examples from Central Texas. *Bulletin Geological Society of America* 88: 1057–1071.
- Beighley RE, Moglen GE. 2003. Adjusting measured peak discharges from an urbanizing watershed to reflect a stationary land use signal. *Water Resources Research* 38(4): 4-1–4-11.
- Bernhardt ES, Palmer MA, Allan JD, Alexander G, Barnas K, Brooks S, Carr J, Clayton C, Dahm C, Follstad-Shah J, Galat D, Gloss S, Goodwin P, Hart D, Hassett B, Jenkinson R, Katz S, Kondolf GM, Lake PS, Lave R, Meyer JL, O'Donnell TK, Pagano L, Powell B, Sudduth E. 2005. Synthesizing U. S. river restoration efforts. *Science* 38: 636–637.
- Biedenharn DS, Copeland RR, Thorne CR, Soar PJ, Hey RD, Watson CC. 2000. Effective Discharge Calculation: A Practical Guide. ERDC/CHL TR-00-15, U.S. Army Corps of Engineers: Washington D.C., 63 p.
- Biedenharn DS, Watson CC, Thorne CR. 2008. Fundamentals of fluvial geomorphology. Chapter 6 In: Sedimentation Engineering: Processes, Management, Modeling, and Practice, Garcia MH (Ed.), American Society of Civil Engineers, Task Committee for the Preparation of the Manual on Sedimentation, Environmental and Water Resources Institute, ISBN 0784408149, 9780784408148, p. 355–386.
- Bledsoe BP, Watson CC. 2001. Effects of urbanization on channel instability. *Journal of the American Water Resources Association* 37(2): 255–270.
- Booth DB. 1990. Stream-channel incision following drainage-basin urbanization. *Water Resources Bulletin* 26(3): 407–417.
- Booth DB. 1991. Urbanization and the natural drainage system impacts, solutions and prognoses. *The Northwest Environmental Journal* 7: 93–118.
- Booth DB, Jackson CR. 1997. Urbanization of aquatic systems-degradation thresholds, storm water detention, and the limits of mitigation. *Journal of the American Water Resources Association* 33(5): 1077–1090.
- Booth DB, Karr JR, Schauman S, Konrad CP, Morley SA, Larson MG, Burges SJ. 2004. Reviving urban streams: land use, hydrology, biology, and human behavior. *Journal of the American Water Resources Association* 40(5): 1351–1364.
- Bray DI. 1972. Generalized Regime-type Analysis of Alberta Rivers. Ph.D. Thesis, University of Alberta: Edmonton, Alberta.

- Brice J. 1973. Meandering pattern of the White River in Indiana – an analysis. In: Fluvial Geomorphology, Morisawa M, Allen G (Eds.), Unwin Ltd: London, England, pp. 178–200.
- Brice, JC. 1984. Planform properties of meandering rivers. In: River Meandering, Elliott, CM (Ed.), Proceedings of the '83 Rivers Conference, American Society of Civil Engineers, New Orleans, Louisiana, October 24-26, 1983, pp. 1–15.
- Brookes A. 1988. Channelized Rivers: Perspectives for Environmental Management. Wiley: Chichester, England, 326 p.
- Brown CB. 1950. Sediment transportation. In: Engineering Hydraulics, Rouse H (Ed.), Wiley: New York, New York, pp. 769–857.
- Brownlie WR. 1981. Prediction of Flow Depth and Sediment Discharge in Open-channels. Report No. KH-R-43A, California Institute of Technology, W.M. Keck Laboratory: Pasadena, California.
- Bunte K, Abt SR. 2001. Sampling Surface and Subsurface Particle-size Distributions in Wadable Gravel- and Cobble-bed Streams for Analyses in Sediment Transport, Hydraulics and Streambed Monitoring. General Technical Report RMRS-GTR-74, U.S. Department of Agriculture, U.S. Forest Service, Rocky Mountain Research Station: Fort Collins, Colorado, 428 p.
- Campo SH, Desloges JR. 1994. Sediment yield conditioned by glaciations in a rural agricultural basin of southern Ontario, Canada. *Physical Geography* 4: 1–5.
- Carlston, CW. 1965. The relation of free meander geometry to stream discharge and its geomorphic implications. *American Journal of Science* 263: 864–865.
- Carter, RW. 1961. Magnitude and frequency of floods in suburban areas in short papers in the geologic and hydrologic sciences. *Geological Survey Research Article* 5: B9–B12.
- Chang HH. 1988. Fluvial Processes in River Engineering. Krieger Publishing Company: Malabar, Florida, 432 p.
- Chapman LJ, Putnam DF. 1966. The Physiography of Southern Ontario. Second Edition, Ontario Research Foundation, University of Toronto Press: Toronto, Ontario, Canada, 386 p.
- Chapman LJ, Putnam DF. 2007. The Physiography of Southern Ontario. Digital Resource – Ontario Ministry of Natural Resources: Peterborough, Ontario, Canada (based on Chapman and Putnam (1966)).

- Chin A. 1999. The morphologic structure of step-pools in mountain streams. *Geomorphology* 27: 191–204.
- Chitale SV. 1970. River channel patterns. *Proceedings of the American Society of Civil Engineers, Journal of the Hydraulics Division* 96: 201–221.
- Chow VT. 1959. Open Channel Hydraulics. McGraw-Hill Book Company Inc.: New York, New York, pp. 109–123.
- Church MA, McLean DG, Wolcott JF. 1987. River bed gravels: sampling and analysis. In: Sediment Transport in Gravel-bed Rivers, Thorne CR, Bathurst JC, Hey RD (Eds.), John Wiley & Sons: London, England, pp. 43–79.
- Curran JC, Wilcock PR. 2005. Characteristic dimensions of the step pool configuration: an experimental study. *Water Resources Research* 41:W02030, doi:10.1029/2004WR003568.
- D'Agostino V, Lenzi MA. 1997. Origine e dinamica della morfologia a gradinata (step-pool) nei torrenti alpini ad elevata pendenza. *Riv. Semestr. Dell'Assoc. for. del Trentino*, pp. 7–39.
- D'Agostino V, Lenzi MA. 1998. La massimizzazione della resistenza al flusso nei torrenti con morfologia a step-pool. Vol. 1, XXVI, Convegno di Idraulica e Costruzioni Idrauliche, Catania, Italy, September 9–12, pp. 281–293.
- Davis JC. 1986. Statistics and Data Analysis in Geology. John Wiley & Sons: New York, New York.
- Davis WM. 1899. The geographical cycle. *Geographical Journal* 14: 481–504.
- Doll BA, Wise-Frederick DE, Buckner CM, Wilkerson SD, Harman WA, Smith RE, Spooner J. 2002. Hydraulic geometry relationships for urban streams throughout the Piedmont of North Carolina. *Journal of the American Water Resources Association* 38(3): 641–651.
- Dyhouse GR. 1982. Sediment analyses for urbanizing watersheds. *Proceedings of the American Society of Civil Engineers, Journal of the Hydraulics Division* 108(HY3): 399–421.
- Edwards TK, Glysson GD. 1988. Field methods for measurement of fluvial sediment. Chapter C2 In: U.S. Geological Survey, Techniques of Water-Resources Investigations Report, Book 3: Applications of Hydraulics, pp. 86–531.
- Emmett WW. 1980. A Field Calibration of the Sediment-trapping Characteristics of the Helley-Smith Bedload Sampler. U.S. Geological Survey, Professional Paper 1139, 44 p.

- Emmett WW, Wolman MG. 2001. Effective discharge and gravel-bed rivers. *Earth Surface Processes and Landforms* 26: 1369–1380.
- Espey Jr WH, Morgan CW, Masch FD. 1966. A Study of Some Effects of Urbanization on Storm Runoff from a Small Watershed. Report No. 23, Texas Water Development Board: Austin, Texas, 109 p.
- Federal Interagency Stream Restoration Working Group (FISRWG) (1998). Stream Corridor Restoration: Principles, Processes, and Practices. GPO Item No. 0120-A, SuDocs No. A 57.6/2:EN 3/PT.653, ISBN-0-934213-59-3.
- Freeman PL, Schorr MS. 2004. Influence of watershed urbanization on fine sediment and macro invertebrate assemblage characteristics in Tennessee ridge and valley streams. *Journal of Freshwater Ecology* 19(3): 353–362.
- Friedman G, Sanders J. 1978. Principles of Sedimentology. Wiley Publisher: New York, New York, 792 p.
- Froude DO, Ireland TR, Kinney PD, Williams IS, Compston W. 1983. Ion microprobe identification of 4, 100-4, 200 myr-old terrestrial zircons. *Nature* 304: 616–618.
- Gingras D, Adamowski KPJ, Pilon PJ. 1994. Regional flood equations for the provinces of Ontario and Quebec. *Water Resources Bulletin* 30(1): 55–567.
- Graf WL. 1975. The impact of suburbanization on fluvial geomorphology. *Water Resources Research* 11(5): 690–692.
- Graf WH. 1984. Hydraulics of Sediment Transport. Water Resources Publications, LLC: Littleton, Colorado, ISBN 0-918334-56-X, 521 p.
- Grant GE., Swanson FJ, Wolman MG. 1990. Pattern and origin of stepped-bed morphology in high-gradient streams, Western Cascades, Oregon. *Geological Society of America Bulletin* 102: 340–352.
- Grant GE, Mizuyama T. 1991. Origin of step-pool sequences in high gradient streams: a flume experiment. In: Proceedings of the Japan-U. S. Workshop on Snow Avalanche: Landslide, Debris Flow Prediction and Control, Organizing Committee, Tskuba, Japan, pp. 523–532.
- Hammer TR. 1972. Stream channel enlargement due to urbanization. *Water Resources Research* 8(6): 1530–1540.
- Hanson GJ. 1991. Development of a jet index to characterize erosion resistance of soils in earthen spillways. *Transactions of the American Society of Agricultural Engineers* 34: 2015–2020.



- Helley EJ, Smith W. 1971. Development and Calibration of a Pressure Difference Bedload Sampler. U.S. Geological Survey, Water Resources Division Open-file Report, 18 p.
- Henderson FM. 1966. Open Channel Flow. Macmillan Publishing Co., Inc.: New York, New York, 522 p.
- Henshaw PC, Booth DB. 2000. Natural restabilization of stream channels in urban watersheds. *Journal of the American Water Resources Association* 36(6): 1219–1236.
- Hey, RD. 1976. Geometry of river meanders. *Nature* 262: 482–484.
- Hey RD. 1997. River engineering and management in the 21st century. In: Applied Fluvial Geomorphology for River Engineering and Management, Thorne CR, Hey RD, Newson MD (Eds.), Wiley: Chichester, England, pp. 3–11.
- Hey RD, Thorne CR. 1986. Stable channels with mobile gravel beds. *Journal of Hydraulic Engineering* 112(6): 671–689.
- Hickin EJ, Nanson GC. 1975. The character of channel migration on the Beatton River, Northeast British Columbia, Canada. *Geological Society of America Bulletin* 86: 487–494.
- Hickin EJ. 1984. Vegetation and river channel dynamics. *Canadian Geographer* 28(2): 111–126.
- Hicks DM, Mason PD. 1991. Roughness Characteristics of New Zealand Rivers. New Zealand Department of Scientific and Industrial Research, Marine and Freshwater, Natural Resources Survey: Wellington, New Zealand, 329 p.
- Hollis GE. 1975. The effect of urbanization on floods of different recurrence intervals. *Water Resources Research* 11(3): 431–435.
- Hollis GE, Luckett JK. 1976. The response of natural river channels to urbanization: two case studies from southeast England. *Journal of Hydrology* 30: 351–363.
- Horton RE. 1945. Erosional development of streams and their drainage basins: hydrophysical approach to quantitative morphology. *Geological Society of America Bulletin* 56: 275–370.
- Hubbell DW. 1964. Apparatus and Techniques for Measuring Bedload. U.S. Geological Survey Water, Supply Paper 1748.

- Hutton NJ. 1788. Theory of the Earth; or an investigation of the laws observable in the composition, dissolution and restoration of the land upon the globe. *Transactions of the Royal Society of Edinburgh* 1(2): 209–304.
- Imhof JG, FitzGibbon JE, Annable WK. 1996. A hierarchical indicator model for characterizing and evaluating watershed ecosystems for fish habitat. *Canadian Journal of Fisheries and Aquatic Sciences* 51(Supl. 1): 312–326.
- Inglis CC. 1949. The behaviour and control of rivers and canals. *Resource Publication*, Poona (India) 2(13): 1–687.
- Johnson PA, Heil TM. 1996. Uncertainty in estimating bankfull conditions. *Water Resources Bulletin* 32(6): 1283–1291.
- Jordan B, Annable WK, Watson CC. 2009. Contrasting stream stability characteristics in adjacent urban watersheds: Santa Clara Valley, California. *River Research Application* 25: 1–17, DOI: 10.1002/rra.1333.
- Julien PY. 2002. River Mechanics. Cambridge University Press: Cambridge; 434 p.
- Karrow PF. 1991. Quaternary Geology of the Brampton Area. Open File Report 5819, Ontario Geological Survey, Ministry of Northern Development and Mines: Toronto, Ontario.
- Keller EA. 1971. Areal sorting of bed material: the hypothesis of velocity reversal. *Geological Society of America Bulletin* 83: 915–918.
- Keller EA, Melhorn WN. 1978. Rhythmic spacing and origin of pools and riffles. *Geological Society of America Bulletin* 89: 723–730.
- Keller EA, Swanson FG. 1979. Effects of large organic material on channel form and fluvial processes. *Earth Surface Processes* 4: 361–380.
- Kellerhals R, Neill CR, Bray DI. 1972. Hydraulic and Geomorphic Characteristics of Rivers in Alberta. Alberta Research Council: Edmonton, Alberta, 52 pp.
- Kennedy JF. 1963. The mechanics of dunes and antidunes in erodible bed channels. *Journal of Fluid Mechanics* 16(4): 521–544.
- Kibler DF, Froelich DC, Aron G. 1981. Analyzing urbanization impacts on Pennsylvania flood peaks. *Water Resources Bulletin* 17(2): 270–274.
- Kleinbaum DG, Kupper LL, Muller KE. 1988. Applied Regression Analysis and Other Multivariable Methods. PWS-Kent Publishing Company: Boston, Massachusetts, 718 p.

- Klingeman PC, Emmett WW. 1982. Gravel bedload transport processes. In: Gravel-bed Rivers, Hey RD, Bathurst JC, Thorne CR (Eds.), John Wiley & Sons Ltd.: London, England, pp. 141–179.
- Kondolf GM, Downs PW. 1996. Catchment approach to planning channel restoration. In: River Channel Restoration: Guiding Principles for Sustainable Projects, Brookes A, Shields Jr FD (Eds.), Wiley: Chichester, England, pp. 129–148.
- Konrad CP, Booth DB. 2002. Hydrologic Trends Associated with Urban Development in Western Washington Streams. U. S. Geological Survey, Water Resource Investment Review 02–4040, 40 p.
- Konrad PK, Booth DB, Burges SJ. 2005. Effects of urban development in the Puget Lowland, Washington, on interannual streamflow patterns: consequences for channel form and streambed disturbance. *Water Resources Research* 41(W07009): 1–15.
- Lacey G. 1930. Stable channels in alluvium. Paper 4736, Minutes of the Proc., Institution of Civil Engineers, 229, William Clowes and Sons Ltd.: London, England, pp. 259–292.
- Lane EW. 1955. The importance of fluvial morphology in hydraulic engineering. *Proceedings of the American Society of Civil Engineers* 81: 1–17.
- Langbein WB, Leopold LB. 1964. Quasi-equilibrium states in channel morphology. *American Journal of Science* 262: 782–794.
- Lawler DM, Thorne CR, Hooke JM. 1997. Bank erosion and instability. In: Applied Fluvial Geomorphology for River Engineering and Management, Thorne CR, Hey RD, Newsom MD (Eds.), John Wiley & Sons: London, England, p. 137.
- Lawler DM, Petts GE, Foster IKL, Harper S. 2006. Turbidity dynamics during spring storm events in an urban headwater river system: the Upper Tame, West Midlands, United Kingdom. *Science of the Total Environment* 360: 109–126.
- Lee JH, Bang KW, Ketchum LH, Choe JS, Yu MJ. 2002. First flush analysis of urban storm runoff. *The Science of the Total Environment* 293: 163–175.
- Leliavsky S. 1955. An Introduction to Fluvial Hydraulics. Constable and Company Ltd.: London, England, 257 p.
- Léonard J, Richard G. 2004. Estimation of runoff critical shear stress for soil erosion from soil shear strength. *Catena* 57: 233–249.
- Leopold A. 1949. A Sand County Almanac: and Sketches Here and There. Oxford University Press Inc.: New York, New York.

- Leopold LB, Wolman MG. 1960. River meanders. *Geological Society of America Bulletin* 71: 769–794.
- Leopold LB, Wolman MG, Miller JP. 1964. Fluvial Processes in Geomorphology. W.H. Freeman and Company: San Francisco, California, 522 pp.
- Leopold LB. 1968. Hydrology for urban land planning – a guidebook on the hydrologic effects of urban land use. U. S. Geological Survey, Circular No. 554.
- Leopold LB. 1973. River channel change with time: an example. *Bull. Geol. Soc. of America* 84: 845–860.
- Leopold LB. 1994. A View of the River. Harvard University Press: Cambridge, Massachusetts, 298 p.
- Lindley ES. 1919. Regime channels. *Minutes and Proceedings of Punjab Engineering Congress Lahore* 7: 63–74.
- MacRae CR, Rowney AC. 1992. The role of moderate flow events and bank structure in the determination of channel response to urbanization. In: Resolving Conflicts and Uncertainty in Water Management, Shrubsole D (Ed.), Proceedings of the 45th Annual Conference of the Canadian Water Resources Association: Kingston, Ontario.
- MacRae CR. 1997. Experience from morphological research on Canadian streams: is control of the two-year frequency runoff event the best basis for stream channel protection? In: Effects of Watershed Development and Management of Aquatic Ecosystems, Roesner LA (Ed.), Proceedings of an Engineering Conference, American Society of Civil Engineers: New York, New York, pp. 144–162.
- Madej MA. 2001. Development of channel organization and roughness following sediment pulses in single-thread, gravel bed rivers. *Water Resources Research* 37(8): 2259–2272.
- Magalhaes L, Chau TS. 1983. Initiation of motion conditions for shale sediments. *Canadian Journal of Civil Engineering* 10: 549–554.
- McGilchrist CA, Woodyer KD. 1968. Statistical tests for common bankfull frequency in rivers. *Water Resources Research* 4(2): 331–348.
- Millar RG. 2000. Influence of bank vegetation on alluvial channel patterns. *Water Resources Research* 36(4): 1109–1118.
- Montgomery DR, Buffington JM. 1997. Channel-reach morphology in mountain drainage basins. *Geological Society of America Bulletin* 109: 596–611.

- Morley SA, Karr JR. 2002. Assessing and restoring the health of urban streams in the Puget Sound Basin. *Conservation Biology* 16(6): 1498–1509.
- Nanson GC, Young RW. 1981. Downstream reduction of rural channel size with contrasting urban effects in small coastal streams of southeastern Australia. *Journal of Hydrology* 52: 239–255.
- National Research Council (NRC). 1999. Improving American River Flood Frequency Analyses. National Academy Press: Washington, D.C.
- O’Neil MP, Abrahams AD. 1984. Objective identification of pools and riffles. *Water Resources Research* 20(7): 921–926.
- Ontario Ministry of Natural Resources (OMNR). 2006. Southern Ontario Land Resource Information System (SOLRIS) – Digital Resources, Ontario Ministry of Natural Resources, Science and Information Branch: Peterborough, Ontario, Canada.
- Packman JC. 1979. The effect of urbanization on flood magnitude and frequency. In: Man’s Impact on the Hydrological Cycle in the United Kingdom, Hollis GE (Ed.), Report No. 63, Institute of Hydrology, Geobooks: Wallingford, England, pp. 153–172.
- Parker G, Anderson AG. 1977. Basic principles of river hydraulics. *Proceedings of the American Society of Civil Engineers, Journal of the Hydraulics Division* 103(HY9): 1077–1087.
- Parker G, Wilcock PR, Paola C, Dietrich WE, Pitlick J. 2007. Physical basis for quasi-universal relations describing bankfull hydraulic geometry of single-thread gravel bed rivers. *Journal of Geophysical Research* 112: F04005. DOI:10.1029/2006JF000549.
- Parker G. 2008. Transport of gravel and sediment mixtures. Chapter 3 In: Sedimentation Engineering: Processes, Management, Modeling, and Practice, Garcia MH (Ed.), American Society of Civil Engineers, Task Committee for the Preparation of the Manual on Sedimentation, Environmental and Water Resources Institute, ISBN 0784408149, 9780784408148, pp. 165–252.
- Paul MJ, Meyer JL. 2001. Streams in the urban landscape. *Annual Review of Ecology and Systematics* 32: 333–365.
- Paulson DS. 2007. Handbook of Regression and Modeling: Applications for the Clinical and Pharmaceutical Industries. Chapman and Hall: Boca Raton, Florida, 520 pp.
- Richard GA. 2001. Quantification and Prediction of Lateral Channel Adjustments Downstream from Cochiti Dam, Rio Grande, New Mexico. Ph.D. Thesis,

Department of Civil Engineering, Colorado State University, Fort Collins, Colorado, 283 p.

- Riley SJ. 1972. A comparison of morphometric measures of bankfull. *Journal of Hydrology* 17: 23–31.
- Rosgen DL. 1996. Applied River Morphology. Second Edition, Wildland Hydrology: Pagosa Springs, Colorado, ISBN 0-9653289-0-L 2, 385 p.
- Rozovskii IL. 1957. Flow of water in bends of open channels. Academy of Sciences of the Ukrainian SSR, Institute of Hydrology and Hydraulic Engineering, pp. 233.
- Rubey W. 1933. Settling velocities of gravel, sand and silt particles. *American Journal of Science* 25(148): 325–338.
- Sauer VB, Thomas Jr. WO, Stricker VA, Wilson KV. 1982. Flood Characteristics of Urban Watersheds in the United States. U. S. Geological Survey, Water-Supply Paper 2207, 61 p.
- Schumm SA. 1960. The Shape of Alluvial Channels in Relation to Sediment Type. U. S. Geological Survey, Professional Paper No. 352-B, 30 p.
- Schumm, SA. 1968. River Adjustment to Altered Hydrologic Regimen – Murrumbidgee River and Palaeochannels, Australia. U. S. Geological Survey, Professional Paper 598, 65 p.
- Schumm SA. 1969. River metamorphosis. *Proceedings of the American Society of Civil Engineers, Journal of the Hydraulic Division* 95(HY1): 255–273.
- Schumm SA. 1977. The Fluvial System. Wiley-Interscience: New York, New York.
- Schumm SA, Harvey MD, Watson CC. 1984. Incised Channels: Morphology, Dynamics and Control. Water Resources Publications: Littleton, Colorado, ISBN 0918334-53-5, 200 p.
- Shields Jr. FD, Copeland RR, Klingeman PC, Doyle MW, Simon A. 2003. Design for stream restoration. *Journal of Hydraulic Engineering* 129(8): 575–584.
- Shugar D, Kostaschuk R, Ashmore P, Desloges J, Burge L. 2007. In situ jet testing of the erosional resistance of cohesive streambeds. *Canadian Journal of Civil Engineering* 34: 1192–1195.
- Simons DB, Albertson ML. 1960. Uniform water conveyance channels in alluvial material. *Proceedings of the American Society of Civil Engineers, Journal of the Hydraulics Division*, 86(HY5): 33–71.

- Simons DB, Richardson EV. 1963. Form of bed roughness in alluvial channels. *ASCE Transactions* 128: 284–323.
- Soar P. 2000. Channel Restoration Design for Meandering Rivers. Ph.D. Dissertation, University of Nottingham: Nottingham, England.
- Stankowski SJ. 1974. Magnitude and Frequency of Floods in New Jersey with Effects of Urbanization. U. S. Geological Survey, Special Report 38, 46 p.
- Stevens MA, Simons DB, Richardson EV. 1975. Nonequilibrium river form. *Proceedings of the American Society of Civil Engineers, Journal of the Hydraulics Division* 101(HY5): 557–567.
- Strickler A. 1923. Beitrge zur Frage der Geschwindigkeitsformel und der Rauhigkeitszahlen fur Strome, Kanale und geschlossenen Leitungen, Mitteilung 16. Amt fur Wasserwirtschaft, Bern, Switzerland.
- Sweet WV, Geratz JW. 2003. Bankfull hydraulic geometry relationships and recurrence intervals for North Carolina's coastal plain. *Journal of the American Water Resources Association* 39(4): 861–871.
- Thorne CR. 1990. Effects of vegetation on riverbank erosion and stability. In: Vegetation and Erosion, Thornes JB (Ed.), Wiley: Chichester, England, pp. 125–144.
- Thorne CR. 1997. Channel types and morphological classification. In: Applied Fluvial Geomorphology for River Engineering and Management, Thorne CR, Hey RD, Newson MD (Eds.), Wiley: Chichester, England, pp. 175–222.
- U. S. Army Corps of Engineers (USACE). 2004. HEC-RAS River Analysis System – User's Manual. U.S. Army Corps of Engineers, Institute for Water Resources, Hydrologic Engineering Center: Davis, California, 687 p.
- U. S. Department of Agriculture Forest Service (USDAFS). 1995. Identifying Bankfull Stage in Forested Streams in the Eastern United States. Video, Rocky Mountain Research Station, Stream System Technology Center: Fort Collins, Colorado.
- U. S. Department of Agriculture Forest Service (USDAFS). 2003. A Guide to Field Identification of Bankfull Stage in the Western United States. Video, Rocky Mountain Research Station, Stream System Technology Center: Fort Collins, Colorado.
- U. S. Geological Survey (USGS). 1982. Guidelines for Determining Flood Flow Frequency. Bulletin 17B of the Hydrology Subcommittee, Interagency Advisory Committee on Water Data: Reston, Virginia.

- Urbonas BR, Roesner LA. 1993. Hydrologic design for urban drainage and flood control. Chapter 28 In: Handbook of Hydrology, Maidment DR (Ed.), McGraw-Hill: New York, New York, pp. 1–28.
- Van Rijn LC. 1984. Sediment transport, Part III: bedforms and alluvial roughness. *Proceedings of the American Society of Civil Engineers, Journal of the Hydraulics Division* 110(11): 1613–1641.
- Whipple Jr W, DiLouie JM, Pytlar Jr T. 1981. Erosional potential of streams in urbanizing areas. *Water Resources Bulletin* 17(1): 36–45.
- Wilcock PR, Kenworthy ST. 2002. A two fraction model for the transport of sand-gravel mixtures. *Water Resources Research* 38(10): 1194–2003.
- Williams GP. 1978. Bank-full discharge of rivers. *Water Resources Research* 14(6): 1141–1154.
- Williams GP. 1986. River meanders and channel size. *Journal of Hydrology* 88: 147–164.
- Wohl E. 2000. Virtual Rivers – Lessons from the Mountain Rivers of the Colorado Front Range. Yale University Press: New Haven, Connecticut, ISBN: 9780300084849, 249 p.
- Wohl E, Merritt DM. 2008. Reach-scale channel geometry of mountain streams. *Geomorphology* 93: 168–185.
- Wolman MG. 1954. A method of sampling coarse river-bed material. *Transactions of the American Geophysical Union* 35: 951–956.
- Wolman MG. 1955. The Natural Channel of Brandywine Creek, Pennsylvania. U. S. Geological Survey, Professional Paper 271, 56 p.
- Wolman MG, Leopold LB. 1957. River Floodplains – Some Observations on their Formation. U. S. Geological Survey, Professional Paper 282C.
- Wolman MG, Miller JP. 1960. Magnitude and frequency of forces in geomorphic processes. *Journal of Geology* 68: 54–74.
- Wolman MG. 1967. A cycle of sedimentation and erosion in urban river channels. *Geografiska Annaler* 49A: 385–395.
- Wolman MG, Schick AP. 1967. Effects of construction on fluvial sediment, urban and suburban areas of Maryland. *Water Resources Research* 3(2): 451–464.



- Wong M, Parker G. 2006. Re-analysis and correction of bedload relation of Meyer-Peter and Müller using their own database. *Proceedings of the American Society of Civil Engineers, Journal of the Hydraulics Division* 132(11): 1159–1168.
- Woodyer KD. 1968. Bankfull frequency in rivers. *Journal of Hydrology* 6: 114–142.
- Yalin MS. 1964. Geometrical properties of sand waves. *Proceedings of the American Society of Civil Engineers, Journal of the Hydraulics Division* 90(HY5):105–119.
- Yalin MS. 1971. On the formation of dunes and meanders. In: Proceedings of the 14th International Congress of the Hydraulic Research Association, Paris, 3(C13), pp. 1–8.
- Yang CT. 1971. Formation of riffles and pools. *Water Resources Research* 7(6): 1567–1574.
- Yang CT. 1979. Unit stream power equations for total load. *Journal of Hydrology* 40: 123–138.
- Yang CT. 1984. Unit stream power equation for gravel. *Journal of Hydraulic Engineering* 110(12): 1783–1797.
- Zimmerman RC, Goodeltt JC, Comer GH. 1967. The influence of vegetation on channel form of small streams. In: Symposium River Morphology, International Association of Scientific Hydrology, Publication 75, pp. 255–275.
- Zimmermann A, Church M. 2001. Channel morphology, gradient profiles and bed stresses during flood in a step-pool channel. *Geomorphology* 40: 311–327.